University of Bath

UNIVERSITY OF BATH

PHD

Control of a Fast Switching Valve for Digital Hydraulics

Sell, Nathan

Award date:
2015

Awarding institution:
University of Bath

Link to publication

Control of a Fast Switching Valve for Digital Hydraulics

submitted by

Nathan Peter Sell

for the degree of Doctor of Philosophy

of the

University of Bath

Department of Mechanical Engineering

May 2015

COPYRIGHT

Summary

Fluid power control is dominated by the throttling orifice. This is an inherently inefficient methodology that is responsible for low system efficiencies. The field of digital fluid power seeks to replace the throttling orifice with on-off valves and in the process greatly improve the efficiency of fluid power systems. One implementation of these on-off valves is the Switched Inertance Hydraulic System (SIHS) which operates in a similar way to Switched Mode Power Supplies (SMPS) in power electronics. In order to realise SIHS it is necessary to have valves that can switch large flow rates between high and low pressure supplies quickly. This report details the development of such a valve. It is demonstrated empirically that by using multiple grooves on a single spool a flow rate of 55L/min (at 10bar pressure drop) can be achieved whilst switching in <1ms. This is achieved through cascading a State Variable Feedback (SVF) controller with Iterative Learning Control (ILC) feedforward. The addition of novel stop learning conditions to the simple proportional lag compensated ILC scheme allow the valve to be tested to the limit of its abilities giving a minimum switching time of 0.5ms, where the limitation proved to be the range of the accelerometer used. Using the valve in a SIHS yielded promising initial results with efficiencies above 80% being achieved across a range of switching ratios.

Contents

List of Figures

List of Tables

Chapter 1

Literature Review

1.1 Introduction

A 2010 paper entitled 'Convicted to Innovation in Fluid Power' [1] dramatically and unequivocally proclaimed the forthcoming death of the fluid power industry if it did not change its ways. The author's contention is that for too long the fluid power industry has used the hydraulic cylinder's unassailable position as the only realistic means of linear actuation, to rest on its laurels. With the fluid power component industry estimated to be worth more than \$49bn in 2011 these are impressive laurels [2] but, if the author is to be believed, in the near future the bastion of the hydraulic cylinder will soon be laid to siege because of two key failings. Firstly, cost. Hydraulic components cost more than twice as much per kilogram as their mechanical counterparts [1]. At the birth of hydraulic engineering, in the late 18th and early 19th century, hydraulics were predominantly used for metal working, cranes and other heavy industry, including raising and lowering Tower Bridge. The inefficiencies of hydraulic systems were not even considered due to the low cost of energy and impossibility of an alternative. Now, however, for every industry that is looking to hydraulics as a transmission system, whether mobile machinery, passenger vehicles [3] or renewable energy [4], system efficiency is no longer a secondary characteristic. It is instead a measure of fitness, with increasing energy cost and tighter emissions regulations serving

1

to compound the problem. Classically, hydraulic components have had good efficiencies with pumps and motors capable of efficiencies in the range of 90% to 95% and cylinders having small frictional losses. Sadly, this potential is not carried forward into efficient systems and losses of more than 50% are not uncommon [5]. The main cause of this is the metering orifice.

The use of throttling as a means of control is ingrained into the fluid power industry. For good reason. Metering orifices provide smooth, simplistic and well understood control. In fact, with the exception of efficiency, it tops all the metrics for a control method. This further complicates the issue of moving away from the intrinsically wasteful throttling control, as expectations of controllability and 'feel' are set very high. The majority of research effort into improving hydraulic system efficiencies has been aimed at more closely matching the flow into the metering orifice with the desired output. It has given rise to variable displacement pumps and motors and load sensing circuits. More recently there have been efforts to do away with throttling losses by the use of direct pump control [6], by introducing common rail techniques to hydraulics [7] - the solution preferred by the author of 'Convicted to Innovation in Fluid Power' - and through digital fluid power systems.

In reply to 'Convicted to Innovation in Fluid Power' another paper, 'Is the Future of Fluid Power Digital?', was written [8]. Whilst acknowledging the accusations levelled at the fluid power industry, the authors suggest that the field of digital hydraulics holds the key to correcting the current failings of fluid power. Digital fluid power systems seek to entirely do away with the ubiquitous throttling valves and instead use digital control elements (on/off valves). There are many possible uses and implementations of these digital control elements, some of which will be covered below.

1.2 Digital Hydraulics

Whilst the field of digital hydraulics is, by academic standards still a fledgling, there is a reasonable body of work in existence, dating back to the 1980s. The

bulk of this research is of a theoretical nature, which is a fitting representation of a field that is, for the most part, the dominion of universities, though with a growing industrial representation. The following sections seek to present a state of the art for some of the various different implementations of digital hydraulics under development.

1.2.1   Digital Pumps

A digital pump comprises a collection of separate pumping elements which can either be off-the-shelf pumps in their own right or custom built. Each element is independently valve controlled, meaning it can either idle, pump or motor. This allows a large number of possible output flow rates and pressures to be created efficiently. A circuit diagram using standard hydraulic parts can be seen in Figure 1-1. Research has shown that a single speed prime-mover providing 1.3kW of power, to meet the duty cycle average, is still able to meet a 10.6kW cycle peak requirement [9].

The design seen in Figure 1-1 will be used to demonstrate the pumping cycle and possible operating modes. Each of the three pump elements can retrieve fluid from the tank or the system and pump it to the system port or back to the tank. It is possible for this system to operate as a traditional pump, with all pumping elements transferring fluid from tank to system, or as a motor with all elements returning fluid from system to tank . The advantage of the digital pump, however, lies in its ability to do both simultaneously. For example, if only partial flow is required, elements 1 and 2 could pump from tank to to system whilst element 3 pumped from tank to tank or, possibly from system to tank. The circuit in Figure 1-1 is relatively simple and, as such, only has a limited number of possible output flows and pressures. By increasing the number of pumping elements significantly smoother operating envelopes can be achieved. One of the few commercially available digital hydraulic products does exactly this. The 'Digital Displacement' pump from Artemis Intelligent Power, unlike the circuit shown in Figure 1-1, doesn't use existing pumps as the individual pumping elements but instead has six cylinders with the necessary valves all

3
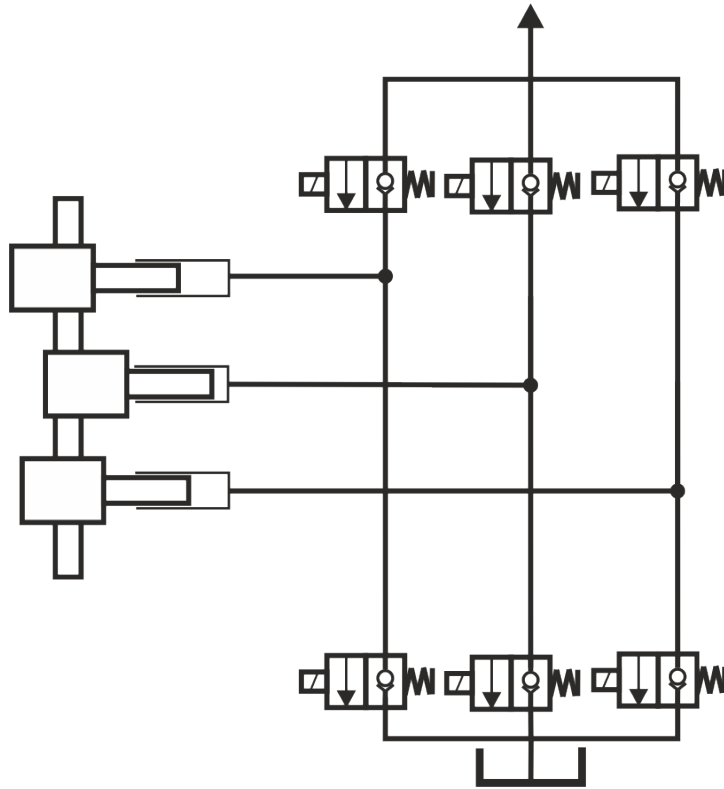
Figure 1-1: Hydraulic circuit diagram for a digital pump

mounted into a single unit. A cross section of the 'Digital Displacement' pump can be seen in Figure 1-2.

When a suitably sized Digital Displacement unit was fitted, using a parallel hybrid architecture, to a bus it was found to give a 24% efficiency gain over an electric hybrid using batteries for storage [11]. The same architecture was used to extract power from a tidal current generator, allowing for a peak efficiency of 94.8% and average efficiency above 80%, over a year's operation [12]. Further work on digital pumps has also been carried out by [13], [14], [15] and [16].

1.2.2 Digital Actuators

Digital actuators apply similar principles to digital pumps, but instead of having separate pumping elements they have separate chambers. This allows a single "actuator" to have multiple selectable areas, giving varied levels of force and
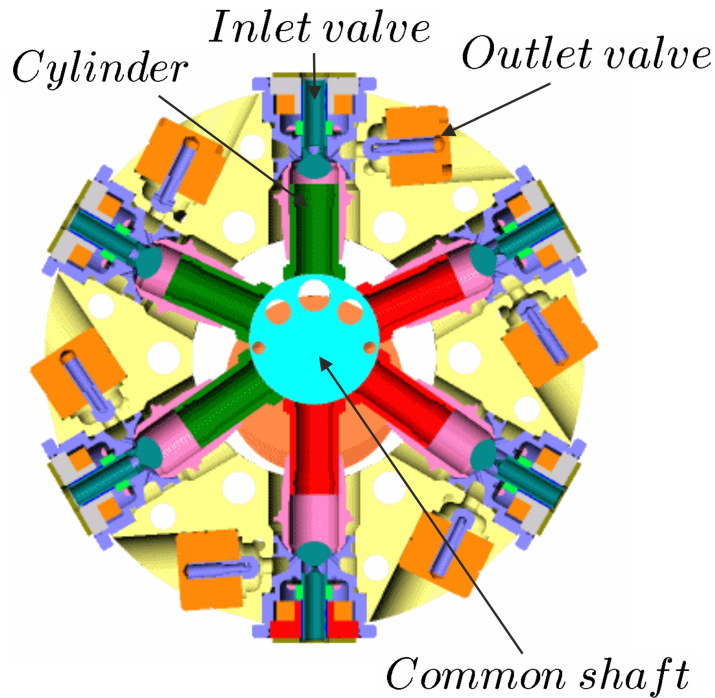
Figure 1-2: Representation of 6 cylinders in the Digital Displacement pump [10]

speed from a fixed source. Figure 1-3 shows a simplified hydraulic circuit for a digital actuator based on standard hydraulic components.

As with the digital pump it is possible to build a digital actuator circuit using off-the-shelf components. However, the need to house and mount multiple actuators is, in most situations, a significant inconvenience and so most research is based on bespoke actuators that incorporate multiple chambers into a single unit. Figure 1-4 shows the cross section of the actuator used by Dell'Amico *et al* [17] within the boom arm of an excavator.

This design has four volumes, with a ratio of 27:3:9:1 (A:B:C:D), and three pressures, giving a total of 81 (3^4) possible force outputs. No efficiency measurements were made. However, in an earlier paper, involving the same rig but using an actuator with only three volumes, a 60% efficiency gain over traditional load sensing systems was found [18]. The possible savings from the use of digital actuators varies based upon the system used and load cycles considered. For example, Linjama *et al* [19] were able to use a digital actuator to obtain 'lossless' control, when compression and valve losses are neglected, for high inertia loads. Whereas
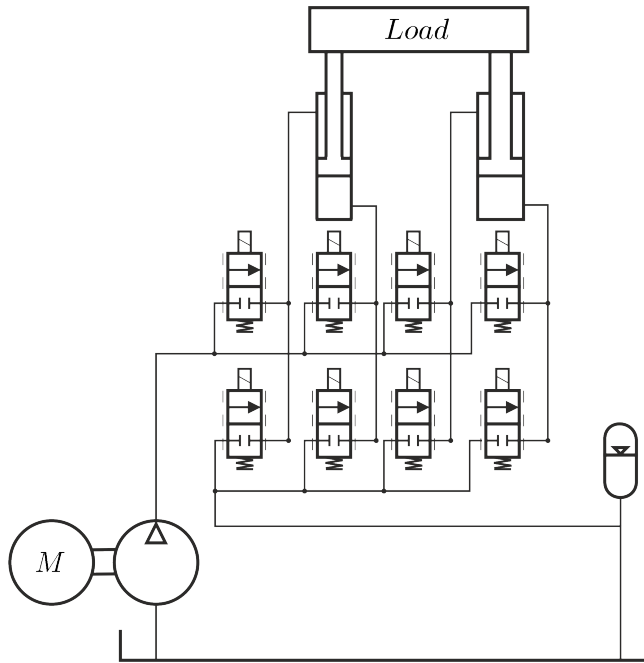
Figure 1-3: Hydaulic circuit for a digital actuator circuit

Huova *et al* [20] found that when operating a mobile boom at three distinct loading conditions - an almost balanced load, a resistive load and an overrunning load - a digital actuator with three volumes gave an average efficiency gain of 33% over a load sensing system. They also hypothesised that this efficiency saving would increase to around 70% in a multi-actuator circuit, as currently most cylinders see overly high pressures. Despite these potential savings, there exist, currently, no commercial systems. There are multiple reasons for this. Firstly, to control four volumes Dell'Amico [17] used 27 discrete valves. This introduced both space and cost increases. Dell'Amico also found issues with obtaining smooth velocity profiles, especially at low loads, due to the nature of a switched controller. It is hypothesised, however, that by replacing the simple PI controller a better response could be expected.

1.2.3 Hydraulic Transformers

Unlike digital pumps or actuators, hydraulic transformers don't really have a commerically available equivalent component in the 'analogue' domain of hydraulics. A transformer is capable of converting pressure and flow from one state

6
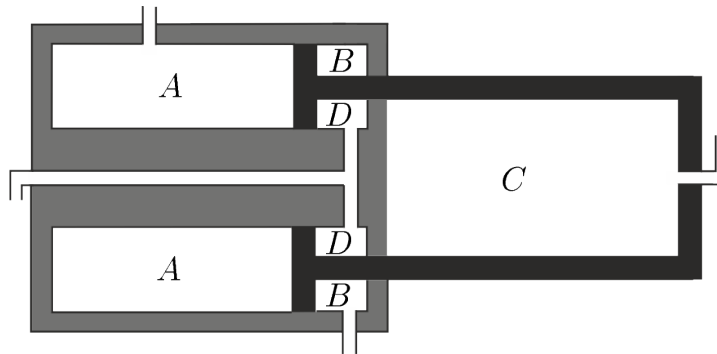
Figure 1-4: Cross section of a digital actuator

to another whilst, in theory, retaining the overall power level. Numerous ways of achieving this transformation have been posited. Classic hydraulic transformers use two hydrostatic devices of which at least one has variable displacement. However, this shares the efficiency issues of all variable displacement devices and suffers severely under certain operating conditions [21]. Research is ongoing into the implementation of the common rail transformer [7]. As a result of the above there is a significant amount of research into 'digital' transformers, three proposed schematics of which will be discussed below. The first to be discussed was proposed in the first known paper on what later came to be called digital hydraulics.

In Brown's seminal paper entitled 'Switched Reactance Hydraulics: A New Way to Control Fluid Power' [22] a basic summary of multiple power electronic devices is presented before proceeding to provide analogous hydraulic circuits. Many similarities can be found between digital fluid power and the field of power electronics, with power electronics literature proving a rich seam of inspiration. Power electronic circuit designs can be easily carried over to hydraulics by exchanging simple electronic components for their hydraulic alternatives. For example, a fluid volume has capacitive effects, hydraulic lines possess inductive behaviour, particularly at small diameters, and a transistor can be considered analogous to a fast switching hydraulic valve. This last analogy proved to be the sticking point as no such valve existed, so Brown designed and manufactured his own rotary valve. More details on this valve can be found in section 1.2.4. By utilising these switched circuits Brown believed that, as well as increased efficiency, a higher bandwidth of control could be gained over conventional orifice

metered circuits. Figure 1-5 shows one of the hydraulic circuits posited by Brown for a simple step up transformer, along with the power electronics circuit which inspired it. Theoretically this circuit would have a 100% efficiency.
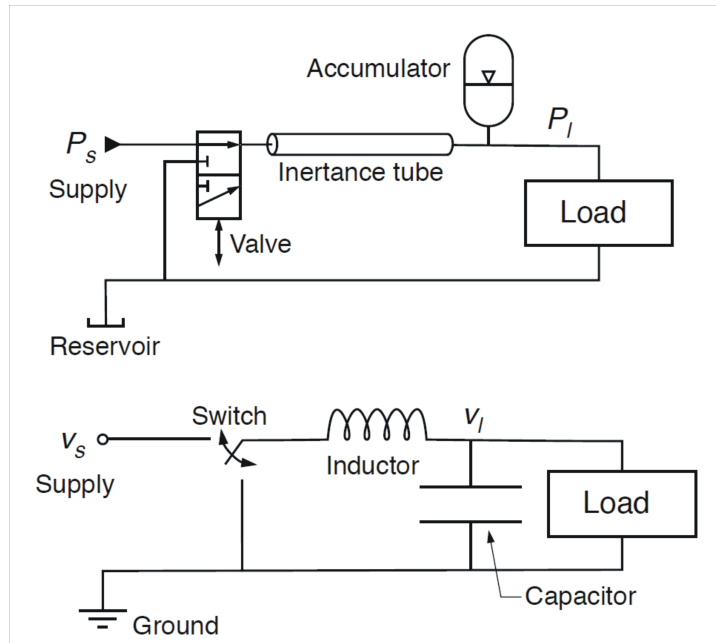
Figure 1-5: Hydraulic switched step-up transformer [5]

When the valve is switched from high pressure to low, the inertia of the fluid in the tube draws flow from the tank, resulting in pulses of fluid alternating between high and low pressure. These pulses are then smoothed over the distance of the inertance tube and by the accumulator at the outlet.

In a further paper in 1988 Brown went on to empirically test this concept of a hydraulic transformer by implementing the circuit shown in Figure 1-6 [23]. It was found that the valve design resulted in too high an inertance in the channel to the tank accumulator which caused significant cavitation. Brown concluded that whilst this cavitation limited the scope of the empirical results, the results themselves supported the belief that a digital transformer could be realised, if two shortcomings could be overcome [22]. The first of these was in fluid modelling - a need for distributed, rather than lumped, systems and the ability to handle frequency dependent parameter values. Secondly, a better valve was needed, the design of which required a better understanding of the fundamental fluid
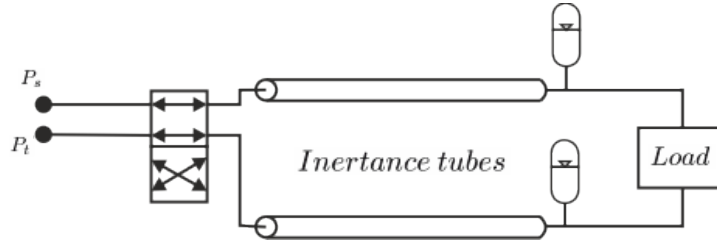
Figure 1-6: Diagram of a switched inertance hydraulic system (recreated from [22])

mechanics than was then available. Given the requirements Brown placed on furthering the digital transformer, and the lack of financial incentive, it is not surprising that it was not until the 21st century that a concerted effort was made to further Brown's work on digital transformers. One of the first papers to cite Brown's 1988 work was Johnston, in 2009 [5]. With 20 years worth of advances in fluid power, particularly modelling, Johnston attempted to recreate the circuit which Brown used in 1988, also utilising a rotary valve. Like Brown, Johnston found what was termed a 'Switched Inertance Hydraulic System' or SIHS (Brown called it a 'Switched-Inertance Servo-Transformer') worked better in theory than in experimentation. This was due to problems with modelling, estimating unknown parameters and valve limitations - mainly excessive leakage. However, the initial results were close enough to those predicted to be considered worthy of further investigation. As with Brown, this further investigation was contingent on a better valve, the development of which will be discussed below. As a result, the follow up paper [24] showed significantly better results using the testing circuit in Figure 1-7. At this juncture it is necessary to introduce the
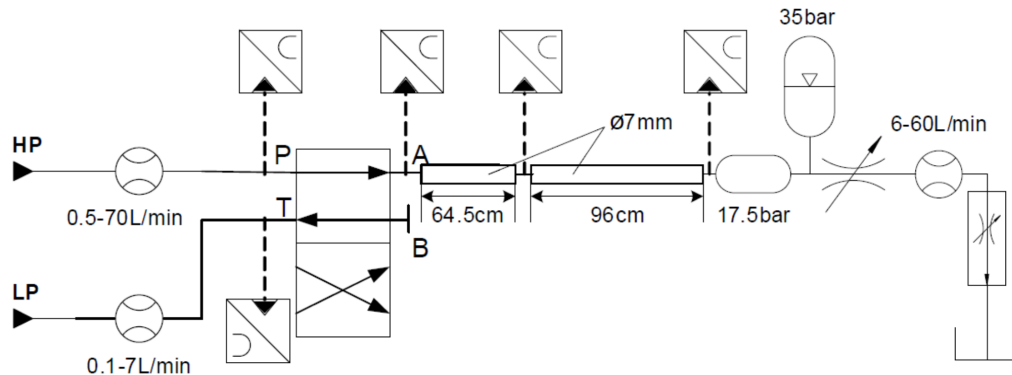
Figure 1-7: Pan *et al* test set-up [24]

concept of flow loss as this provides a helpful metric for evaluating a transformer's performance. This is done in Equation 1.1:

$$q_{loss} = \bar{q}_{HP} - \bar{q}_{out} \cdot \alpha$$

$$or$$

$$q_{loss} = \bar{q}_{out} \cdot (1 - \alpha) - \bar{q}_{LP} \tag{1.1}$$

where $\bar{q}_{HP}$ is the measured flow from the high pressure port and all other flows are defined similarly. Effectively, it is a measure of how much flow, in excess of the figure indicated by the switching ratio (α), is supplied by the high pressure port. It therefore provides an indication not only of the efficiency of the circuit. Pan *et al* experimentally validated the conclusion drawn from a detailed hydraulic model in [25]. Namely, they found that for each switching ratio there existed a switching frequency which minimised the flow loss. This switching frequency could be theoretically calculated using:

$$f = \begin{cases} \frac{\alpha \cdot c}{2 \cdot L} & 0 \le \alpha \le 0.5 \\ \frac{(1-\alpha) \cdot c}{2 \cdot L} & 0.5 \le \alpha \le 1 \end{cases} \tag{1.2}$$

Where L is the length of the inertance tube used and c is the speed of sound in this tube. This leads to the conclusion that there is an upper limit past which faster switching provides no benefit for each tube length. Instead fast switching frequencies can be utilised to minimise the tube length and, thus, losses in the tube. With a tube and fitting length of 1.66m it was found that the highest frequency required would be 189Hz at a 0.5 switching ratio. Using these optimised switching frequencies an average q_{loss} of 0.8L/min was found for a delivery flow rate of 7L/min, over a range of switching frequencies - from 0 to 1 - with LP held at 20bar and HP at 30bar. This gives an efficiency between 83% and 90%. When the flow rate was increased to 20L/min and the HP supply increased to 60bar the q_{loss} increased somewhat to 3L/min.

Kogler *et al* [26] also took inspiration from the work of Brown to create what was dubbed a Hydraulic Buck Converter (HBC). Due to its intended purpose in the field of mobile robotics, it was designed for significantly lower flows (5 L/min) than either Brown's or Johnston's work and, consequently, made use of

smaller components. This allowed it to be packaged into a single unit containing inertance tube, switching valve and accumulators, as can be seen in Figure 1-8. It was found that by using the HBC an energy saving equivalent to 34% was achieved, over metering control, when following a 1Hz sine wave from 45bar to 65bar.
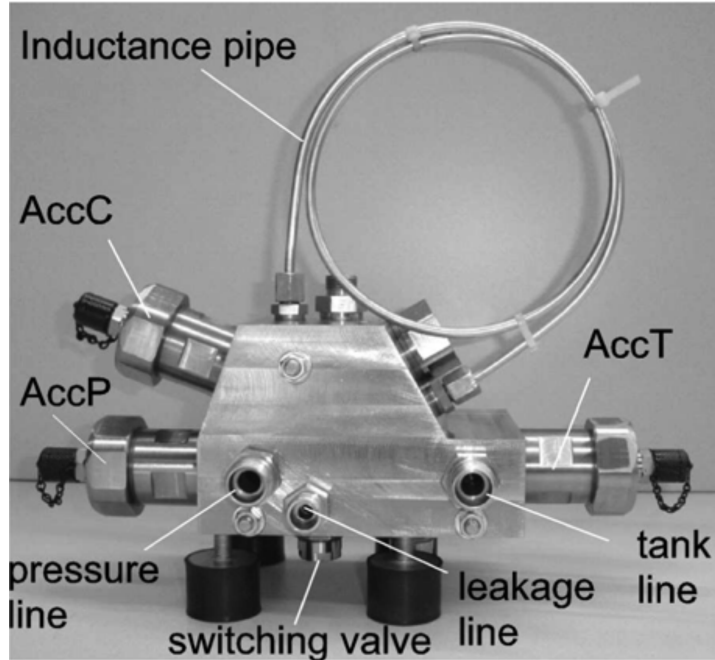
Figure 1-8: Hydraulic Buck Converter [26]

Whilst the switched inertance transformers use a combination of valve and inertance tube to transform, there are other designs based on more classic hydraulic components. Namely, the hydraulic actuator and pump. Bishop proposed what was termed a 'Digital Hydraulic Transformer', DHT, which is based on the concept of a digital actuator, the circuit for which is in Figure 1-9. By swapping each
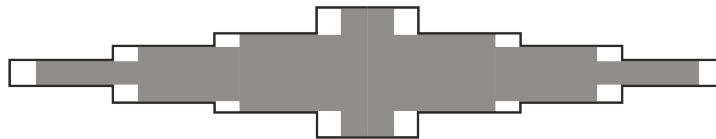
Figure 1-9: Digital Hydraulic Transformer

of the multiple chambers between pump pressure, tank pressure or the transform pressure (pressure in the transformer), it is possible to create 143 different pressure transform ratios ranging between 0.7 and 15. This allows it to transform the

flow with an average efficiency of more than 80% and peak efficiency of 92% [27].

The final transformer to be discussed here has been named the Digital Hydraulic Power Management System (DHPMS), Figure 1-10. This is an evolution of the digital pump and has a similar mode of operation to the DHT but, where the latter uses a digital actuator to transform the input, it makes use of a digital pump. The DHPMS has three key advantages over the DHT. Firstly, it is sig-
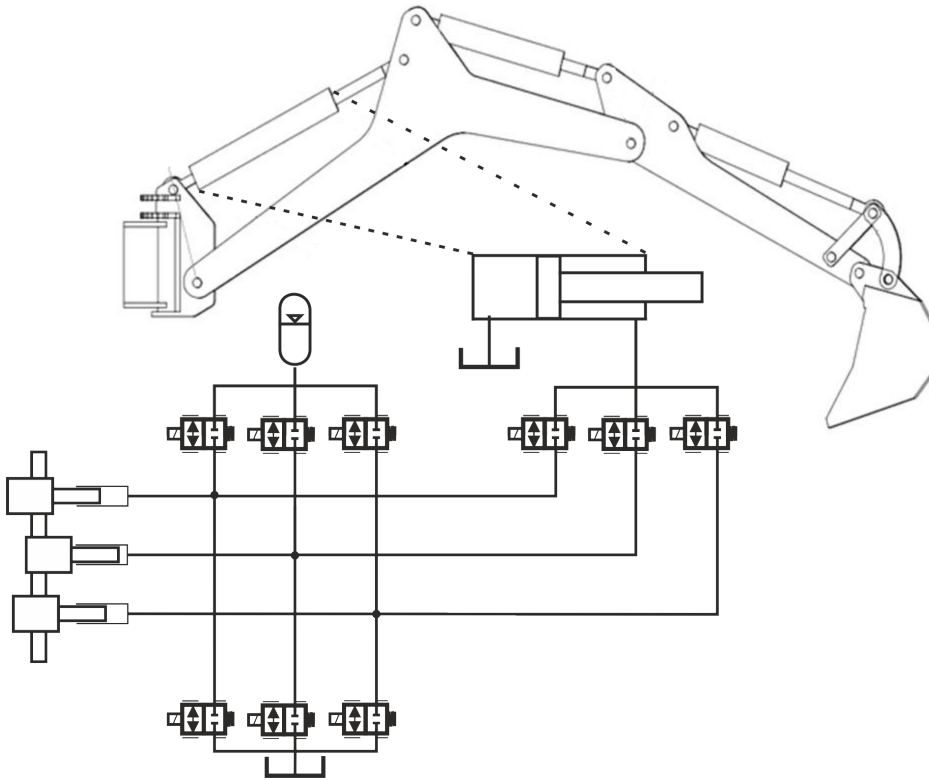
Figure 1-10: Digital Hydraulic Power Management System (modified from [28]

nificantly more compact as the ratio of flow to total volume is much better for a pump than for a cylinder. Secondly, the DHPMS can be achieved using off-the-shelf components [14]. Finally, the DHMPS is currently configured to have multiple output ports. This enables significantly more possible transformations with little increase in complexity and is theoretically expandable to any number of pumping elements and output ports. A six piston, two port DHMPS was found to have an efficiency of 80% which proved constant whether pumping or

transforming. However, the flow capacity of the valves was too small and the system suffered from internal leakage, both factors believed to have limited its efficiency [14]. Further research into the DHPMS found that when connected directly to a double acting cylinder on an excavator arm a position accuracy of 2mm was achievable regardless of the load on the arm, though this became more difficult at low velocities. It was also suggested that the efficiency could be further improved by using leak-free control valves and by increasing the number of pistons in the unit, whilst reducing the volume of each cylinder and by adding accumulators for energy recovery [28]. Currently no valves exist that are able to meet the optimal requirements of the DHPMS. For a 15 pumping element system, believed to be the minimum required for completely smooth flow [29], with a flow of 100 L/min at 1500rpm the valves would need to be durable over 10^9 cycles, have a response time below 2ms repeatable to within 0.1ms and a flow capacity of 30 L/min at 0.5 MPA whilst consuming less than 1J per cycle [29].

1.2.4 Digital Valves

Digital fluid power advocates would like to see the similarities with power electronics extended to the same uptake in technology that saw power electronics go from having no commercial units at the beginning of the 1950s to being a ubiquitous part of the technology landscape. As the power electronics revolution began with one component, the mercury arc rectifier, the hoped for digital fluid power revolution is also contingent upon a single component, the fast switching valve. Whilst many possible applications of these fast switching valves have been proposed, modelled, optimised and published, as can be seen from the above paragraphs, there does not currently exist the standardised unit that Scheidl, Linjama and Schmidt [8] argue will lead to a drop in component cost and allow the many efficient system designs laid out above to be proved. It is the lack of these valves which proves to be the biggest problem for most digital hydraulic systems. They either suffer compromised performance using existing valves or cannot be realised outside of the world of simulation and postulation. There are multiple valves currently under development that set out to achieve different flow rates and switching rates and thus utilise different mechanisms. A selection of these valves are discussed below.

13

The first valve designed specifically for digital hydraulics can be seen in Brown's 1988 paper, discussed above. This was a 2-position, 4-way valve designed to enable fast switching from high pressure to tank at the output ports, in order to follow a pulse width modulation (PWM) signal from 0%-100%, at the high frequencies required for the Switched Inertance Hydraulic Transformer. Figure 1-11 shows the internal geometry of the rotary valve. It can be seen that due to the design of the rotary valve the control of the switching rate and PWM ratio were separated. The velocity of the rotor is controlled by the rate of the electric
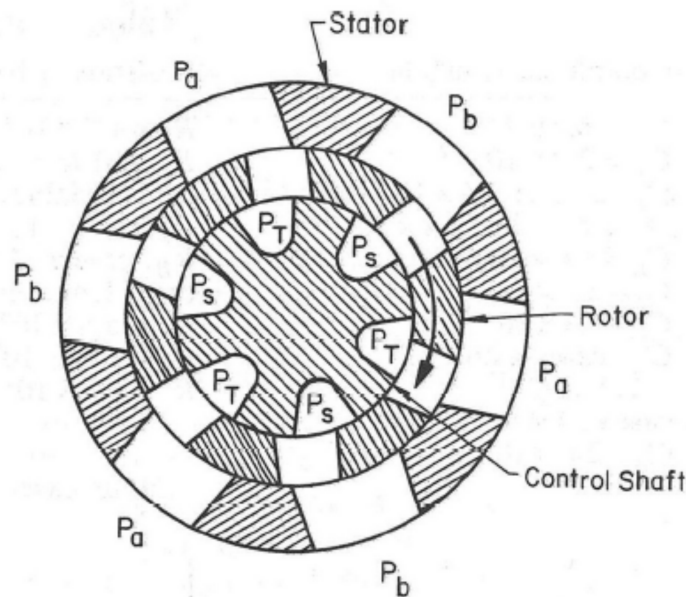
Figure 1-11: Internal geometry of Brown's rotating valve [23]

motor driving it and the duty cycle is set by the position of the control member. The rotor has six slots on it meaning a switching rate of 500Hz is achieved at the motor operating condition of 5000rpm. This could be easily controlled by a simple speed control loop. The duty cycle is controlled by rotating the control shaft from $0°$ to $60°$. Brown did this manually but it could easily be achieved using a servo motor. It was found that due to the sharpness of the switching there were large pressure spikes that interacted with the inertance tube. This could be overcome by changing the valve geometry slightly to give a less abrupt switch. The largest problem encountered with this valve design was the severe cavitation that occurred due to insufficient compliance in the tank side, arising from the high inertance within one of the valve's channels. It was concluded that

14

a redesign was required but further papers were not forthcoming.

Tu *et al* also believed that the best way to achieve the fast switching required in digital hydraulics was to use a rotary, rather than a linear, valve. Unlike Brown, Tu *et al* conceived of a valve that was fluid driven i.e. one that uses the flow it is directing to drive itself. As the valve was intended for use at a fixed frequency it is only necessary to overcome the viscous friction within the valve itself. A separate gerotor pump is driven by a DC motor for the purpose of controlling the linear position, and thereby the duty cycle of the valve. If the power required to drive this is not included then modelling puts the valve losses at 28.9% of the energy passing through it, when operating at 84Hz and 40 L/min. This is a result of transition losses and overcoming viscous friction [30]. In 2009 experimental results showed energy losses to be 35% at 15Hz and 50% duty cycle. An updated model predicted 27% losses at 75Hz [31]. Suggested improvements to the internal flow paths were made as a result of CFD analysis [32] but it was concluded that the requirement on the valve to be self spinning placed too many limitations on the design. In 2011 it was found that an improvement in efficiency of between 7% and 15% could be achieved by actuating the valve externally, though it is unclear whether this figure includes the energy required by the external drive, or only losses within the valve. This change also allowed for a variable switching rate between 50-100Hz widening the possible uses for the valve. External actuation also allowed for the addition of a second inlet port [33] significantly increasing the possible uses of the valve. Figure 1-12 shows the single inlet self-actuated valve. For the dual inlet, externally actuated valve, the overarching geometry remains unchanged, but with an additional middle section. This may well not be optimised for an externally actuated design.

Katz and Van de Ven [34] also suggest a rotary solution to the need for a fast switching digital valve. A three plate design is proposed. The geometry of the plates can be seen in Figure 1-13. In this configuration the switching rate is controlled by the speed at which the valve plate rotates, and the duty cycle by the relative angle of the top and bottom plates. The set up in Figure 1-13 would give a 50% duty cycle. Experiments were carried out using a prototype valve switching at 64Hz. It was found that a maximum efficiency of 38% could be achieved at 100% duty cycle. This was a result of leakage issues and higher
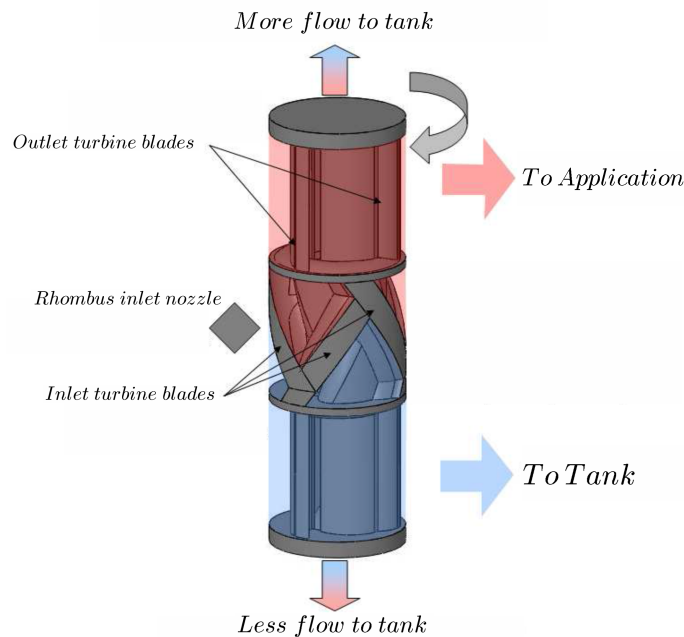
Figure 1-12: Diagram of Tu *et al* rotating valve models (from [30])

than expected torque requirements [34]. This design was developed further in subsequent papers [35] [36] and an updated version of the valve was used in a switch mode hydraulic circuit [37]. No results for the performance of the valve are forthcoming in this paper and it is not possible to infer fully the valve's performance from the circuit's performance. It should, however, be noted that the valve's efficiency must be in advance of 75.4% in some conditions as this was the peak system efficiency [37]. However, the valve was only able to rotate at 10Hz, significantly lower than required for most digital hydraulic circuits, suggesting that there are still limitations with the valve's design.

The rotary valve used in the SIHS study discussed above [24] was designed with the specific application of the SIHS in mind. It is very similar in design to that created by Brown *et al* - a rotor powered by a brushless motor, housed inside a stator with the four ports, HP, LP and two service ports, with a control rod nested inside the rotor. This allowed the motor speed control to govern the switching frequency whilst switching ratio was a function of the control shaft's angular displacement. Figure 1-14 shows the geometry of the valve and the two separate actuators. Whilst based on Brown's ideas this valve did not suffer from the same shortcomings as Brown's. It was theoretically able to switch at up to

16
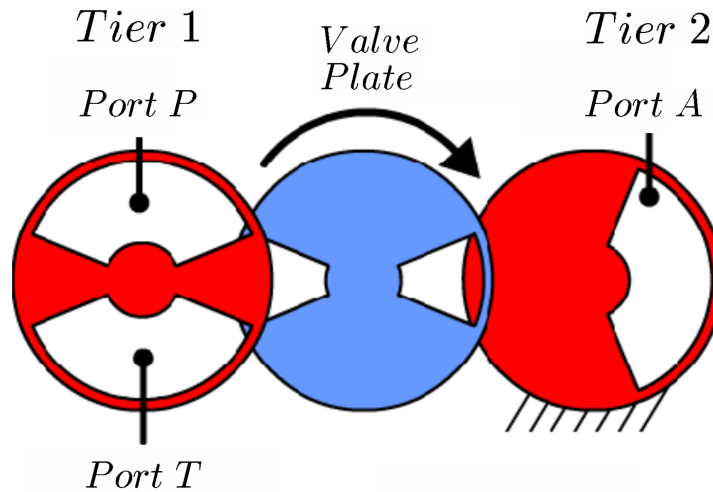
Figure 1-13: Geometry of plates in rotating valve design (taken from [34])

255Hz, though the highest frequency tested was 189Hz, without any noticeable cavitation and had an average leakage of less than 0.2L/min with the control shaft set for a switching ratio of 0.5 and a pressure difference of 20bar. There was, however, a leakage peak of 2L/min when the valve switched between LP and HP ports. This was believed to be a combination of a zero lap design and manufacturing tolerances.

Whilst rotary valves offer the opportunity to separate the control of duty cycle and switching rate, they are not currently very common within the industry. They present issues of their own, such as the need for rotary seals, the need for electrical motors, in many cases, and difficulties with miniaturisation. The rotary valves discussed are also only suitable for use in continuously switching systems such as the transformers mentioned above. They aren't applicable to the digital pumps and actuators discussed which do not require constant switching. In general, linear valves also require less energy to operate as rotary valves, generally, must rotate continuously where as linear valves usually operate an actuate-hold cycle. This helps to further recommend them for use in digital hydraulic circuits which aim to increase total circuit efficiency. Therefore there are also a number of linear digital hydraulic valves that have been proposed and developed.

Yokota and Akuta developed an early linear digital valve in 1991. Using commercially available multilayer piezoelectric transducers they were able to design
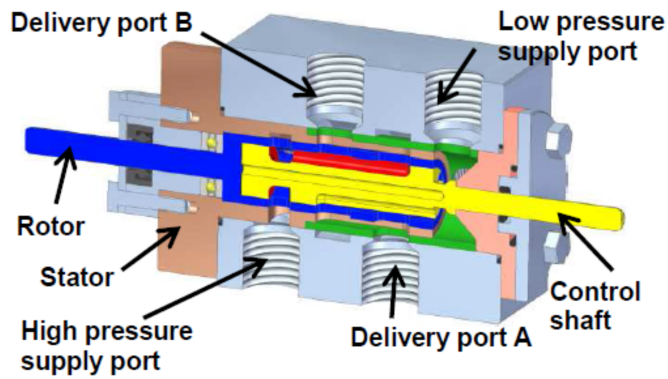
(a) Geometry of a rotating valve
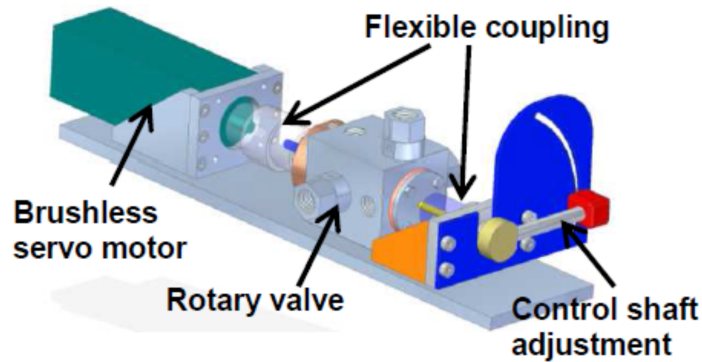
(b) Rotary valve with actuators assembled

Figure 1-14: Diagrams taken from [24]

a dual poppet valve that was capable of tracking a 2kHz rectangular wave [38]. However, the maximum flow that could pass through this valve was 7.2 L/min at a 100bar pressure drop which is much too small for the vast majority of digital hydraulic applications. Therefore this valve was used as the pilot stage of a two stage servovalve which was shown to be capable of producing a 350Hz sine wave, though the flow rate and pressure drop were not reported.

Zhang and Haran presented a valve design based on a small ultrasonic motor which was capable of a relatively fast movement of 13mms^{-1} when unloaded and requiring only 0.9W [39]. However, there have been no publications about the prototype that was being manufactured and therefore although the actuation method seems credible there is no information regarding its use in a valve.

To meet the concurrent requirements for large flows and fast switching times Karvonen *et al* proposed using multiple small valves connected in parallel. To

achieve this they designed a spring return needle valve with an orifice diameter of 0.5mm and opening of 0.3mm resulting in a flow of 0.5 L/min for a 20bar pressure drop. It was able to open in 2ms but due to thermal losses in the actuator it was only able to switch at 22Hz. The outer diameter of the needle valve was only 10mm allowing large numbers of them to be accommodated in relatively small spaces [40]. In a follow up paper in 2011 the valve was shown to have withstood 10^6 actuations once the shape and material of the needle point had been modified, these changes also allowed the switching time to be reduced to 1.2ms [41].

A similar approach was taken by Winkler, Plöckinger and Scheidl who used multiple poppets all located on a single valve and actuated by a joint pilot stage. This allows the sensing and actuating requirements to be centralised, which should ultimately save both money and space. By using needle bearing rollers as poppets and 'ballising' the poppet bores, the cost of manufacturing is kept low [42]. A prototype was manufactured with a bore diameter of 2.7mm, a stroke of 0.675mm and 14 separate poppets. A pilot valve capable of switching within 2ms and providing a flow of 10 L/min at 5bar was used to actuate the poppets with a wave spring being used for the return stroke. This valve was able to provide 85 L/min at 5bar, lower than the design flow of 100 L/min, but this could easily be increased by increasing the number of poppets. A schematic representation can be seen in Figure 1-15. By slightly increasing the overall diameter it is clear that more poppets could be added as necessary. The valve was esti-
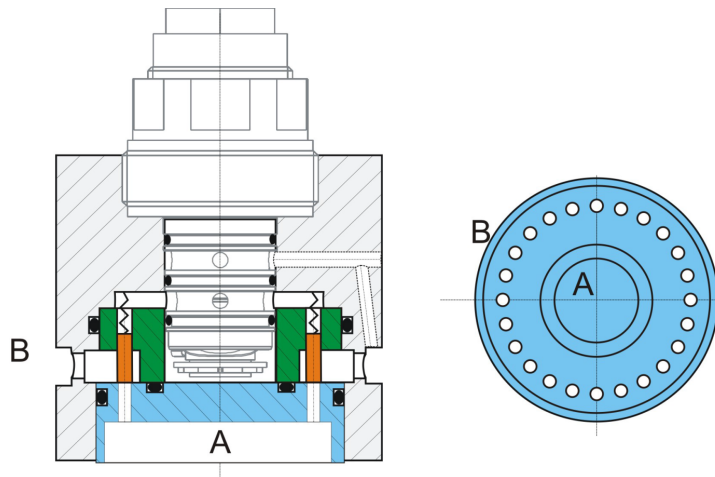
Figure 1-15: Schematic of multipoppet valve (taken from [42])

mated to switch in about 1ms but due to deformation of some components during

switching it was not possible to provide an entirely accurate measure. Whilst the prototype proved the applicability of the approach there are a few key areas in which further work is required. Firstly, there appears to be some leakage which the authors confess to having not studied sufficiently. Secondly, the pilot valve used was not optimised, providing a significantly larger than required flow which could be exchanged for a faster switching time. Thirdly, the lack of accuracy in the position measurement is limiting, especially from a control perspective and the design or sensing method would need to be modified to allow for an accurate and high bandwidth measurement of position. Finally, it also remains to be seen how the valve responds to prolonged use both with regards to wear and durability but also with regards to repeatability of the step responses shown within the paper.

Kudmza *et al* take a similar approach to achieving high flow rates but, rather than using multiple poppets, a spool with multiple grooves is used [43]. This resulted in an equivalent orifice area of 37.7mm^2 [44] for a spool displacement of 0.1mm. This gives a theoretical flow of 65 L/min at a 10bar pressure drop, though experiments showed this to be only 15 L/min as a result of manufacturing errors [43]. The valve was designed with the expressed purpose of being used in the SIHS circuit discussed above. It was, therefore, intended to achieve a switching frequency of 200Hz in keeping with the simulations conducted in [5]. To achieve this a three stage design was realised. A high speed servovalve from Moog was used to direct high pressure flow into an equal area actuator which is on a common shaft with the multiple grooved main stage. All the other digital hydraulic valves mentioned thus far have only two states, on or off. However, the actuation method used by Kudzma *et al* means that it is capable of proportional control. There are a few advantages to this. Firstly, as the valve is position controlled rather than being 'bang-bang' there is less concern about the durability and wear on the valve given the high frequencies it is intended to operate at. Secondly, Tu *et al* [30] found that at very high or low duty cycles proportional control was actually more efficient than switching control. Finally, if the switching mode control were to fail for some reason the valve would not lose all functionality but could instead be used as a simple proportional valve. Due to the specifics of the valve's design it is considerably larger than the other proposed linear designs.

Lantela *et al* [45] perhaps most closely answered Scheidl *et al*'s call for a standardised on/off valve that could be cascaded and combined to meet the needs of the larger digital fluid power community. By developing a valve requiring only 4cm^3 of volume whilst still flowing 9L/min at a 35bar pressure drop and having multiple instances machined onto a block, the dream of a single valve design that can be utilised through the field is closer. The valve uses a spool actuated by a spring and solenoid combination to connect a chamber behind the main stage sealing element, a ball bearing or, in later iterations, a poppet ground from a roller bearing, to either tank or supply pressure. When connected to tank the bearing or poppet moves up allowing flow from supply to outlet, when connected to supply this flow path is closed. Figure 1-16 shows the four layer construction of the valve which is crucial to allowing the creation of multiple valves on a single block. The manufacturing and assembly methods also meant it was possible to
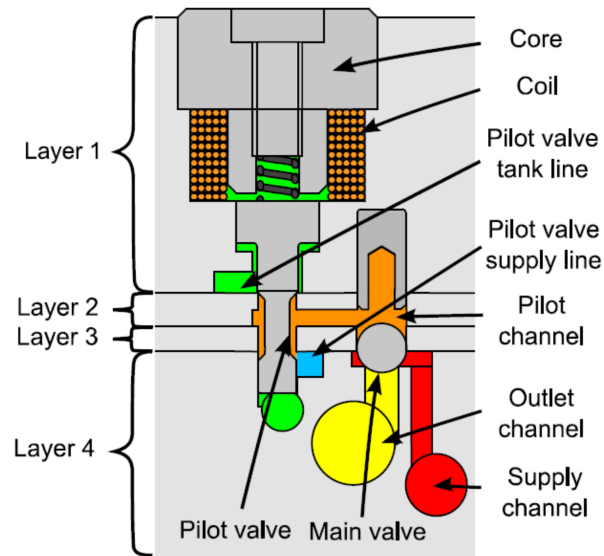
Figure 1-16: Cross section of a fast switching valve showing manufacturing and assembly features (taken from [45])

easily create valves of differing areas, a prototype valve block with four valves with orifice diameters of 2mm, 2.58mm, 2.58mm and 3mm was manufactured. This prototype was found to have leakage of 0.02L/min at 100bar, no figures were provided for the maximum tested pressure of 250bar. The valve was switched from 10% open to 90% closed in around 1ms when the pressure drop across the pilot stage was greater than 20bar. The authors postulated that using this design

it would be possible to create a valve system with a flow capacity of 70L/min at a 35bar pressure drop and a 1.5ms 0-100% rise time with dimensions similar to those of a standard sized (CETOP3) proportional valve.

Lantela *et al* also provide a useful comparison of their valve, some commercial valves and some of the prototypes which are under development.

Table 1.1: Comparison of digital hydraulic valves (modified from [45])

	Valve from [45]	Valve from [41]	Valve from [46]	Valve from [47]	Hydac [45]	Parker [45]
Response Time (ms)	0.9-1.3	1.2-1.5	2	1.5-2	12	3.5
Max. Pressure (bar)	>300	200	21	30	25	35
Flow(L/min@10bar)	4.7	0.3	3.3	15	17	21
Volume (cm^3)	4	2.4	7	88	73	559
Specific Flow $(L/min)/cm^3$	1.18	0.13	0.47	0.17	0.23	0.15

These figures are slightly misleading as all the prototypes, except that discussed in [42], use the volume of only the switching element to calculate the flow density ignoring the need for manifolds, fluid connections and in some cases electrical connections. This obviously severely biases the result. There is also some discrepancy with the reporting of response times. Lantela *et al* use the time from the demand signal reaching the solenoid to when 90% of the steady state pressure is first reached in the volume between main stage and a throttle valve. Uusitalo in [46] used the time from the control signal being sent to the first noticeable change in pressure in an attempt to compensate for the estimated delay time in the pressure sensor of 0.4ms, this approach is sufficiently accurate to measure the order of magnitude of the valves response but not its actual response. In [41] the time from the command signal being sent to the valve being measured as fully open was used. Obviously all these methods are attempting to show the same characteristic but given the scale of the response times the differences between the measurement methods may prove as important as the valves themselves. Thus, whilst informative, the table does not provide a metric by which to judge the valves' performance. It should also be noted that little to no information is available on the controllers used with the valves reported in this section, it is therefore difficult to confirm whether the results published are a good representation of each valves performance or instead of their respectively control strategies. The lack of information would imply however that the control

was not given much consideration, this thesis will demonstrate that significant improvements in performance can be realised by replacing a Zieger-Nichols PID controller with a more carefully designed one.

1.3 In Summary

The case for replacing the metering orifice with digital hydraulics has been laid out, however this case currently is built mainly on theoretical and simulation work rather than the realising of real world systems. To take digital hydraulics forward it is necessary to create valves which are capable of the fast switching times and high flow rates needed in many applications. The general approach to this need is to design small switching units which can be grouped in different ways in order to provide a single solution to all valve requirements. The modular designs presented by Karvonen *et al* , Winkler *et al* and Lantela *et al* show promise in this area but appear to be limited currently in their switching speed, controllability and flow rates respectively. All these valves also rely upon a bang-bang form of actuation rather than position control. A position controlled valve of the form proposed in [43] should offer greater robustness than the alternatives as it will not be undergoing near continuous impacts. It also offers the ability to use a combination of digital (switching) and analogue (throttling) control whether for better dynamics or, in some cases, efficiency However, it requires significantly more complicated control. The discussion of control within the existing digital hydraulic valve literature is all but non-existent but what is said in [17,48] would suggest that control of digital hydraulic valves generally remains quite simplistic. Kudzma *et al* found a lower than desired flow rate and were able to provide only steady state results [43], thus precluding a comparison to the valves mentioned above which also gave dynamic results. This thesis therefore presents the development of valve initially proposed in [43] and details the development of the control strategy for the valve and shows the benefits of exchanging a Zieger-Nichols tuned PID compensator with one created from a more complex design process by providing dynamic results.

1.4 Aims and Objectives

The aim of this thesis is not as grand as the creation of a single standard digital hydraulic valve. Rather, it is the more humble, and achievable, goal of adding to the commonwealth of knowledge from which that valve may one day be created. The design and control of the valve elucidated within this thesis are, however, specifically and intentionally geared towards the intended application of a Switched Inertance Hydraulic System (SIHS) as investigated by [5], [49] and [24]. The implications of this statement will be unpicked in later chapters. To state explicitly the objectives of this research project:

1. To further the development of the valve first proposed in Kudzma *et al* [43].

2. To design a control system for said valve which is capable of meeting the requirements of operating in a SIHS. Namely, that it switch in 1ms or less and minimise flow resistance. These requirements are derived from the literature in Chapter 2.

3. To benchmark the valve's performance against those presented in Lantela *et al.*

4. To apply the valve to an experimental SIHS in order to show its applicability.

1.5 Statement of Originality

In order to meet these objectives this thesis contains original work in both digital hydraulics and control as detailed below:

1. Development of a novel valve design.

2. Novel lag compensation scheme for application to Iterative Learning Control (ILC) systems.

3. Proposal of Stop Learning conditions and proof that they do not contravene asymptotic stability criteria.

4. First application of a linear valve to SIHS which is capable of achieving >100Hz switching frequency.

1.6   Thesis Structure

Having provided a background to the field of digital hydraulics with a focus on the valves needed to make the proposed circuits a reality, the remaining six chapters proceed as follows:

Chapter 2 will detail the design of the valve and the initial modelling work conducted based on this design.

Chapter 3 focuses on the test set-up and steady-state performance of the valve.

Chapter 4 elucidates the development of the feedback controller and shows its ability to meet the 1ms switching time.

Chapter 5 shows the improvements gained by the addition of a feedforward controller and suggests novel additions to Iterative Learning Control.

Chapter 6 discusses what has been learnt from the development of the valve and its control system before presenting some initial results from applying the valve to a SIHS.

Chapter 7 concludes the thesis and lays out suggested further work.

1.7   Published Works

A number of conference papers have been, or will shortly be, presented based on the work within this thesis a list of them can be found in Appendix A.

Chapter 2

Valve Design and Modelling

A specific set of requirements for the valve in a SIHS circuit can be drawn from existing SIHS research, both theoretical and experimental . From these sources, it can be concluded that a switching rate above 100Hz (or settling time $\leq$ 1ms) [49] and minimal flow resistance are the key properties of a valve, with the exact size being dependant upon the intended flow rate. In order to utilise the circuit design seen in [24] it is necessary for the valve, or valve pack, to be able to switch two supply lines to one output. Due to the large number of existing valves able to switch small flow rates (below 10L/min) it was determined that a single, large flow valve presented the best opportunity for furthering knowledge, as well as limiting the number of components needed to realise a reasonable size SIHS circuit and simplifying the manufacturing of a prototype. Details of the first iteration of this valve can be found in Kudzma *et al* [43]. This report will concern itself strictly with results taken from the second iteration. The difference between the iterations is one of accuracy and ease of manufacture along with some minor corrections to tolerances to lessen the expected breakaway force.

2.1 Fast Switching Valve Design

In order to achieve the seemingly paradoxical requirements for fast switching times and low resistance a novel, multi-grooved spool was designed for the main

stage. By having four metering edges for each port, seen in Figure 2-1, an exceptionally high flow gain can be achieved. With a displacement of 0.1mm a flow area of 37.7mm² is opened and thus the design flow of 65L/min at 10bar can be calculated, based on a discharge coefficient (C_d) of 0.6 and density (ρ) of 870kgm^{-3} [43].

0.6mm overlap
0.1mm gap
0.1mm overlap
0.4mm overlap
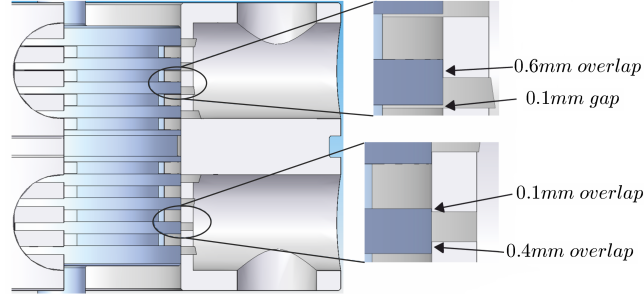
Figure 2-1: Multiple grooves on spool and sleeve (modified from [43])

$$Q_{mainstage} = A \cdot C_d \cdot \sqrt{\frac{2 \cdot \Delta P}{\rho}}$$

$$= 37.7 \times 10^{-6} \cdot 0.6 \cdot \sqrt{\frac{2 \cdot 10 \times 10^5}{870}}$$

$$= 65L/min \tag{2.1}$$

Where A is the flow area and ΔP is the differential pressure across the orifice. The main spool is zero-lapped meaning that at 0mm there is, theoretically, no flow. At +0.1mm the estimated 65L/min at 10bar should flow from HP to common port A and at -0.1mm flow should be from LP to A. This can be seen in Figure 2-2.

The actuation of the spool is achieved through an equal area actuator, the position of which is controlled by a Moog E050-899 servovalve. A sectioned view of the actuation module can be seen in Figure 2-3. Due to the experimental nature of this valve two pressure tappings can be seen. Dynamic pressure sensors were installed into the valve during experimentation for monitoring purposes, whilst the accelerometer mounted on the central rod is used via sensor fusion to provide measurements for the controller elucidated in later chapters. In contrast to the
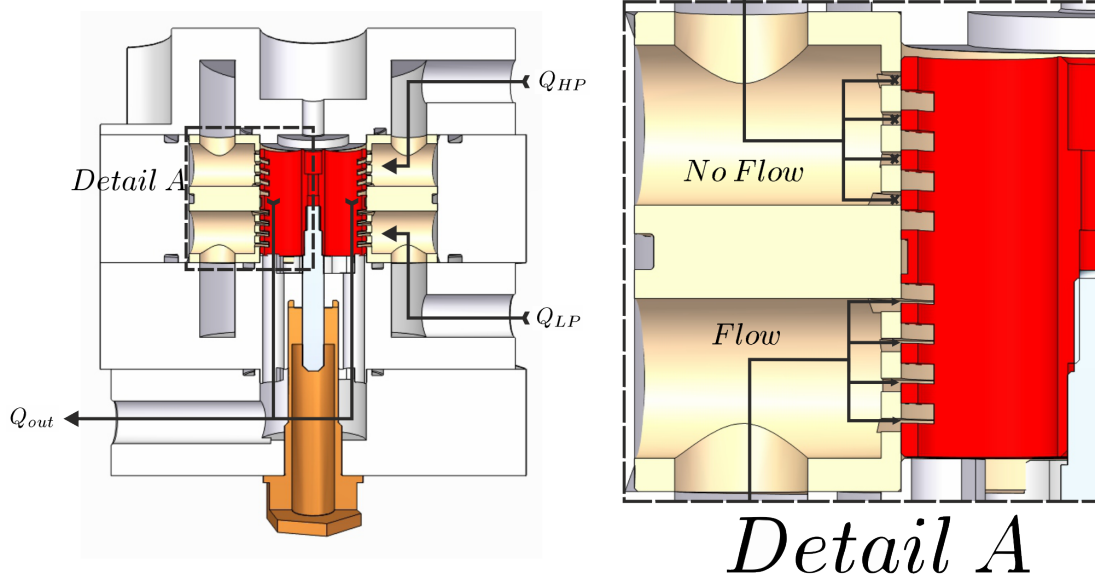
Figure 2-2: Flow paths through the valves main stage
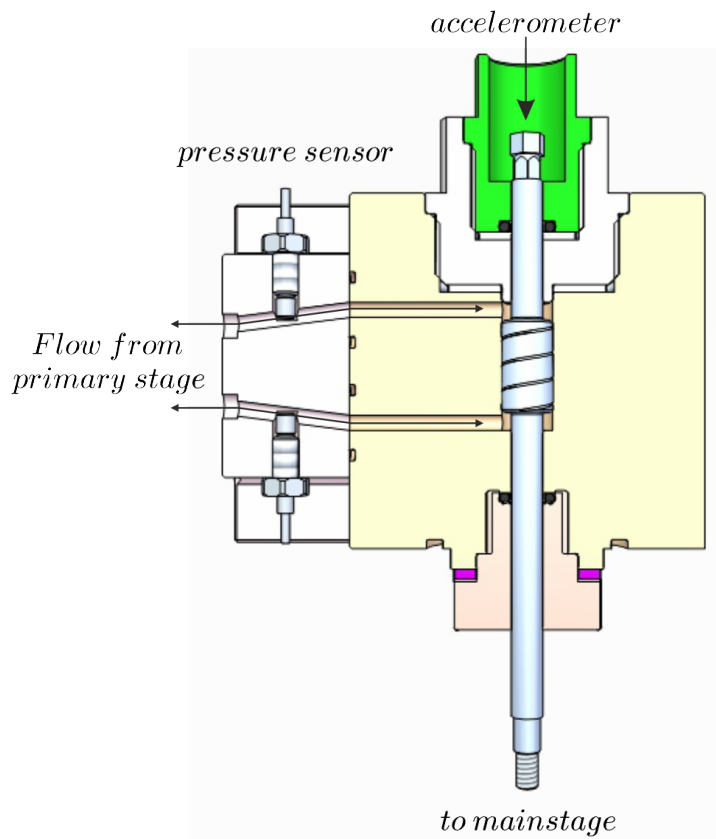
Figure 2-3: Sectional view of actuation module

majority of digital hydraulic valves under development [41] [42] [45], endstops are not utilised for the purpose of fast switching. Instead position control is used which offers multiple advantages. Namely, fewer vibrations, less stress on components and the ability to use the same valve as either a switching element or proportional control valve. This is advantageous not just for robustness but also because at the extremes of switching ratios proportional control proves to be more efficient [30]. Conversely, there is a need for more intricate control, a topic covered in depth in Chapters 4 and 5. A picture of the finished valve can be seen in Figure 2-4 and a complete set of technical drawings found in Appendix B.

Figure 2-4: Picture of assembled valve

It can be seen that the main body of the valve is made up of four machined rounds of steel. This is one of the design compromises made in order to accommodate the need to prototype manufacture the valve. As well as making the valve considerably larger than need be, this introduced a risk of misalignment between the various components and particularly between the main and actuation stages. Bosses were used to maintain alignment between these various pieces

with bolts providing the fastenings. This risk of misalignment coupled with the tight tolerances needed in order to stop leakage between the two stages results in multiple pinch points at which any misalignment could result in bending or damage to the central shaft. These sites are indicated in Figure 2-5. Two other
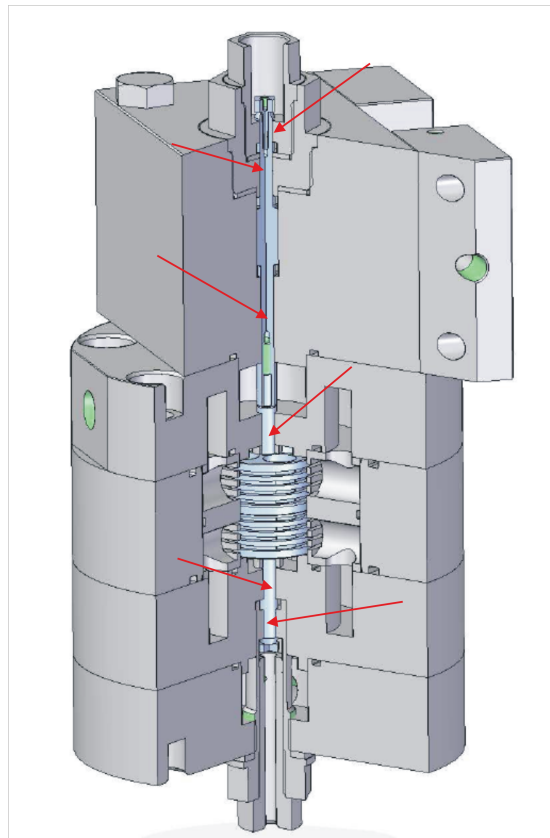
Figure 2-5: Sites of possible interference from misalignment

compromises were made in order to prototype the valve. Firstly, all seals were made with o-rings, except across the piston in the actuation stage which was a gap seal. These are well suited to providing static seals - the majority required - but are less well suited to providing dynamic seals on the reciprocating piston rod. However, due to the very small expected displacements (fractions of a millimetre), the hope was that the o-rings would be able to deform sufficiently that the piston rod would not need to break away, as this would cause control and longevity issues. Ideally these o-rings would be replaced with PTFE seals designed for sliding contacts, such as those manufactured by Parker [50], but due to the minimum batch size this was not tenable for the prototype. Finally the

Moog servovalve used for the primary stage has a flow of 29.5L/min at 69bar, less than half the intended operating pressure, which is significantly larger than required based on half the switching time proposed by De Negri *et al* [49]:

$$
\begin{aligned}
max(Q_{actuation}) &= \frac{Displacment}{Switching\ Period} \cdot Area \\
&= \frac{0.2 \times 10^{-3}}{0.5 \times 10^{-3}} \cdot 5.02 \times 10^{-5} \\
&= 2 \times 10^{-5} m^3 s^{-1} \\
&= 1.2 L/min
\end{aligned}
\tag{2.2}
$$

With a smaller valve, the large flow rate could be exchanged for an increased bandwidth. It can be seen from Figure 2-6 that it would be sensible, with the current pilot valve, to band limit control signals to less than 1000Hz in order to avoid the resonant peak. In order to achieve good tracking it is beneficial to have the closed loop bandwidth of a system an order of magnitude higher than the plant bandwidth. This would limit the valve to switching at around 100Hz, or around 1ms (based on switching time being 10% of cycle time).
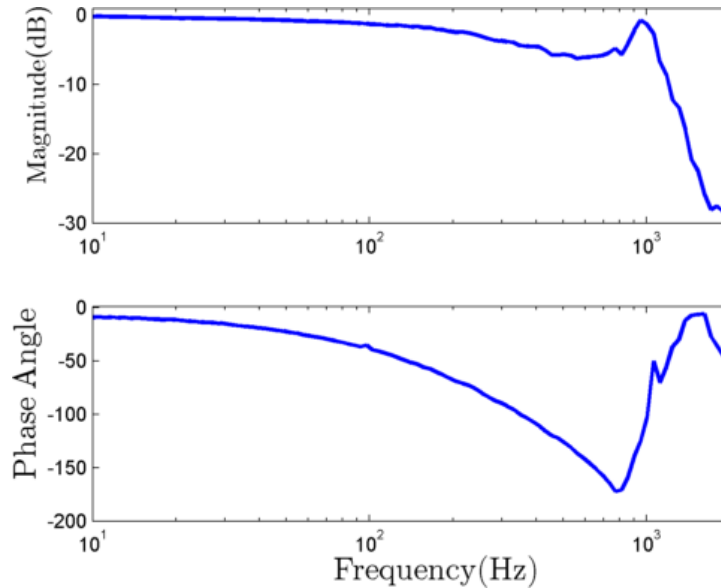
Figure 2-6: Frequency response of Moog pilot valve

2.2 Modelling of Fast Switching Valve

The modelling of an SIHS is well documented in [49] and [24]. This means it is only necessary to model the position of the main spool. Existing models can then be utilised for the SIHS behaviour with just some basic design parameters of the main stage. For simplicity, therefore, the main stage will be considered to be a simple mass as it is pressure balanced. The valve can therefore be considered to be analogous to the simple hydraulic circuit in Figure 2-7. Assuming a fixed
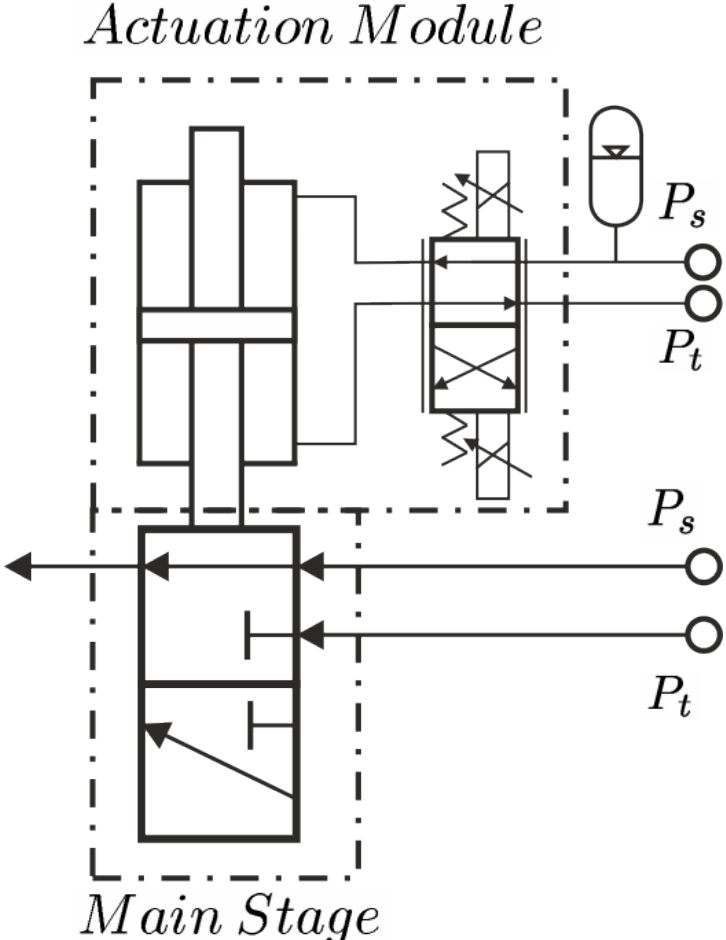
Figure 2-7: Hydraulic circuit representation of valve

supply flow and pressure to the actuation module then the relatively simple model relating a normalised pilot stage input signal, $0 \leq i \leq 1$, to valve position, x,

seen in Equation 2.3, can be derived:

$$y = \frac{\omega_n^2}{s^2 + 2 \cdot \omega_n \cdot \zeta \cdot s + \omega_n^2} \cdot i$$

$$Q_{actuation} = Q_s \cdot y$$

$$x = \int \frac{Q_{actuation}}{A_p} dt$$

$$While$$

$$P_s{\cdot}A_p - P_t \cdot A_p > F_L$$

$$Where$$

$$F_l = M \cdot \ddot{x} + Friction \tag{2.3}$$

Where y is the displacement of the pilot stage, ω_n is its natural frequency, ζ its damping ratio and i is the normalised control input such that 1 is fully open and 0 is fully closed. x the displacement of the main spool. P_s and P_t are the pressure at the supply and tank sides of the pilot valve respectively, A_p is the piston area of the second stage and F_L is the load force at the second stage.

The natural frequency and damping of the pilot stage can be found from the data supplied by the manufacturer (Appendix C). For this simple model they were estimated to be 364Hz and 1 respectively. A comparison of this and the measured frequency response of the valve can be seen in Figure 2-8.

$$y = \frac{(364 \cdot 2\pi)^2}{s^2 + 2 \cdot 364 \cdot 2\pi \cdot 1 \cdot s + (364 \cdot 2\pi)^2} \cdot i \tag{2.4}$$

It can be seen that the second order model selected provides a reasonable approximation of the valve's behaviour at frequencies below 700Hz but does not take into account higher order harmonics. However, as it is intended to avoid exciting the resonant mode in the valve, at 1000Hz, this inaccuracy is deemed a reasonable trade off for maintaining the simplicity of the model.

Due to the large number of difficult to quantify variables, the estimation of friction forces present within the valve is not trivial. Such variables include cleanliness of oil, lubrication provided by oil, clearances, surface finish and the alignment along the central shaft. However, it is possible to accurately calculate
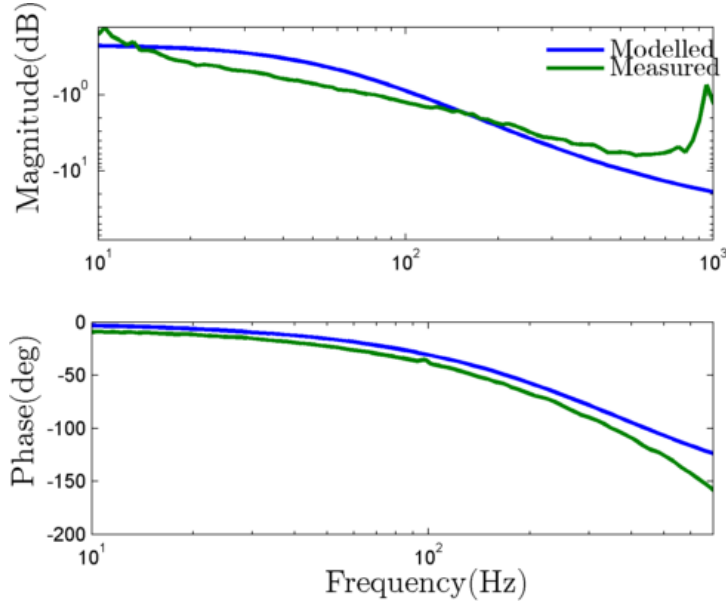
Figure 2-8: Comparison of Moog e501 measured frequency response ($\frac{y}{i}$) and model

the force due to acceleration by first calculating the mass of the piston spool and attached components, Table 2.1. Given the fast switching nature of the valve the inertial forces should dominate, assuming there isn't a serious misalignment. Therefore, initially F_L will be equal to inertial forces plus a simple viscous friction model:

$$F = \lambda \cdot \dot{x}$$

$$where \ \lambda = \frac{A_{spool} \cdot \mu}{x_{gap}} \qquad (2.5)$$

$$(2.6)$$

A_{spool} is the surface area of the spool ($\pi d \cdot L = 0.03 \cdot \pi \cdot 0.012 = 0.0011m^2$) where d is the spool diameter and L is the contact length, found by subtracting the length of the grooves from the total spool length. μ is the dynamic viscosity of the hydraulic oil taken to be $\nu \cdot \rho = 55 \times 10^{-6} \cdot 870 = 0.048$ and x_{gap} is the clearance between the spool and sleeve assumed to be 10μm. This gives an estimated λ value of 5.43Ns/m. The numbers used above are for the case where the valve is in the zero position, as the valve opens L will reduce by the valve opening, this is accounted for in the model. Both soft and hard cushions are included at

34

the extreme ends of the actuator to aid the solver. However, these are located beyond the expected operating envelope and so shouldn't unduly affect the valve control. The model can be further improved by including the expected leakages
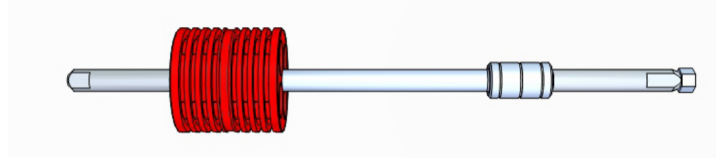
Figure 2-9: Components on central shaft

Table 2.1: Masses of components on central shaft

No.	Part	Mass (g)
1	Accelerometer	2
2	Piston	26
3	Spool	81
4	Spool Rod	9
	Total	118

across the piston. These can be calculated from the maximum clearance, as in Equation 2.7.

$$Q_{leak} = \frac{\pi d \cdot \Delta P \cdot x_{gap}^3}{12 \cdot \mu \cdot L} \tag{2.7}$$

Instead of the nominal viscosity value used to calculate friction the minimum viscosity value of 32cSt was used to find the maximum expected leakage. The length of overlap in this equation cannot be lumped as in the friction equation, instead the leakage for each overlap between spool and sleeve must be calculated then summed. As we are concerned with the fully open case rather than the closed case used above there are four overlaps of 0.1mm, three of 0.4mm and one of 1.15mm. This gives a total leakage of 0.82L/min when there is 10bar pressure drop across the valve. All dimensions used for this calculation can be found on the component drawings located in Appendix B. The leakage forms a very small percentage of the expected flow rate, Equation 2.2. There maybe a slight increase in leakage in the actual valve due to manufacturing defects but it can still be seen to not be a defining factor in the valve's response. There is the possibility of a second leakage path as shown in Figure 2-10. As mentioned in Section 2.1 it is hoped that the o-ring seal will be sufficient as the reciprocating motion is quite
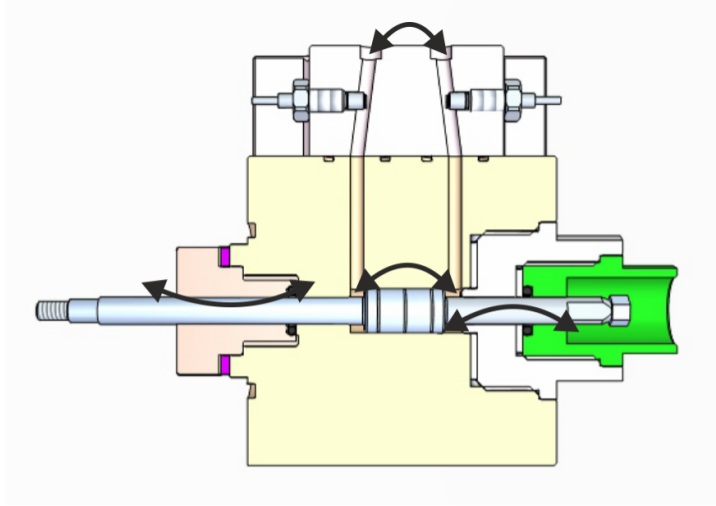
Figure 2-10: Leakage paths in actuation module

a low magnitude. However, if this is not the case then the leakage past this seal may have a noticeable effect on the valve's performance.

Thus far the model has been built around hydrostatics, meaning that it has ignored the effects of compressibility, pressure waves and other dynamic effects. For many hydraulic systems this is acceptable. However, due to the high frequency switching, these effects are likely to have a noticeable effect on the valve's response. In order to model these effects it is necessary to utilise the bulk modulus of the fluid to link fluid flow and pressure. This was achieved using the approach used in [51]. A block digram representation of this dynamic model is shown in Figure 2-11. Once the size of the pilot valve's opening has been determined it
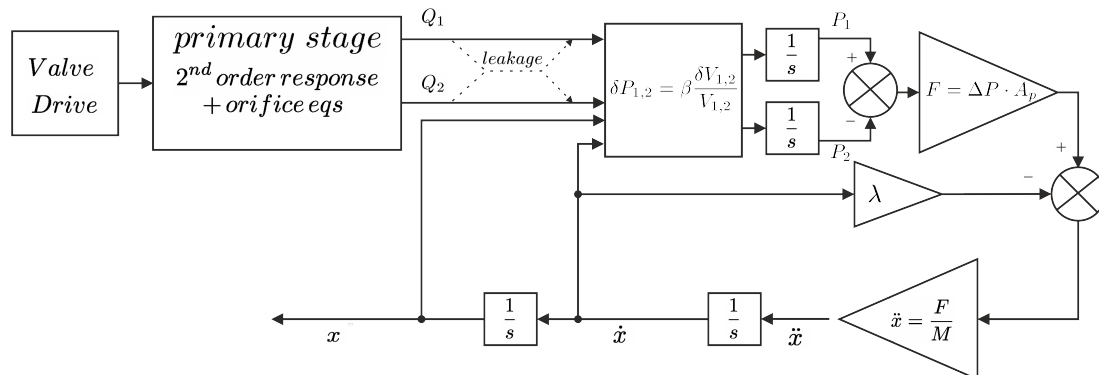
Figure 2-11: Block diagram of actuation model

can be used to calculate the flow into or out of the two chambers of the second

36

stage using the orifice equation.

$$Q = K_v \sqrt{\frac{P_1 - P_2}{\rho}} \cdot y \qquad (2.8)$$

Where K_v is a constant which includes the orifice discharge coefficient and circumference and P_1 and P_2 are the pressures either side of the orifice. This flow can, in turn, be converted into force by considering the bulk modulus of the fluid and the piston area of the actuator as demonstrated in Equation 2.9 below.

$$\beta = -V_{1,2} \frac{\delta P_{1,2}}{\delta V_{1,2}}$$

$$\delta P_{1,2} = \beta \frac{\delta V_{1,2}}{V_{1,2}}$$

$$\Delta P = \beta \int \frac{\delta V_1}{V_1} dt - \beta \int \frac{\delta V_2}{V_2} dt$$

$$where \quad \delta V_{1,2} = Q_{1,2} - A_p \cdot \pm \dot{x}$$

$$F = \Delta P \cdot A_p \qquad (2.9)$$

To make the model more accurate the model of viscous friction discussed above was added along with a simple Coulomb friction.

Having calculated the force provided by the first two stages it is a relatively trivial exercise to calculate the position of the valve. The equations required can be found in Equation 2.10 below. The position and velocity responses, to an impulse, of the resulting model can then be seen in Figure 2-12 and 2-13.

$$\ddot{x} = \frac{F}{M}$$

$$\dot{x} = \int \ddot{x} \, dt$$

$$x = \int \dot{x} \, dt \qquad (2.10)$$

The integrative action is clear from the position response whilst the velocity response gives an indication of the minimum switching time expected from the valve; around 1ms, in keeping with the parameters set out by DeNegri for use with a SIHS [49]. Due to the geometry of the valve overshoot does not affect

37
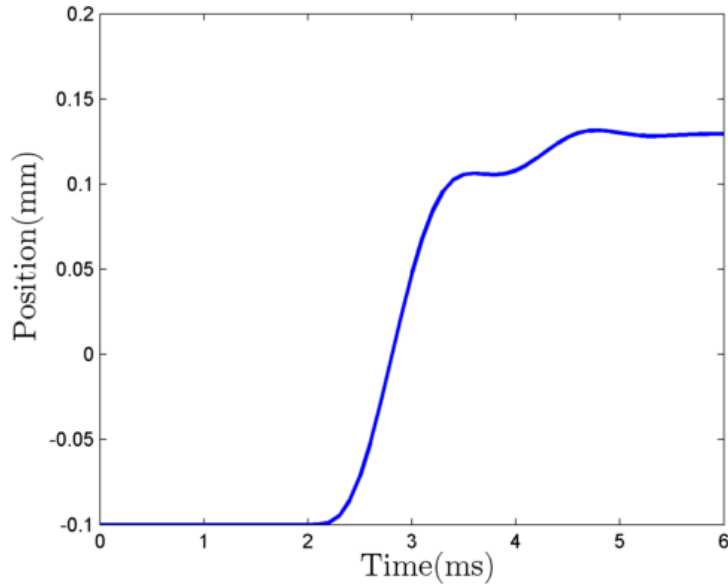
Figure 2-12: Position response of valve model to impulse signal

valve performance as long as it remains below ±0.3mm. Therefore, instead of the more commonly used *rise* time metric, a *switching* time metric will be used in this report. This is defined as the time taken for the valve to transition from one 'fully' open position to another. ±0.1mm for HP and LP ports respectively. Because of this settling time is of no import except as an indication of the controller's stability. Similarly, overshoot is not treated as a parameter but rather as a binary acceptance test. Any overshoot below 0.15mm is acceptable, to allow for tolerancing on the spool, and any above that not so. A simple PID controller was added to the valve model and tuned empirically using Zieger-Nichols [52]. Figure 2-14 shows the model's response to a range of square wave references. It can be seen that by 100Hz the valve's response is no longer fast enough with a switching time of around 2ms - 40% of the whole cycle time. Given the simplicity and unoptimised nature of the control used this is not surprising. However, it was decided to proceed with validating the model experimentally before detailed controller design was undertaken.
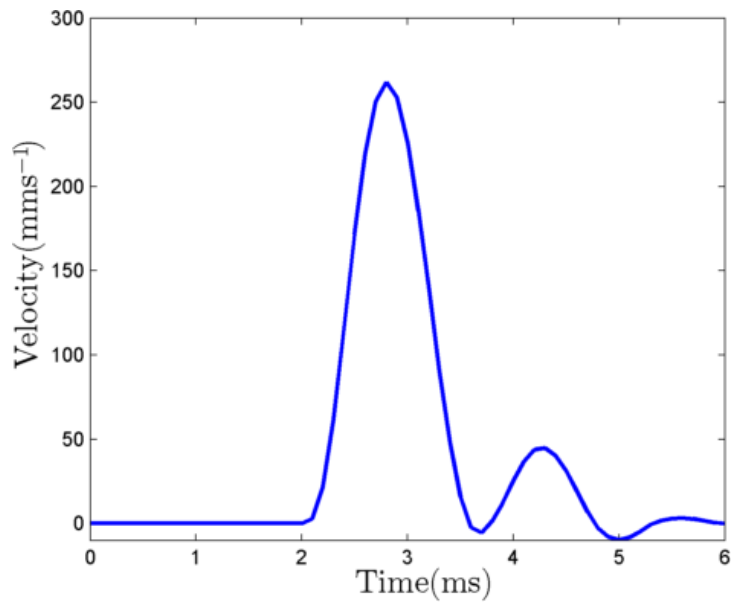
Figure 2-13: Velocity response of valve model to impulse signal
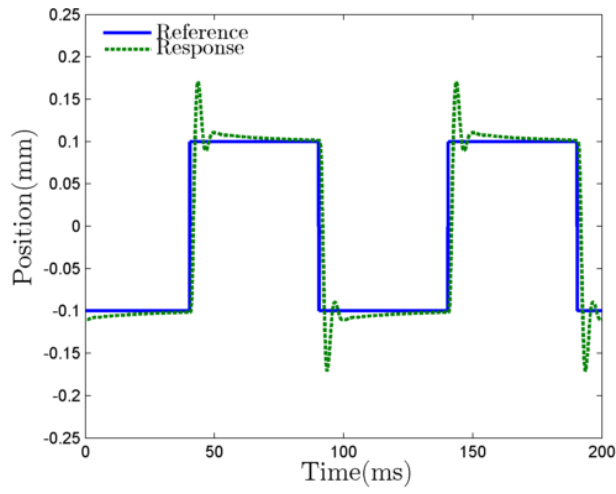
(a) 10Hz
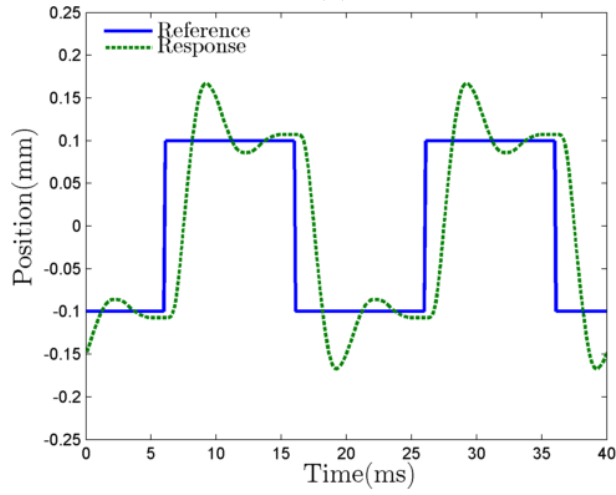
(b) 50Hz
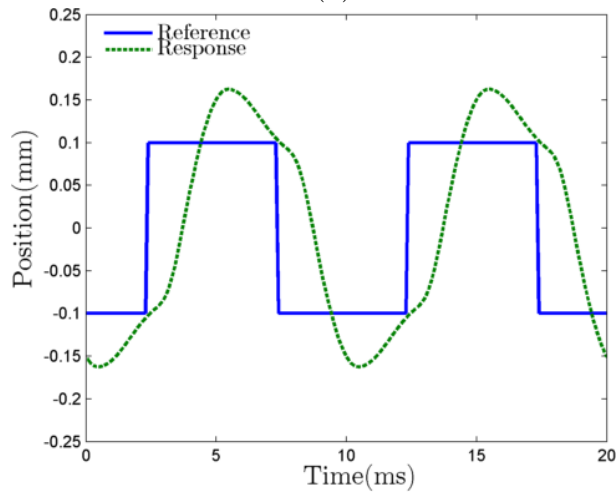
(c) 100Hz

Figure 2-14: Postion response of valve model under PID control

40

Chapter 3

Experimental Set-up

The test set-up used with the fast switching valve consists of two separate hydraulic circuits. One is the main stage, which treats the valve as a simple block. The second is the actuation stage of the valve, wherein the main spool is considered a simple mass. Both of these circuits can be seen in Figure 3-1.

Whilst the hydraulic circuits of the different stages were handled separately, the instrumentation was all processed using an xPC system. This enabled a maximum sample rate of 100kHz. However, due to hardware limitations and the number of sensors used, this was reduced to 10kHz in practice. Given the intended switching frequencies, tens and hundreds of Hz, this was deemed sufficient not just for monitoring purposes but also for the control as given the intended switching time of 1ms a sample rate of 10kHz provides 10 samples during each switching event.

3.1   Instrumentation

As mentioned above, signal processing, data logging and control were all managed via the MathWorks xPC platform. A National Instruments PCI6220 card, along with various peripheral hardware such as isolation amplifiers and anti-aliasing filters, was used to interface with the platform. There were four separate types of sensor - pressure sensors, flow meters, positions sensors and accelerometers - used in the test rig. An overview of each is given below.
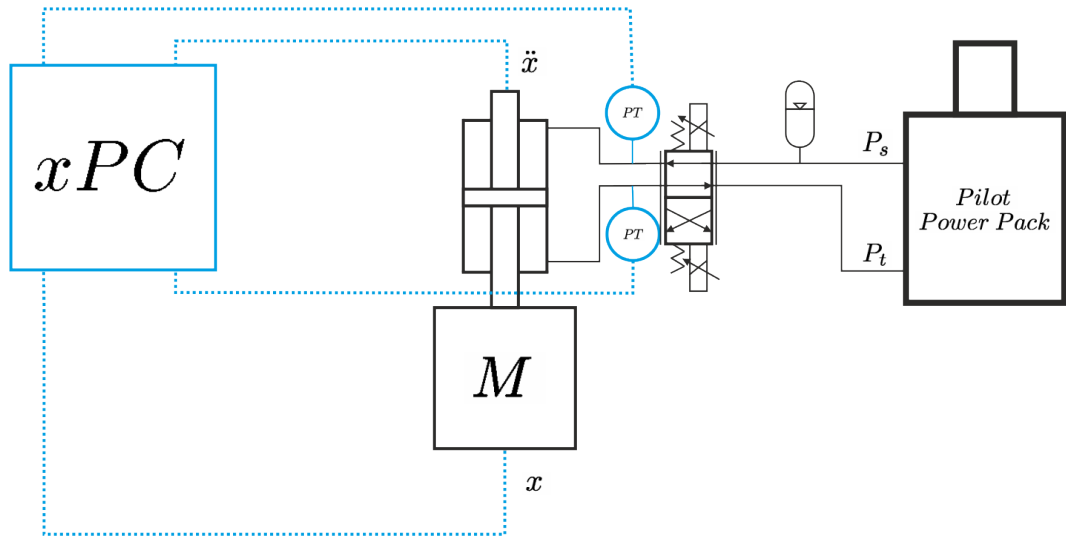
(a) Diagram of hydraulic circuit for pilot stage
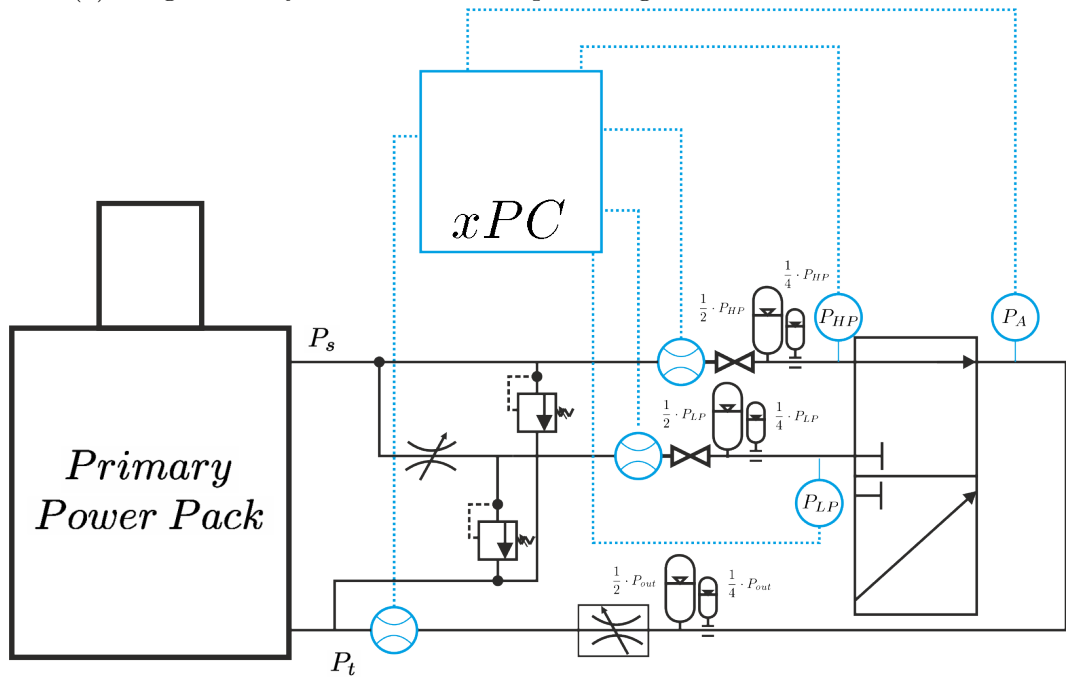
(b) Diagram of hydraulic circuit for main stage

Figure 3-1: Experimental test set-up

3.1.1   Pressure Sensors

The majority of the pressure sensors used on the test rig were XP5 miniature dynamic sensors, from Measurement Specialities, and their predecessor the EB100. These were selected for their small size and high bandwidth of measurement. It was important that they could be placed as close as possible to the valve's ports without unduly increasing the dead volume between the ports and the accumulator, for the sake of SIHS operation. Wave effects are very important to the operation of an SIHS and, thus, it was important to be able to log pressure changes within a switching cycle rather than just average pressure. It was found during testing that the zero measurement of these dynamic sensors was fairly sensitive to temperature, especially the FP5's. Therefore a single static pressure sensor was placed in the system to allow for calibration and checking. Some key specifications of the two sensors can be found in Table 3.1.

Table 3.1: Properties of pressure sensors

Specification	XP5	EB100
Fixing	M5 stud	M5 stud
Range	1-350bar	2-350bar
Linearity	0.25% F.S.	1% F.S.
Bandwidth	3kHz	1kHz

3.1.2   Flow Meters

As with the pressure sensors, the dynamics of the flow were more important in the SIHS experiments than in most hydraulic tests. Of particular importance was the ability to measure flow bidirectionally as one of the expected losses was flow from the HP to LP, either as a result of leakage or back flow from the inertance tube due to insufficient inertance or slow switching. It was also important to be able to measure flow over a very large range, 0 - 60L/min, within the whole system. Fortunately, this can be broken down into slightly different specifications for the LP, HP and outlet. If external leakage is assumed to be negligible then the flow from HP and LP can each be calculated by subtracting the flow from the opposite inlet from the outlet. This means that as long as the combined

43

range of the two flow meters covers the operating range, with some overlap, each individual flow meter is not required to do so. The range can also be modified slightly for the outlet flow meter as it will only see the outflow of the inertance tube. A minimum flow rate of 6L/min can be set for this, so a sensor need only measure from 6-60L/min. It also has no need to be bi+−+directional. The specification of the three flow meters can be found in Table 3.2.

Table 3.2: Properties of flow sensors

Specification	HP port	LP port	Outlet
Make	AW Gear Meters	AW Gear Meters	Hydac
Model	JVS-60KG	JVS-20KG	EV3100
Measuring element	Gears	Gears	Impeller
Range (L/min)	0.2-90	0.01-9	6-60
Bidirectional	Yes	Yes	No
Max. pressure (bar)	344	344	400

3.1.3   Kinematic Sensors

A theme throughout this chapter has been the high bandwidth that both valve control and SIHS measurement require. This is, perhaps, most imperative when it comes to the position signal due to its usage in feedback. The position sensor available for testing was an inductive proximity sensor, a Keyence EX-110, for which no information regarding frequency response was available. However, the documentation does mention a low pass filter, the cut off point of which which must be at 1kHz or below, suggesting the sensor's limit exists around this point. Therefore, in order to extend the signal's bandwidth, information from an accelerometer, in this case a Kistler 8730AE500, was utilised. How this was achieved is discussed in detail in Section 3.2. The accelerometer was mounted on top of the central shaft, while the position sensor was located at the bottom of the valve and measured the distance from the bottom of the spool rod to the sensor head. A diagram showing the locations of the sensors within the valve can be found in Figure 3-2.
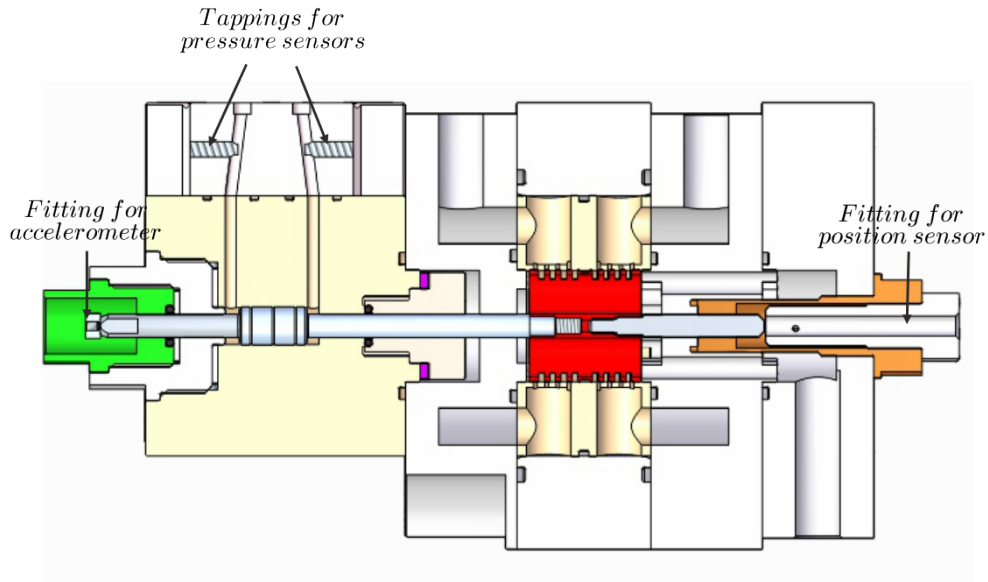
Figure 3-2: Locations of sensors within the valve

Table 3.3: Properties of position and acceleration sensors

Specification	Keyence EX-110	Kistler 8730AE500
Fixing	held by grubscrew	M1 stud
Range	0 to 2mm	-1000 to 1000g
Linearity	0.3% F.S.	1% F.S.
Freq. response	0-1kHz (assumed)	2Hz-7kHz

3.2 Sensor Fusion

The idea of integrating the measurements from multiple different sensors in order to take of advantage of their various benefits, or make-up for their short comings is not new. Indeed, an example can be found in most pockets - smart phone navigation software often makes use of GPS signals and internal accelerometers to provide location and direction information. A particular application of this technique, discussed in [53], is the fusing of information of data from a Linear Variable Differential Transformer (LVDT) and accelerometer to provide a better estimation of acceleration and position than the individual sensors could, as well as a good estimation of velocity. The filters used to combine the signals were based on Butterworth filters and were designed to be complementary i.e. at all frequencies their magnitudes sum to unity. This was further developed in [54] by replacing the Butterworth filters with optimal filters. This showed a marked

reduction in peak error but requires knowledge of the sensors' limitations. With regard to fusing displacement and acceleration signals, the most important parameter is the frequency at which the two signals are crossed over. It is important that the cross over occurs in an area where both signals are accurate and in phase with each other. Due to the lack of data provided with the sensors a simple experiment was undertaken in order to determine where this cross over should be. With both sensors mounted on the valve a filtered chirp signal between 0 and 500Hz was sent directly to the pilot stage after a simple PI controller had been used to centre the piston. This signal was filtered in order to avoid saturation of the second stage. The acceleration signal was then integrated twice and the magnitude and phase plotted on the same graph as the position signal, Figure 3-3. It can be seen that between 40Hz and 80Hz the two signals have good agreement
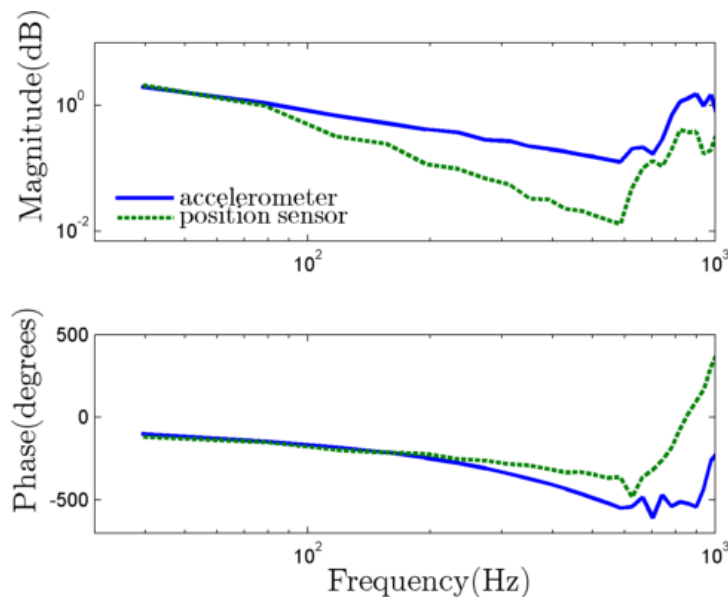
Figure 3-3: Frequency response of position and acceleration sensors

in both phase and magnitude. This agreement is closest at 50Hz with the two magnitude traces crossing over. Figure 3-4 shows the position measured by each sensors after being highpass filtered at 5Hz. With the exception of a slight offset it can be seen that the two signals are in very good agreement. This offset is not of concern as it is a low frequency phenomenon and so will be attenuated by the complementary filters. It does, however, highlight that the acceleration signal can be improved by using a twice differentiated position crossed over at 50Hz. It
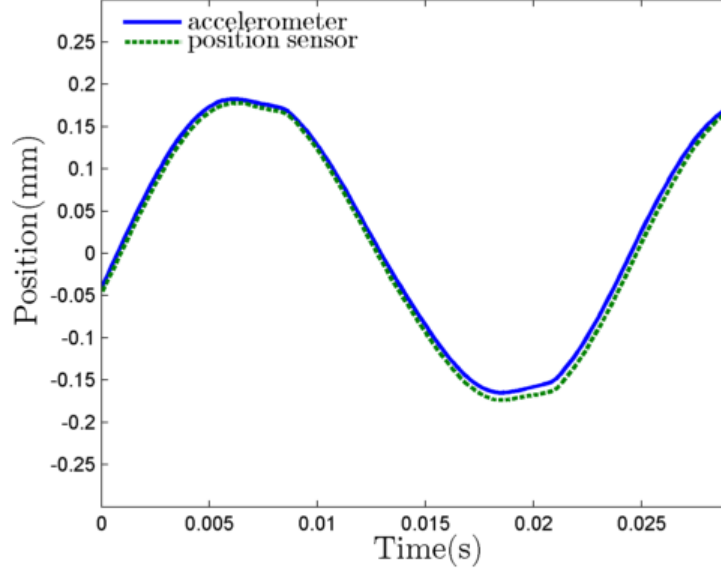
Figure 3-4: Position estimation at 50Hz

is also possible to use the same methodology to estimate velocity by integrating acceleration and differentiating position. The collection of H_∞ optimal filters used to achieve this were designed based using the frequency response data and the method in [54] and can be seen in Equations 3.1 - 3.5.

$$LPF = \frac{4.74 \times 10^{-4}s^2 + 3.09 \times 10^{-2}s + 1}{3.26 \times 10^{-13}s^5 + 9.98 \times 10^{-10}s^4 + 1.51 \times 10^{-6}s^3 + 4.74 \times 10^{-4}s^2 + 3.09 \times 10^{-2}s + 1} \tag{3.1}$$

$$HPF = \frac{3.26 \times 10^{-13}s^5 + 9.98 \times 10^{-10}s^4 + 1.51 \times 10^{-6}s^3}{3.26 \times 10^{-13}s^5 + 9.98 \times 10^{-10}s^4 + 1.51 \times 10^{-6}s^3 + 4.74 \times 10^{-4}s^2 + 3.09 \times 10^{-2}s + 1} \tag{3.2}$$

$$x_f = LPF \cdot x + HPF \cdot \frac{1}{s^2} \cdot \ddot{x} \tag{3.3}$$

$$\dot{x}_f = LPF \cdot s \cdot x + HPF \cdot \frac{1}{s} \cdot \ddot{x} \tag{3.4}$$

$$\ddot{x}_f = LPF \cdot s^2 \cdot x + HPF \cdot \ddot{x} \tag{3.5}$$

Figure 3-5 shows the magnitude and phase of the complementary filters without any extra integrators or differentiators added.

47
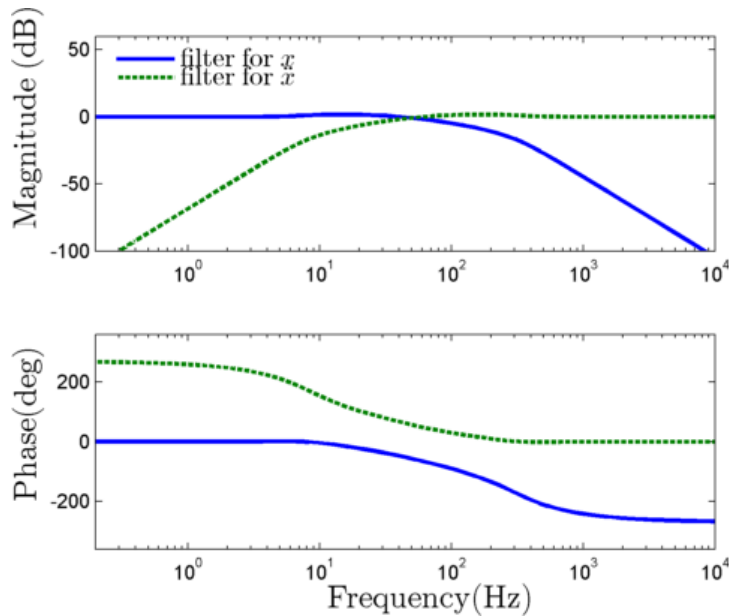
Figure 3-5: Bode plots of complementary filters

3.3 Steady State Tests

As the position sensor is secured by means of a grub screw there is no simple means of determining the spool's zero position. For the purpose of testing the sensors, therefore, an arbitrary zero was chosen (at the centre of the stroke) however this is not suitable in the long term. Figure 3-6 shows the spool open to HP, closed (the zero position) and open to LP. In order to find this zero position, a sweep was made from one extreme position to the other, firstly with HP open and LP closed and then with LP open and HP closed. By plotting the outlet flow of these experiments against each other, Figure 3-7, it is possible to see where the valve switches from HP to LP - the zero position. All flow tests were conducted with oil at 20℃.

It can be seen that maximum flow from HP occurs around 0.5mm and from LP at 0.3mm. Therefore 0.4mm was determined to be the zero point and the port openings of $\pm$ 0.1mm validated, though it can be seen that there is a slight increase in flow past the 0.1mm port openings. The difference in flow rate between the two ports is likely to due to a difference in pressure between LP and HP as only a cursory effort was made to ensure both were at 20bar for the tests. By repeating this test for a third time, with both LP and HP open but outlet

48
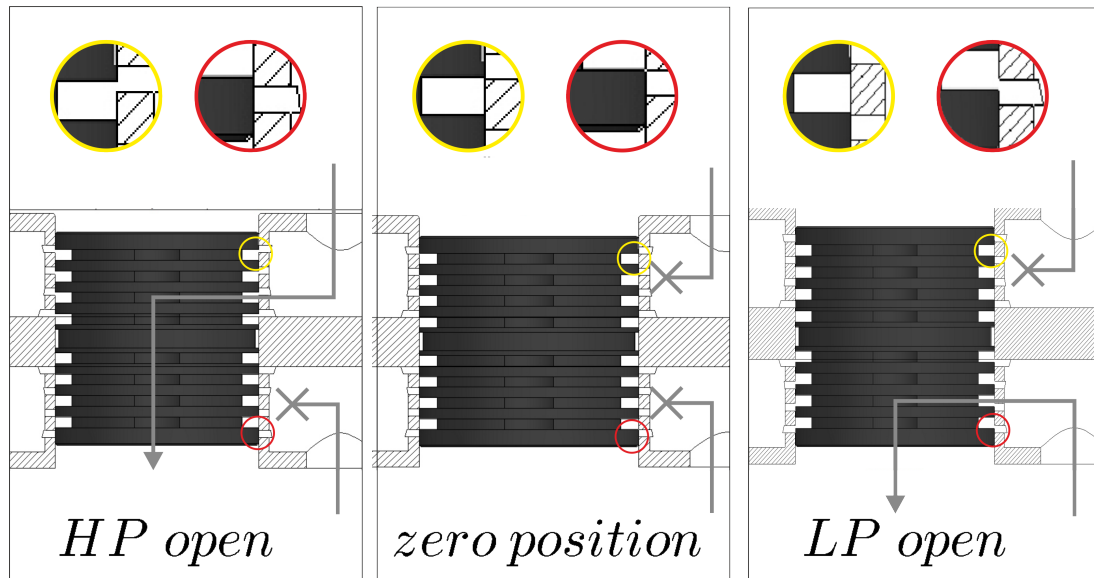
Figure 3-6: Spool locations

blocked, it is possible to investigate leakage between the two ports. Figure 3-8 shows these results when there is a 50bar pressure difference between HP and LP. There is a clear hysteresis effect, it is believed that this is a result of the inertia in the flow meter and accumulators recharging rather than a real effect. It is therefore likely that the real leakage can be found from the internal curve with a small leakage at -0.1mm and 0.1mm and maximum leakage in the zero position as expected. This suggests that the spool is actually slightly overlapped rather than zerolapped. However, given the relative size of the anticipated flow rate (65L/min at 10bar HP > A) and the leakage ($\approx$1L/min at 50bar HP > LP) the choice of zero position and port openings seems valid. It should also be noted that the opening and closing of the ports was conducted over 5s to ensure the flow meters could respond sufficiently whereas the anticipated switching time is 1ms suggesting that leakage as a result of switching will be minimal.

In order to quantify the effect that manufacturing had upon the resistance of the valve, a series of tests were conducted at different opening positions. With the HP port open to A and LP closed, the pressure at HP was increased until a 10bar pressure drop was measured across the valve and then the output flow was plotted against pressure drop. The result can be seen in Figure 3-9. The flow rate achieved through the valve at 10bar is lower than designed, 50L/min as opposed to 65L/min. However, this will increase as temperature increases giving

49
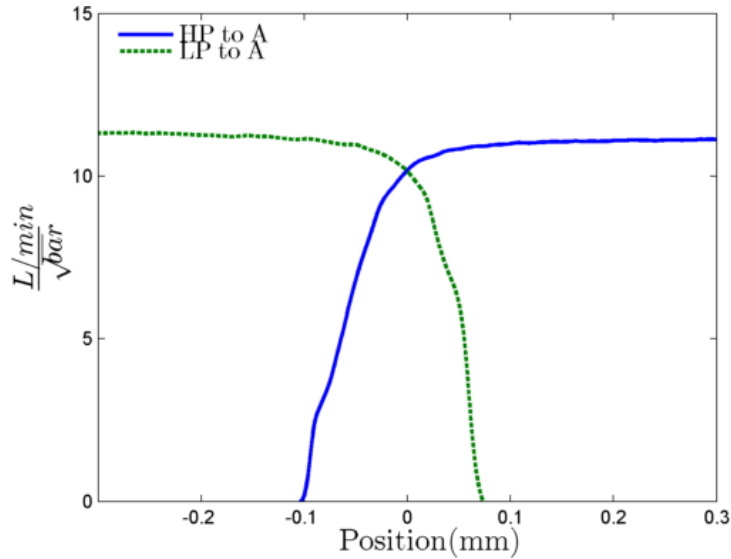
Figure 3-7: Outlet flow against position

more than enough flow rate to prove the SIHS concept and still providing a larger flow than any other known digital hydraulic valve.

3.4   Model Validation

In order to validate the model discussed in Chapter 2 the Ziegler-Nichols (Z-N) design method, used to form the PID controller for the model, was also applied to the controller for the valve. This resulted in different gains to the controller but ensured the stability and suitability of the controller as opposed to copying the gains from the model. The differences in these gains imply that the model and valve are not in complete agreement. It can be seen, however, from the traces in Figures 3-10a to 4-7b that there is a good modelling of the underlying behaviour, with the actual valve appearing to have less damping than the model but otherwise similar dynamic response, though a difference in steady state results. As predicted by the model, the Z-N PID controller is not capable of providing adequate control at 100Hz. Given that the largest control signal was 6% of the pilot stage's full scale output, this is not surprising. The switching time of the valve is 1.5ms, similar to that predicted in the model though as noted above there is less damping in the valve than the model. One possible explanation of this is
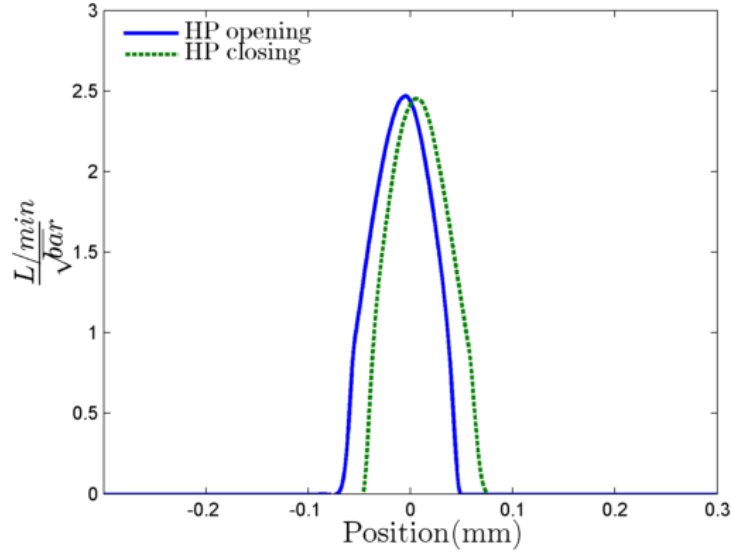
Figure 3-8: Leakage from HP to LP

that the bulk modulus used in the model is likely to be higher than in reality as it doesn't account for entrained air. The model used to represent the pilot stage was also deliberately kept simple and may be, as a result, over estimating the pilot valve's damping. In order to improve the quality of the model, therefore, Simulink's parameter optimisation tool was used to run a non-linear least squares algorithm which sought to minimise the error between the measured and modeled position. More specifically a constrained Trust-Region-Reflective algorithm was used which is based upon the work in [55, 56]. The parameters that were optimised, along with their optimisation ranges and final optimised values, can be seen in Table 3.4. If these parameters are used in the model then a better fit can

Table 3.4: Parameters used in model optimisation

Parameter	Lower Limit	Nominal	Upper Limit	Final Value
Bulk Modulus (GPa)	0.7	0.9	0.9	0.72
Mass of shaft (g)	100	112	120	112
ω_n (Hz)	300	361	400	343
ζ	0.8	1.1	1.1	0.8
Coulomb friction (N)	0	12	20	0
Coefficient of viscous friction	0.07	0.12	0.17	0.09
Input Delay (ms)	0	0	0.2	0.01

be found between the model and valve responses. However, it can be seen from examining the velocity traces, Figure 3-11, that the valve exhibits some higher

51
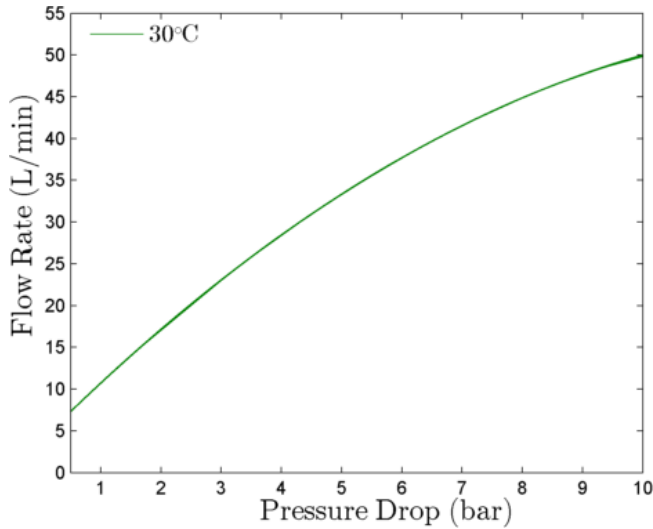
Figure 3-9: Flow against pressure drop for different valve openings

order behaviour that is not accounted for within the valve model.

Therefore a higher order model of the pilot stage valve was used in an attempt to model these effects. The fit of this model in comparison to the second order model can be seen in Figure 3-12. The optimisation procedure was then repeated giving the final values shown in Table 3.5 and response shown in Figures 3-13a. It can be seen that the velocity trace is still missing some high frequency

Table 3.5: Parameters used in second model optimisation

Parameter	Lower Limit	Nominal	Upper Limit	Final Value
Bulk Modulus (GPa)	0.7	0.9	0.9	0.81
Mass of shaft (g)	101	112	123	106.5
Coulomb friction (N)	0	12	24	0
Coefficient of viscous friction	0.07	0.12	0.17	0.06
Input Delay (ms)	0	0	0.2	

information captured on the valve but does a better job of fitting the overall trend of the velocity, giving a good fit between the measured and modelled positions, though the model slightly overestimates switching time and there appears to be an unmodelled leakage or some other effect which stops the valve maintaining a steady state position. Given the focus on achieving a suitable switching response it was deemed that these shortcomings should not impede a successful controller design.
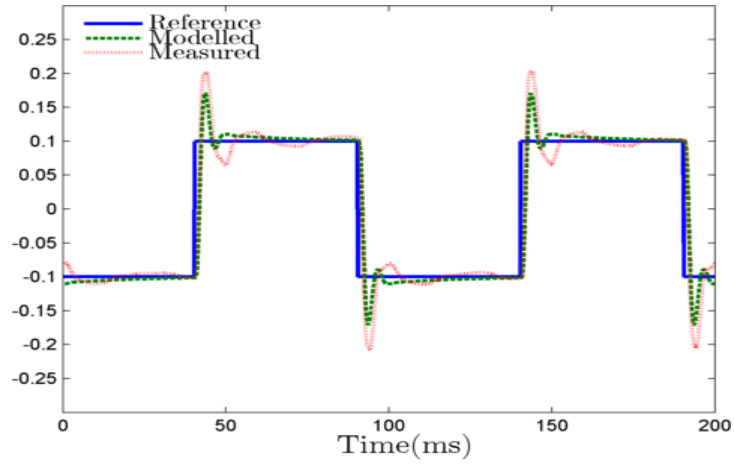
(a) 10Hz
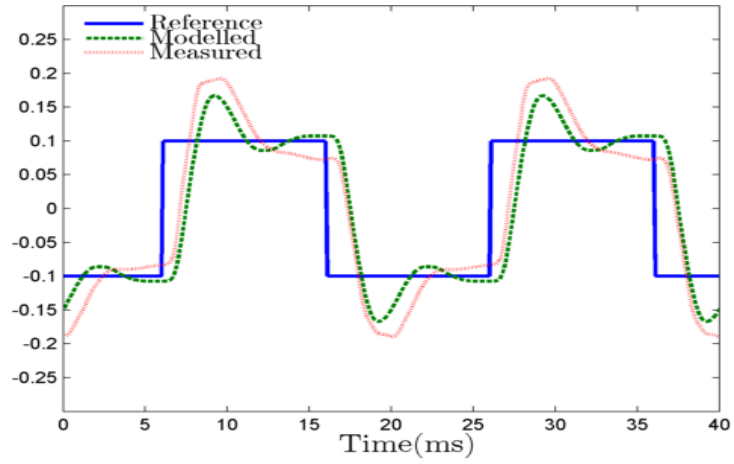
(b) 50Hz
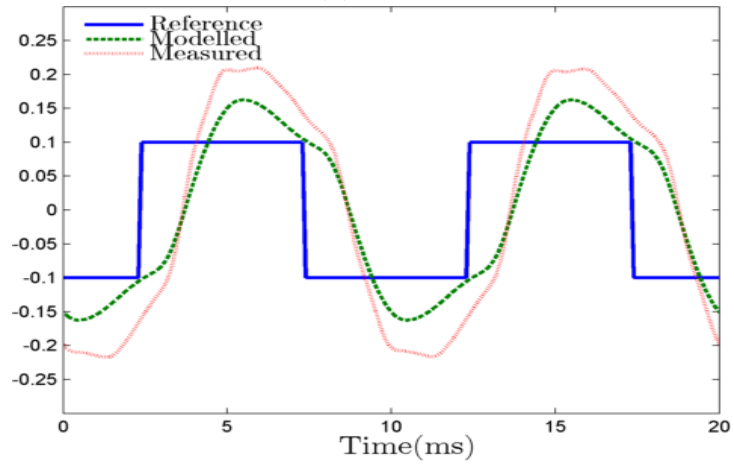
(c) 100Hz

Figure 3-10: Comparison of model and valve under PID control

53
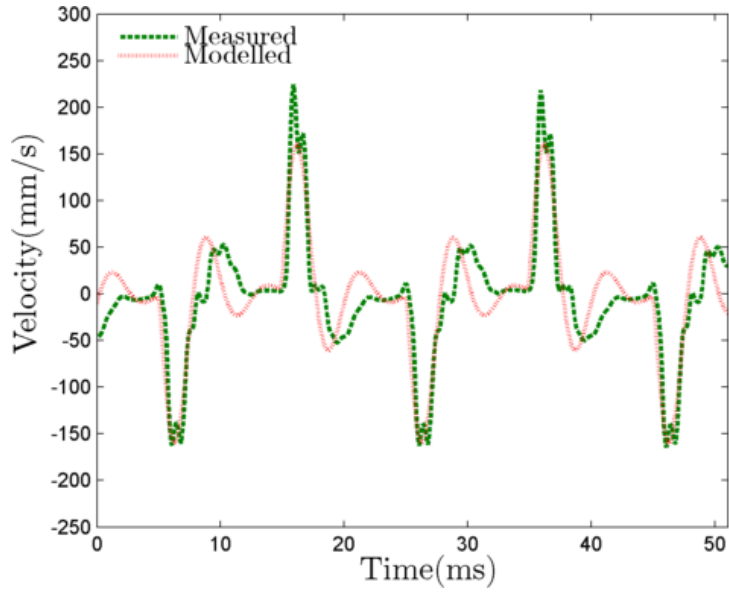
Figure 3-11: Velocity response of valve and optimised model to a 50Hz square wave under PID control
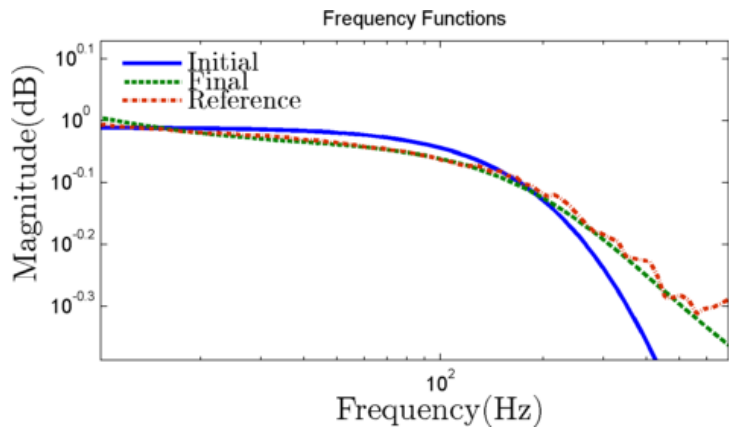
Figure 3-12: Frequency response of pilot valve models
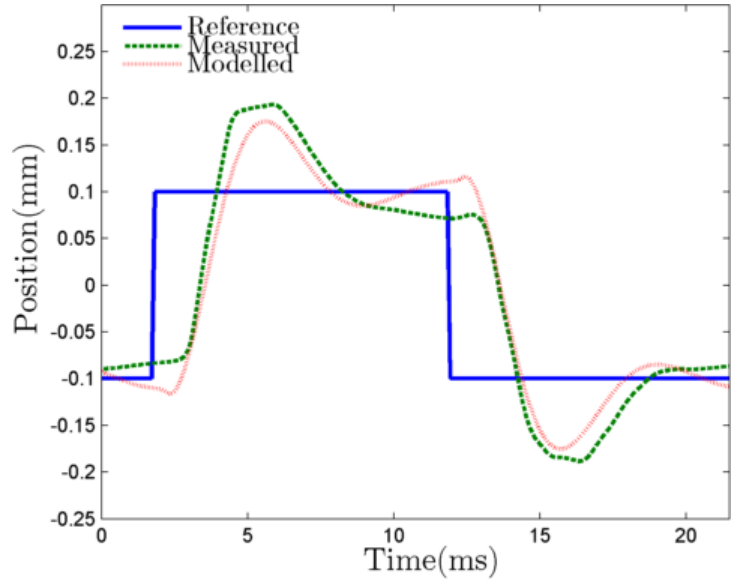
(a) Position response
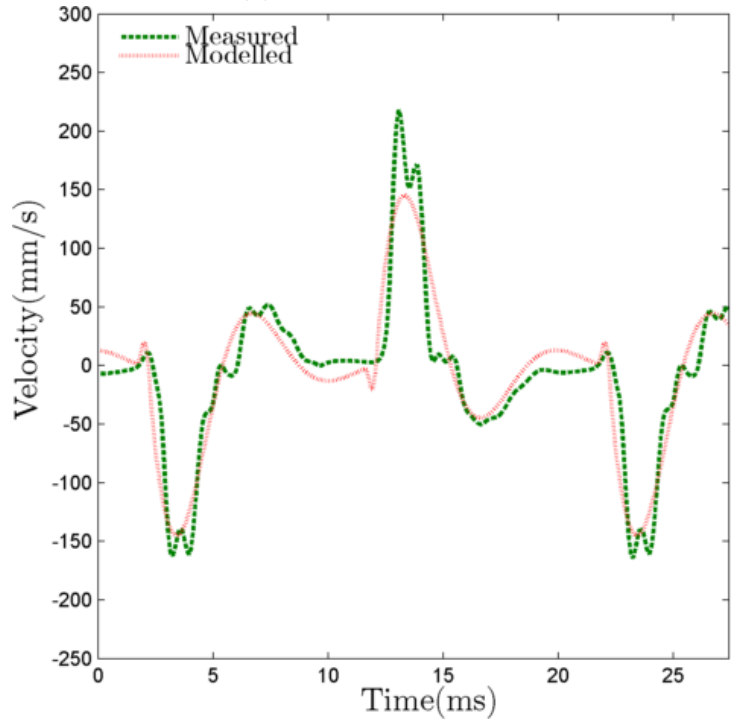
(b) Velocity response

Figure 3-13: Response of valve and optimised model to a 50Hz square wave under PID control

3.5 Conclusions

The valve agrees well with the model of it discussed in Chapter 2 as well as meeting most of the design criteria. The use of simple PID control proved to be incompatible with the switching time desired. However, there is reason to believe that the aim of a 1ms switching period is well within the valve's ability. There is leakage during valve switching but this is in keeping with the design of the valve, some leakage is also present when the valve is open to HP likely due to a slight overlap in the spool. A detailed feedback controller design will be described in the next chapter.

Chapter 4

Feedback Control

4.1 Model Linearisation

The vast majority of control design techniques require, as a prerequisite, a Linear Time Invariant (LTI model) of the plant to be controlled. The model elucidated in Chapter 2 and validated in Chapter 3 is non-linear. Whilst it proved to be accurate at predicting the valve's behaviour it is not well suited to controller design, though some methods such as Fuzzy logic control [57] or Lyapunov stability analysis [58] can be used directly with non-linear models to aid in the design and evaluation of controllers. It was decided to instead identify a simpler, linear model from experimental data for control design purposes. The more complex model was then used to validate the controller design. The chirp data used to determine the phase coherence of the position and accelerometer sensors, and the PID results were good candidates for both identification and validation. The chirp data was used as it covered the full frequency range within which the valve was expected to operate, whilst the PID data provided focus on the effects that would be key to the valve's mode of operation. The use of complementary filters meant that three kinematic states - position, velocity and acceleration - were observable and thus it was decided that a third order model provided a good compromise between accuracy and control design requirements. The model was identified using the identification toolbox within MatLab. This made use

of a proprietary algorithm which is based on the ARMAX algorithm but with modifications to the calculation of prediction errors and gradients [59]. An instrument variable (IV) method was used to initialise the estimable parameters of the model. This method is discussed in [60] where it is referred to as the SRIVC. The identified model can be seen in Equation 4.1 and a comparison of this model and experimental data in Figures 4-1,4-2 and 4-3.

$$\dot{r}(t) = \begin{bmatrix} 0 & 1 & 0 \\ 0 & 0 & 1 \\ -9.02 \times 10^7 & -3.15 \times 10^6 & -4747 \end{bmatrix} r(t) + \begin{bmatrix} 0 \\ 0 \\ 1.28 \times 10^9 \end{bmatrix} u(t)$$

$$x(t) = \begin{bmatrix} 1 & 0 & 0 \end{bmatrix} r(t) + [0]u(t) \tag{4.1}$$

Where the state vector $r(t)$ is made up of three states $[x, \dot{x}, \ddot{x}]$ and the output $x(t)$ is the position of the main spool.

It can be seen the the magnitude of the model and system are in reasonable agreement over a good range of frequencies though at very low frequencies and frequencies above 350Hz there is less agreement. Looking at individual sine waves the phase agreement of the two can also be inferred.

The model appears to lead the measured signal at lower frequencies, where there also appears to be some amount of stiction in the valves response which is not captured in the linear model. At higher frequencies the model lags the valves response somewhat. This behaviour along with the differences in gain can be seen when comparing the modelled and measured results under PID control.

The salient features of the responses are well modelled. The switching period appears to be well modelled but modelling of the steady state behaviour of the valve is less accurate. A more accurate representation could likely be achieved with a higher order or non-linear model. However, given the focus on achieving fast switching times this was deemed an acceptable state of affairs, particularly in light of the non-linear model which is available to confirm the suitability of any controller designed using the linear model and the desire to keep all states meaningful and measurable.
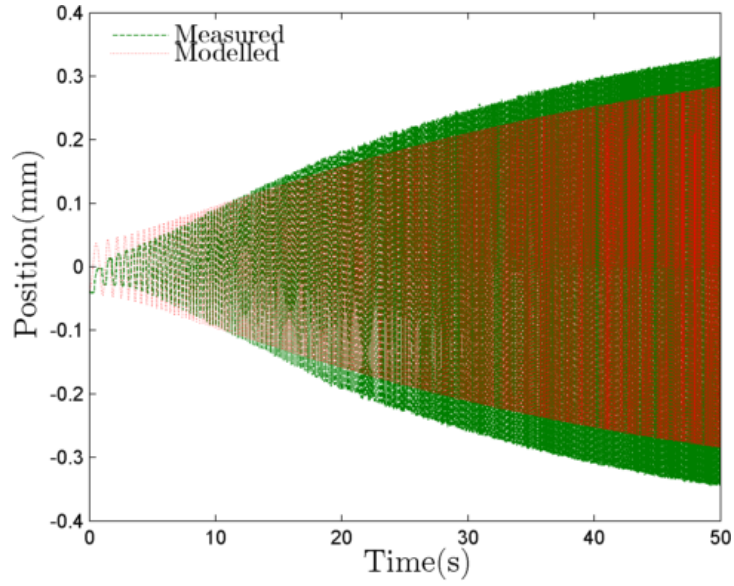
(a) Fit to chirp data between 0-20Hz
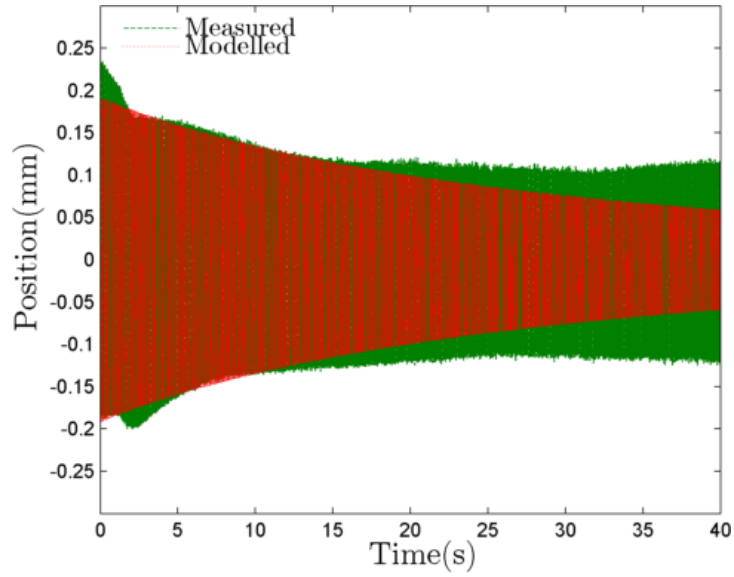
(b) Fit to chirp data between 300-500Hz

Figure 4-1: Comparison of measured and modelled data to two chirp tests
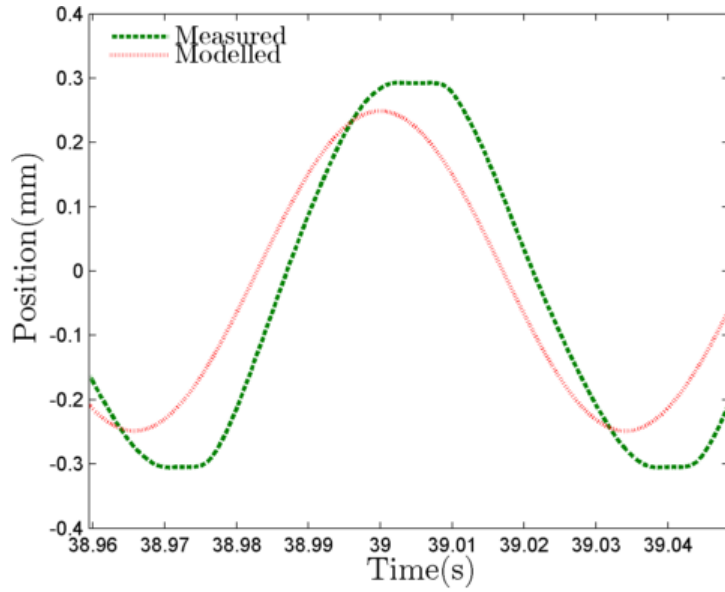
(a) Low frequency phase alignment
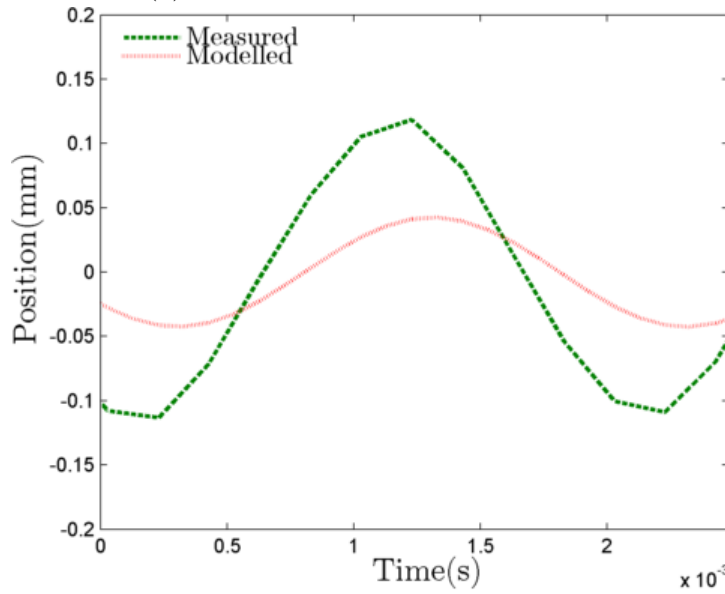
(b) Higher frequency phase alignment

Figure 4-2: Comparison of measured and modelled phase
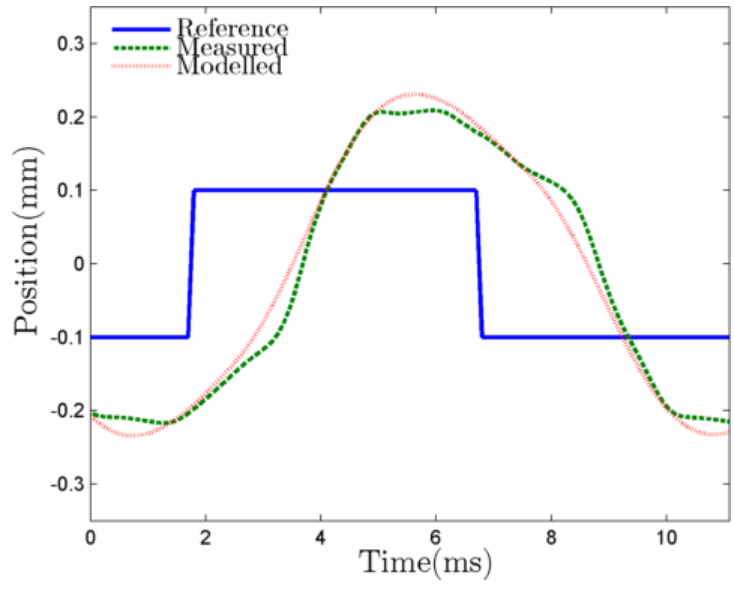
(a) 100Hz Square wave
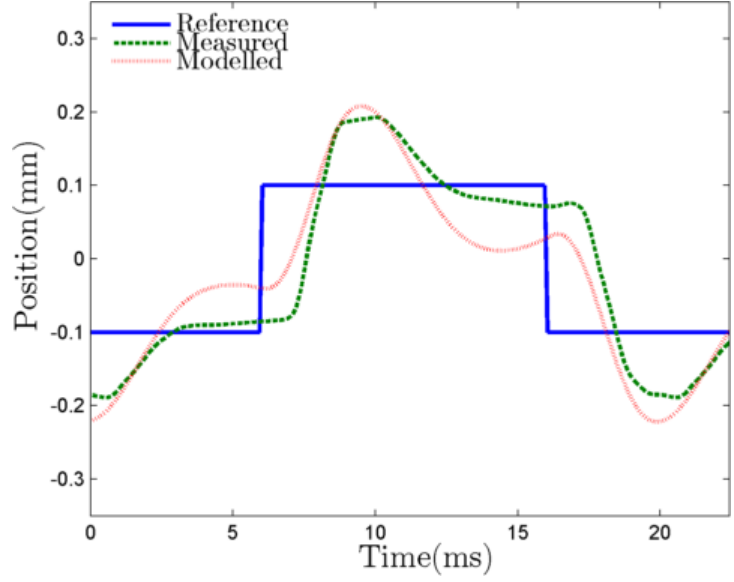
(b) 50Hz Square wave

Figure 4-3: Comparison of modelled and measured responses

4.2 Controller Selection

There is a wealth of control structures including PID and State Variable Feedback (SVF) control that can be used with LTI models and correspondingly a large number of design methods such as root-locus design, H_∞ control and intelligent control design. In choosing a control structure, the form of the model identified and the availability of high bandwidth position, velocity and acceleration signals served to recommend the use of SVF control. The reasoning for this is provided below along with a discussion of some of the various design methods applicable to SVF.

4.2.1 SVF control

As the name implies SVF feeds back multiple states and compares each of these to an input. Consider the state-space representation of a system:

$$\dot{r} = Ar + Bu$$
$$x = Cr + Du \tag{4.2}$$

For a system with n states and m inputs the feedback matrix, $\mathbf{K}$, must be an $n \times m$ matrix. This results in the closed loop state equation in Equation 4.3:

$$\dot{r} = \mathbf{A}r + \mathbf{B}u$$
$$= \mathbf{A}r + \mathbf{B}(x_d - \mathbf{K}r)$$
$$= [\mathbf{A} - \mathbf{B}\mathbf{K}]r + \mathbf{B}x_d \tag{4.3}$$

where x_d is a vector of desired outputs. If $\mathbf{D}=[0]$ then the output equation remains unchanged, giving a model relating the desired output to measured output, with the same state vector as the open-loop plant. This can be seen in Figure 4-4. Because the closed loop system has the same order as the open-loop feedback then, if the open-loop system is fully state controllable, gains can be selected to give the required closed loop characteristic equation (CLCE). This method will invariably produce regulators which seek to reject disturbances to the system. It is
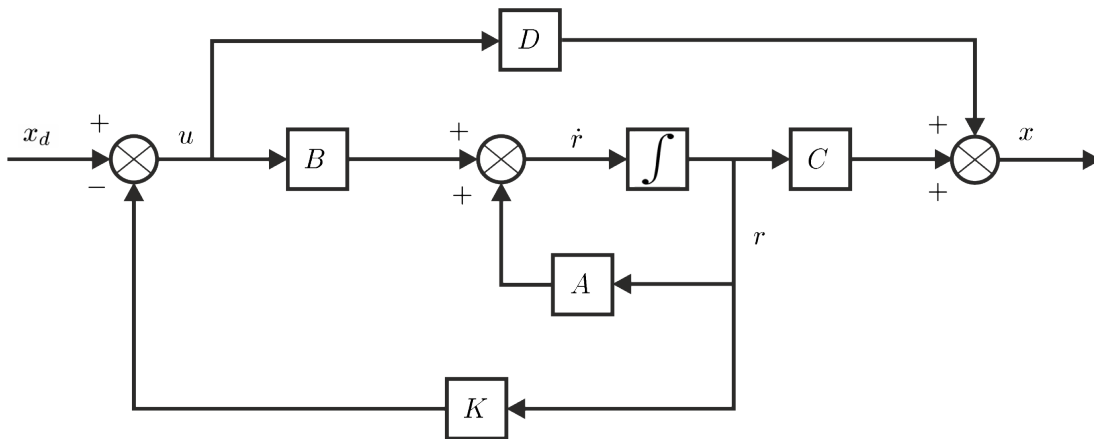
Figure 4-4: Generalised block diagram of a SVF system
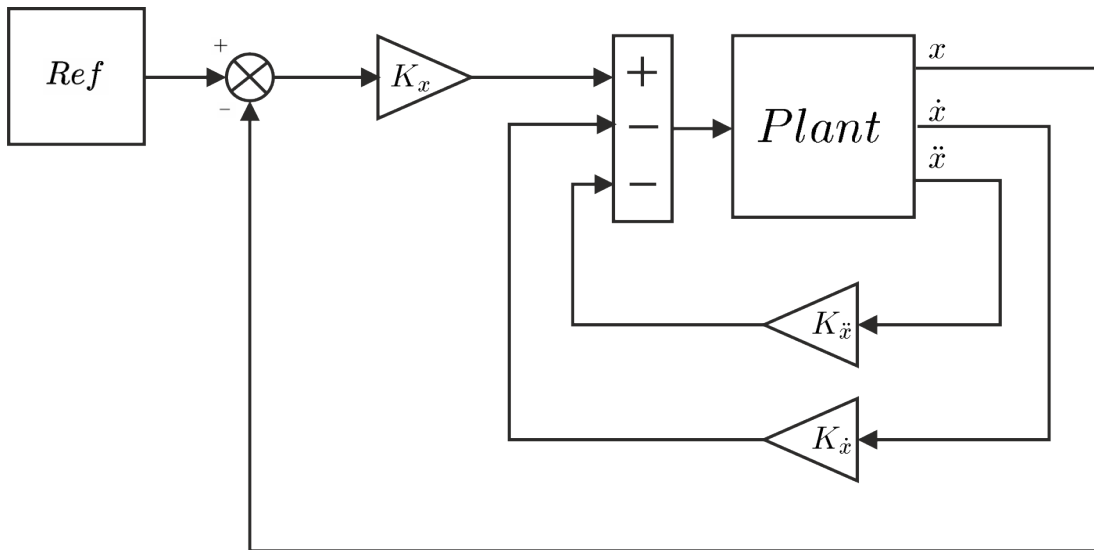
Figure 4-5: SVF control system for fast switching valve

possible however to modify the system's set-point and thus make these regulators perform as tracking systems. This design will, in most cases, give rise to steady state errors due to the resulting system having a type number of zero. However, for the subset of systems which have integrators in their open-loop forward path a similar design approach can be used to produce tracking control systems. The natural integral action will seek to follow the input given to it while the other states will seek to return the system to rest. A block diagram of the modified SVF circuit, needed to provide position tracking for the valve, can be seen in Figure 4-5.

It is clear that SVF is capable of, theoretically, producing a tracking system

with any desired CLCE as long as two conditions are met: all states are fully controllable and the forward path open-loop gives zero steady state error. Examining the linear model in Equation 4.1 shows that both of these conditions can be met. The rank deficiency of the test matrix, as outlined in [61], is zero, which means there are no uncontrollable states. It is also possible to set controller values such that zero steady state error is guaranteed. The DC gain of the forward path is equal to $1.28 \times 10^9/9.02 \times 10^7$ and in the closed loop is equal to $1.28 \times 10^9 \cdot \mathbf{K}(1)/(1.28 \times 10^9 \cdot \mathbf{K}(1) + 9.02 \times 10^7)$ therefore steady state tracking is guaranteed when $1.28 \times 10^9 \cdot \mathbf{K}(1) >> 9.02 \times 10^7$. This places an extra constraint onto the range of acceptable $\mathbf{K}$. It is these particular properties of the model identified - along with the full state observability, achieved courtesy of the complementary filter network - that mean SVF is possible.

There are many ways of selecting the gain matrix $\mathbf{K}$. Perhaps the simplest is Ackermann's pole placement method which appears in many modern control textbooks such as [62]. Ackermann's algorithmic approach enables controller gains to be set from desired pole locations. Many methods have been suggested for selecting the closed loop locations. For example, Franklin *et al* suggest designing a second order system with the desired characteristics (such as rise time and overshoot) and then placing any further poles at four times the natural frequency of the second order system [62]. In [52] it suggests basing two pole locations on a suitable second order system, but adds that if poles in the right-half-plane are to be moved then a reflection in the imaginary axis is a good starting point, and that having a combination of fast and slow poles is inefficient. Thus a Butterworth filter of the required order and suitable cut-off point was suggested because all poles are the same distance from the origin. It should be noted that while it is theoretically possible to produce any desired CLCE if the states are controllable, in reality this is unlikely to be the case. Most real world systems are non-linear. Whilst accurate linear approximations of these models may be made, around setpoints and away from any extremes, seeking to substantially modify the open-loop pole location is likely to cause the linear model to be inaccurate. The inclusion of very fast poles (orders of magnitude faster than the plant) will also serve to increase sensitivity to measurement noise and reduce the systems robustness. This means that Ackermann's pole placement method is more limited in scope than it first appears.

As well as the heuristic methods suggested above, the use of SVF and pole placement has found widespread usage in the field of optimal control. Before proceeding it is important to clarify what is meant by optimal in this context. Namely, that the controller is optimal for minimising the performance index used to formulate it. This does not make it categorically optimal for controlling the plant to which it is applied. Designing the feedback matrix $\mathbf{K}$ using optimal control methods shifts the focus from choosing pole locations, to choosing what governs good pole locations. When the feedback control is $u = -\mathbf{K}x$ then the performance index (PI) generally takes the form seen in Equation 4.4:

$$J = \int_0^\infty [x^T(t)\mathbf{Q}x(t) + u^T(t)\mathbf{R}u(t)]dt \tag{4.4}$$

where $\mathbf{Q}$ is an $n \times n$ symmetric positive semidefinite matrix and $\mathbf{R}$ is an $m \times m$ symmetric positive definite matrix. Effectively, $\mathbf{Q}$ weights the relative importance of errors in each of the states whilst $\mathbf{R}$ is used to limit the controller effort. Once formulated the solution of this minimisation problem is very well documented in [63]. Dutton *et al* [52] suggests a few practical tips for choosing the values of $\mathbf{Q}$ and $\mathbf{R}$.

- If $\mathbf{Q}$ and $\mathbf{R}$ are chosen to be diagonal matrices then it is easy to establish the correct 'definiteness'. It also means that each entry corresponds to a single input or state, making them meaningful.

- An investigation of the structure of the system model can prove useful, as information on the relationship between states can help choose which states to penalise and how heavily.

- The values chosen for the PI are, in general, artificial and thus, generally, testing and iteration are required to achieve the desired results. Testing can be done either in simulation or by investigating the closed loop eigenvalues resulting from the selection of $\mathbf{Q}$ and $\mathbf{R}$.

It should be noted that if the above PI is used to generate a tracking controller by means of inherent integration, then the resulting controller will be suboptimal.

However, given point three above, this is of little concern as the pretence of the controller being optimal in a global sense has been dispensed with. Fortunately though the resulting controller retains one of optimal control's other advantages: that of intrinsically producing stable controllers as long as the **R** matrix is diagonal. It can be shown that the closed loop system will remain stable for gains upwards of about half of those designed [64]. Though at the cost of conservative stability margins. This guarantee of stability extends only to the linear model from which the feedback gains were computed and therefore the level to which these conservative margins are transferred to the actual plant is a function of the model's accuracy.

4.3   Controller Design

Based upon the recommendations from Dutton *et al*, the SVF controller design was undertaken in an iterative manner. The process was as follows:

1. Select a best guess at initial weights based on knowledge of plant.

2. Calculate gains from these weights using linear model.

3. Check that $1.28 \times 10^9 \cdot \mathbf{K}(1) >> 9.02 \times 10^7$.

4. Test gains on linear model with a 50Hz square wave

5. Calculate switching time and overshoot, compare against requirements.

6. If not suitable modify weights and iterate steps 2-4.

7. If suitable test on non-linear model to confirm.

Initially, it was decided to weight only position and acceleration. It was deemed unnecessary to weight velocity as in this situation it will be sufficiently regulated by regulating acceleration which also serves to explicitly increase damping. Given the relative size of acceleration and position signals, along with the importance of fast tracking over minimising overshoot, a big difference in their

66
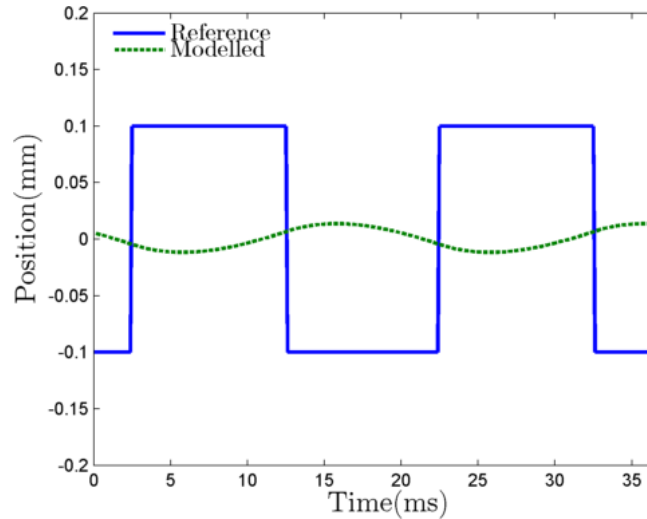
Figure 4-6: Modelled response to SVF control with initial weightings

relative weightings was used. Figure 4-6 shows the modelled response when $\mathbf{Q} = [1000 \quad 0 \quad 10^{-5}]$ and $\mathbf{R} = [1]$.

It is clear that this response is not acceptable as the maximum position is just over 10% of that required. Examining the input which gave rise to this response, it is clear that the desire to limit the velocity and acceleration is too strong. The gain contribution from the acceleration term is larger than that from the position term during the switching phases of the cycle. Ideally the position should dominate this period and then the acceleration and velocity terms should work to return the valve to rest once switching is complete. In order to achieve this the difference in weighting between position and acceleration needs to be bigger.

Table 4.1 shows the development of the weighting matrices along with the resulting gains and model response. For all cases $\mathbf{R} = [1]$. The final iteration

Table 4.1: Development of LQR

Q matrix			K matrix			Switching Time	Overshoot
1000	0	1×10^{-7}	31.6	0.14	3.1×10^{-4}	10ms	0μm
1000	0	1×10^{-9}	31.6	0.043	2.9×10^{-5}	3.5ms	5μm
1000	0	1×10^{-11}	31.6	0.018	2.8×10^{-6}	1.3ms	10μm
2000	0	0	44.7	0.023	3.3×10^{-6}	1ms	11μm

meets the specification given in Chapter 2, switching in 1ms or less with an

overshoot of less than 0.1mm. However, to achieve this it used 80% of the input range as oppose to the 5% required to achieve a 1.5ms switching time using PID control. This is a result of the heavy damping in the SVF response as can be seen from the minimal overshoot. A comparison of this modelled response and control input with those measured using the PID controller is shown in Figure 4-7.
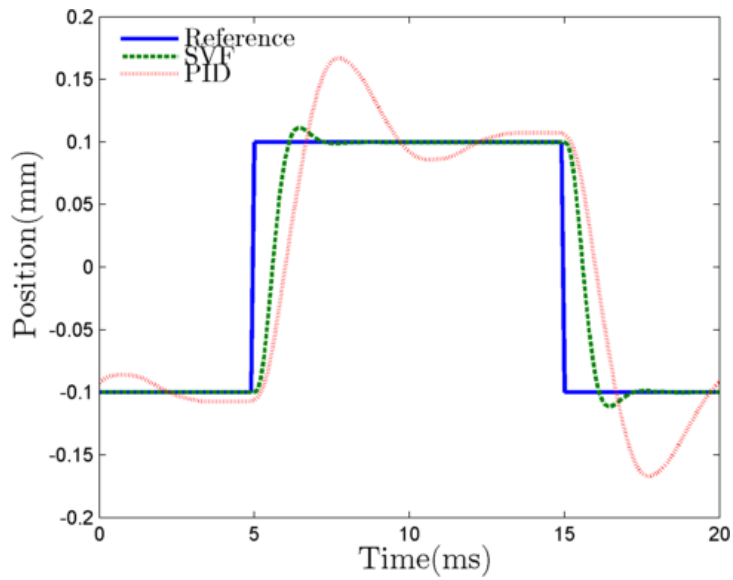
(a) Valve response
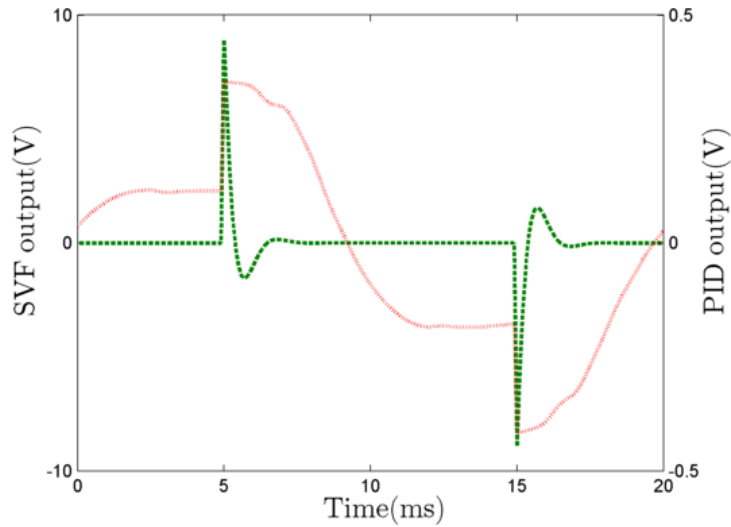
(b) Control Input

Figure 4-7: Comparison of modelled SVF and measured PID control

At this juncture it was determined that the insight gained from the optimal tuning could be used to empirically tune the feedback matrix. It was determined that the gains should all be scaled down with the relative importance of acceleration or velocity error decreasing in order to decrease the damping. A **K** matrix used in a previous iteration of the valve was found to achieve both of these things and gave the poles seen in Figure 4-8. It can be seen that the dominant pair of
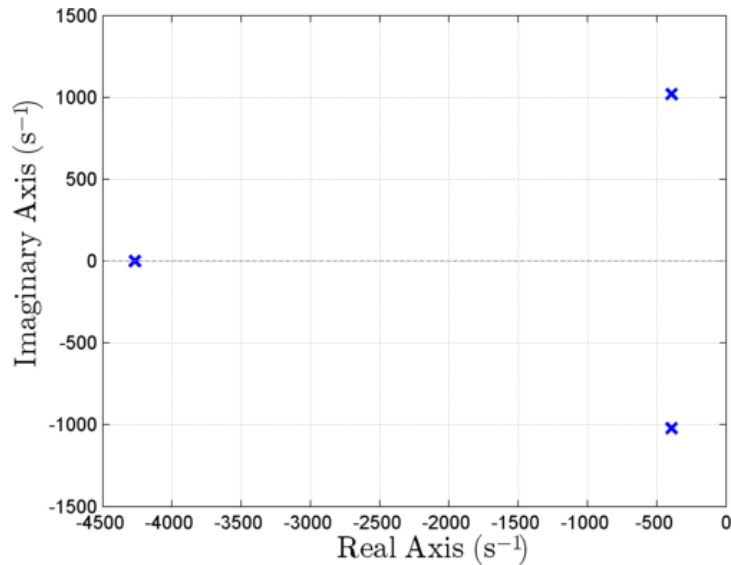
Figure 4-8: Pole locations with proposed **K**

poles give a low damping ratio and provide good bandwidth (ζ=0.36 ω_n=174Hz) since the response of the pilot valve, shown in Figure 2-6, is known to taper off above 300Hz. When this gain matrix was used in the non-linear model to follow a 50Hz square wave a switching time of 1.2ms and overshoot of 35μm were found, Figure 4-9.
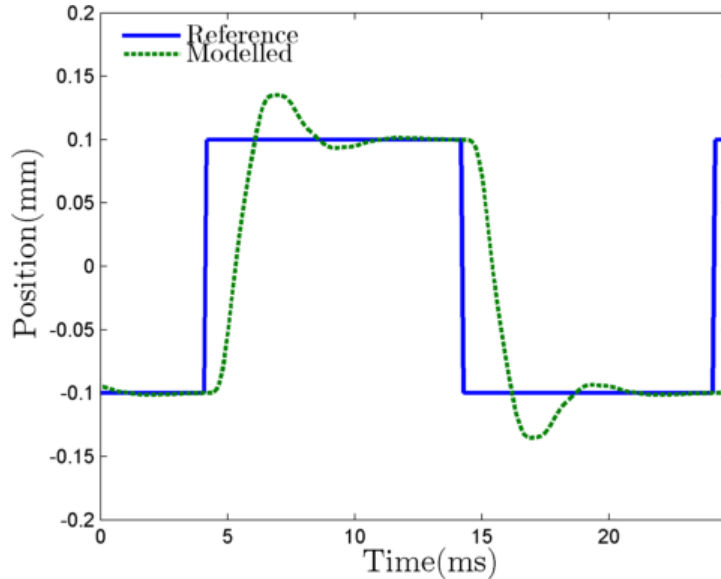
Figure 4-9: Non-linear simulation of valve response with SVF controller

These results are a significant improvement with regards to damping but slightly slower than desired, though the input range drops down to 8%. To confirm these performance estimates the feedback matrix was then used to control the valve itself. A comparison of the non-linear model's response and valve's response can be seen in Figure 4-10. When applying the controller a pragmatic decision to add a small integral gain (0.2) was made to allow for possible offset within the pilot stage and other small effects that have not been considered. This will have limited effect above 0.2rad/s, significantly lower than the other terms in the open-loop frequency response and so will hardly affect the dynamics of the system. The high frequency effects ignored in the modelling of the valve appear to be important enough to change the 1.2ms modelled switching time into a 1ms measured switching time. This means that the SVF controller posed above fulfils the design criteria, with a significantly smaller input than estimated from Table 4.1 - only 9% of the input range instead of 80%. This small input range suggests

that faster switching times could be possible with a better control scheme. The SVF results shown below also highlight other possible areas for improvement in the control scheme that will be discussed at the end of this chapter.

4.4 SVF Results

The switching times obtained from the valve are actually slightly better than those predicted by the model, whilst the overshoot is similar to that predicted. This can be seen in Figure 4-11. At all frequencies the valve switched in 1ms and overshot by less than 0.1mm, as specified. The steady state position at 50Hz was below the required 0.1mm but at higher frequencies this does not appear to be an issue. Figure 4-12 provides further insight into this.

It can be seen that the lower than desired settling position happens in Figure 4-12b but not in Figure 4-12a. This would suggest a lack of symmetry in the valve's response. One possible explanation for this could be leakage from the second stage to the main stage which would only manifest itself when the lower chamber of the second stage is pressurised i.e. when trying to hold a high position.

4.5 Conclusions

The SVF controller detailed in this chapter has shown that it is capable of meeting the two primary design requirements of switching in $\leq$1ms and limiting overshoot to 0.1mm. However, it is let down slightly by its position holding in the positive direction. This could be easily corrected by either demanding a slightly larger positive position - for example, 0.11mm - which would perhaps also serve to speed up the switching time or; by increasing the integral gain in order to stop the leakage sooner. However, it was also observed that only 9% of the total input range was utilised and thus a third path was taken; that of using an learning feedforward controller to not only improve the position holding capabilities of the control but also, to try and achieve even faster switching times and thus provide the possibility of reaching high frequencies in the SIHS.
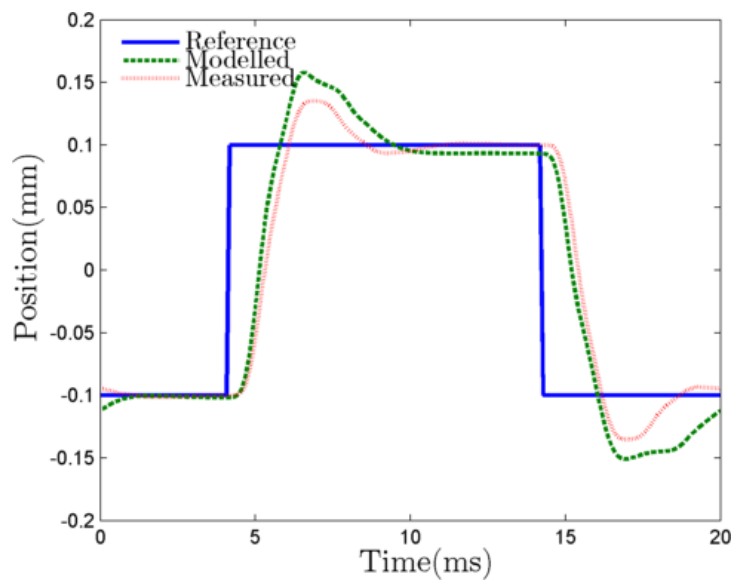
Figure 4-10: Comparison of modelled and measured response
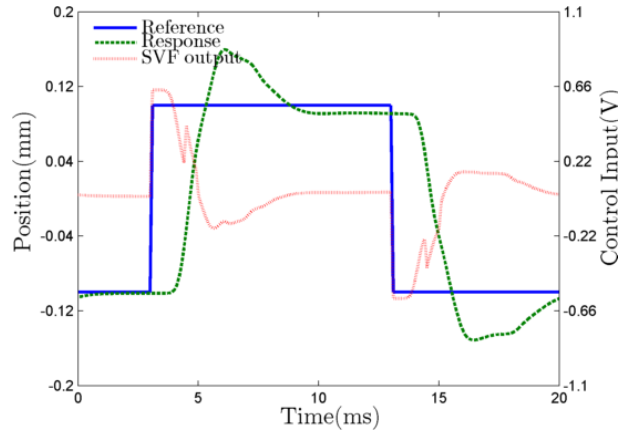
(a) 50Hz
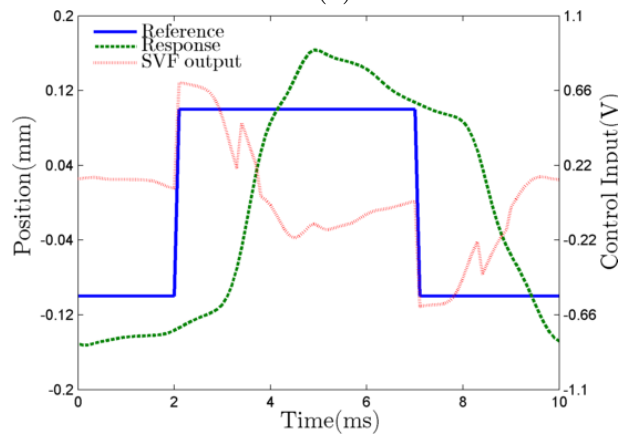
(b) 100Hz
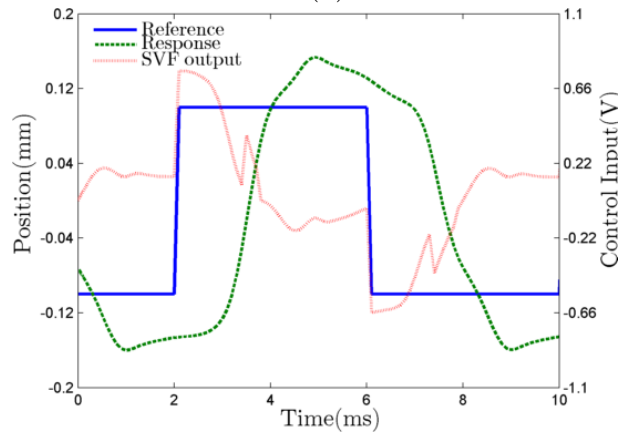
(c) 125Hz

Figure 4-11: Response of valve under SVF control to square waves
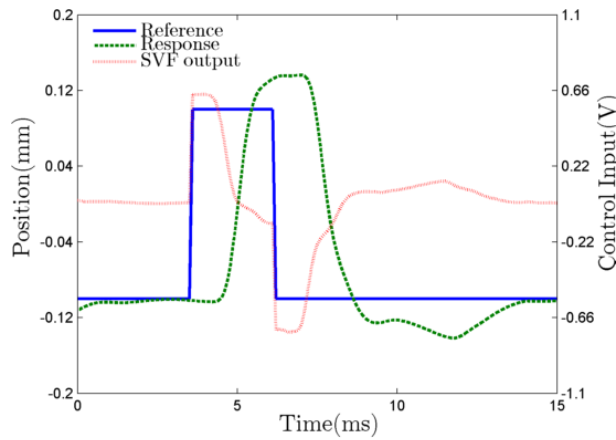
(a) 20% PWM signal at 77Hz
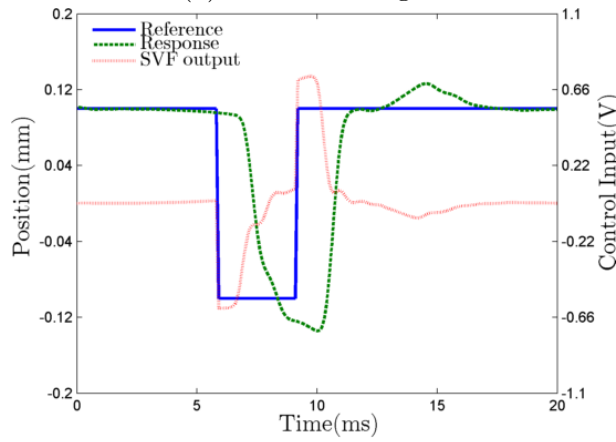
(b) 85% PWM at 45Hz

Figure 4-12: Response of valve with SVF control to PWM signals giving 2.5ms pulse width

Chapter 5

Feedforward Control

5.1 Learning Control

The SVF controller laid out in the previous chapter was adequate to achieve the intended switching time of 1ms. However, looking at the control signal, it was believed that an even better response could be achieved. It was also found that the SVF+I controller struggled to hold a high position, possibly due to leakage. It may have been possible to address both of these observations with further tuning of the SVF system, but the repetitive nature of the valve's operation makes the use of learning control an intriguing and more methodical option. In their survey paper of learning control techniques Wang *et al* state;

'In general, for a process that is repetitive and/or cyclic in nature, the learning-type control method should be the first choice for control.' [65].

They suggest that the question is not whether to use learning control but only which type of learning controller to employ. This is a bold claim to make given the wealth of different control techniques and subjectivity surrounding choice of control, the validity of which will be examined later.

Learning control is, broadly speaking, made up of Iterative Learning Control (ILC) and Repetitive Control (RC). The difference between these two is fairly

slight with ILC being concerned with control problems which are reset at the end of each cycle and RC dealing with continuously running systems that have a repetitive task. Based on these descriptions RC would appear the natural choice for the problem at hand as the valve is not reset before each cycle but runs continuously. However, a large amount of RC literature focuses on dealing with problems like unknown cycle times, non-integer numbers of samples in a cycle and disturbance rejection. Conversely ILC focuses on servo-tracking problems with fixed and known cycle times which are integer multiples of the sampling rate. There also exists a body of literature which discusses the effect of non-zero resetting (for example [66]) on ILC and literature that discusses how to modify ILC laws to account for this (for example [67]). Further to this it can be seen from [68] that a control law which works for ILC will work for RC and vice versa, except for RC problems with a non-integer number of samples within a cycle. Therefore, given that the ILC was intended to only modify what was already a good response it was determined to view the problem as an ILC problem with non-zero resetting.

In their analysis of some different ILC schemes Xu *et al* [69] state that the cascading of an ILC with a stabilising feedback controller is the most common use of ILC. Unlike the previous cycle learning, current cycle learning and the fusion of the two into previous-and-current cycle learning schemes, this form does not require a redesign of the feedback controller, making it suitable for our purposes. Instead the ILC provides a means of modifying the reference signal given to the existing controller in such a way as to make use of the information from previous iterations to reduce errors in the current iteration. Indeed, this form of ILC was used in [70] to improve the tracking response of a hydraulic cylinder with a simple PID feedback controller. A mathematical and pictorial description of this will be provided in Equations 5.3 and Figure 5-1 but first a more practical explanation will be given.

When presented with a repeated task a classic feedback controller will, ideally, provide the same output every single time. This can be a great strength and, indeed, the entire field of robust control exists to confirm and maintain this property in the face of disturbances and uncertainty. However this can also be a weakness when the response is non-optimal as this non-optimal response is

given time and time again. Information is fedback from one time step to the next but not from one iteration to the next. ILC on the other hand is open loop with regards to time but closed loop with regards to iterations, meaning it can use the error from past iterations in order to improve the current one. The similarity to organic learning, that of doing a task, being shown the errors in it and trying again to correct those errors, is why it is named Iterative Learning Control. Mathematically ILC can be most easily demonstrated on a LTI SISO system of the form:

$$y_j = G(s)u_j \tag{5.1}$$

$$e_j = y_d - y_j \tag{5.2}$$

where y_d is the desired output and y_j is the output from the jth iteration. Direct ILC works by using this calculated error to modify the input signal applied to plant at the next iteration, as shown below.

$$
\begin{aligned}
u_{j+1} &= u_j + L(s)e_j \\
&= u_j + L(s)(y_d - y_j) \\
y_{j+1} &= y_j + G(s)L(s)(y_d - y_j)
\end{aligned}
\tag{5.3}
$$

There are also indirect forms of ILC which use the error to tune parameters within an existing controller, such as modifying models [71] or tuning a PID controller [72], but these will not be discussed here. In the cascaded form of ILC, the input being modified is the reference to the feedback controller. This has been shown to be mathematically equivalent to changing the actual plant input but avoids the need to modify the existing controller [73]. The block diagram of this cascaded ILC is shown in Figure 5-1.

Bristow *et al* are more reserved in their review of ILC. They do however give a number of advantages that ILC has over a good feedback/feedforward control design which are discussed below [74].
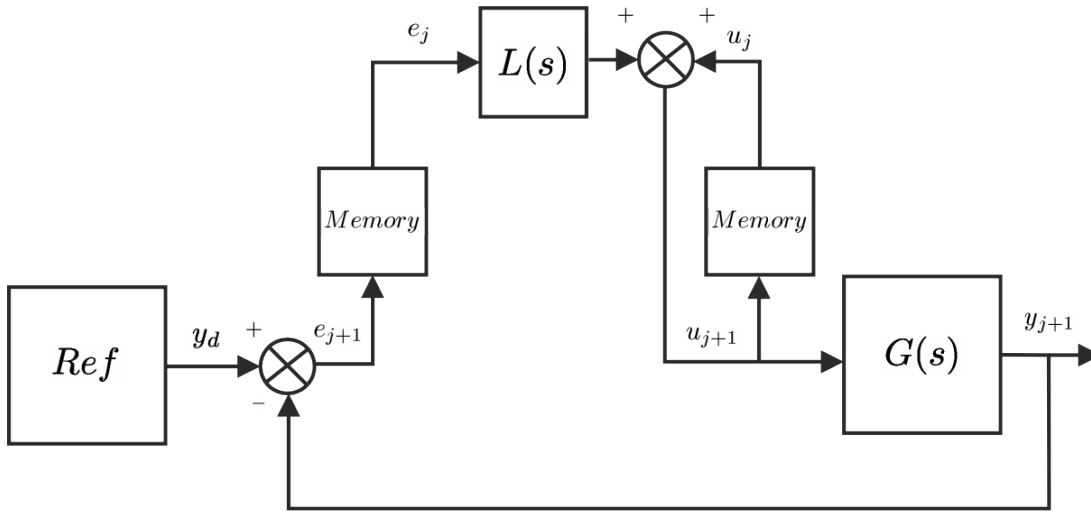
Figure 5-1: Block diagram of a cascaded ILC

5.1.1 Lag Compensation

By its very nature feedback control is reactive, this means it will always lag behind input signals to some degree and that disturbances must manifest themselves in the plant's output before they can be corrected. Classic feedforward controllers can eliminate this lag but only if it is known about when the controller is designed. ILC increases the instances in which this lag can be compensated for, from those that are known to those that repeat from iteration to iteration. For example Chen and Zeng [70] use the update rule in Equation 5.4 which is a modification of that used in Equation 5.3 above:

$$u_{j+1}(t) = u_j(t) + L(e_j(t + \tau_e)) \tag{5.4}$$

where τ_e is the estimated time delay in the system, which is used as a tunable variable to create the desired response. Whilst a classic feedforward could apply a phase lead of a similar magnitude this would not be as effective as the actual time shifting achieved in ILC. Further to this if the exact length of the delay is unknown then as long as the upper limit is known then Park *et al* [75] suggest the ILC can still compensate for the delay. This is achieved by maintaining the initial control input for the duration of the delay uncertainty. When this was done on a numerical model of a batch chemical process perfect tracking was achieved at discrete points spaced equal to the uncertainty. Park and Bien then published

78

a further paper [76] suggesting that another way for overcoming incorrectly estimated time delay would be to utilise an input saturation to bound the control input based on the estimation bound and selected saturation bound. As long as the saturation bound is greater than the highest control input desired this modification does not affect the quality of the converged result. It is suggested that a time-varying saturation function could be a way of tightening the control bound without compromising the final result.

5.1.2 Robustness

Classic controller design is generally based upon a linear model of the plant. How accurate a representation of the plant this is varies from case to case, but changes over time and non-linearities within the plant are not considered in these models. Methodologies such as H_∞ control do exist which can account for modelling error during the design phase and ensure that controllers remain stable and perform appropriately in the face of these effects. However, these still rely upon the designer to determine and accurately model the uncertainties and operating conditions which the plant includes and thus still fail to offer any protection from the unexpected. ILC however is effectively open-loop (though closed loop in the iterative domain) and so can have high stability robustness within each cycle to system uncertainties dependent on the algorithm used. As it is designed not to produce a particular performance but, instead, to be able to converge to the best possible performance then modelling errors are more likely to affect convergence rate than final converged performance.

5.1.3 Advanced Signal Processing

Whilst ILC can compensate for repetitive disturbances it cannot naturally compensate for non-repeating or aperiodic disturbances and noise. However, the use of a cycle delay within the ILC scheme makes it possible to use many signal processing techniques that cannot be applied in real time, such as zero-phase filtering. As zero-phase filters are non-causal they find application mainly in post-processing rather than control. However, their ability to provide filtering without

introducing any lag makes their application in control very useful [77]. Another possible use of this non-causality is time shifting, as mentioned above. As all the data points for the next iteration exist at the beginning of the iteration it is possible to shift the start point. Verwoerd *et al* also found that for non-minimum phase systems the causality imposed by closed-loop control could impede control performance and thus ILC's ability to perform non-causal operations was of great benefit [78].

5.1.4   Ease of Design

This is not part of Bristow *et al*'s list but rather one arising from observation. It can be seen from Equation (5.3) that the design task for an ILC consists solely of designing the learning function $L(s)$. Many forms and design methods of $L(s)$ have been proposed these include both the complex and the simple. Many of the simple forms of $L(s)$ can be designed with no knowledge of the plant using heuristic design methods. The advantage of using a heuristic ILC feedforward controller over a classic feedforward design of similar design complexity is that the ILC can be shown to act as an integral control in the iteration domain in order to reduce errors:

$$u_{j+1} = u_j + L(s)e_j = u_0 + L(s) \sum_{l=0}^{\infty} e \qquad (5.5)$$

where the middle equation can be seen to be the same as the update rule given above and is the recursive form used within the ILC, and the right hand side is the time form of the same rule showing the natural integrative action. In other words a poorly designed ILC is sub-optimal at learning whilst the classically designed controller produces a sub-optimal response.

5.2   Learning Functions

5.2.1   Inverse Model Type

It is apparent that the ideal learning function is a perfect inversion of the closed loop plant as this would converge to a perfect solution after only a single iteration.

$$L(s) = G(s)^{-1}$$
$$\therefore G(s)L(s) = 1$$
$$y_{k+1} = G(s)L(s)y_d - G(s)L(s)y_k + y_k$$
$$= y_d - y_k + y_k$$
$$= y_d \tag{5.6}$$

The most obvious limitation of this method is that the direct inversion of non-minimum phase plants will result in unstable models. There do exist methods to ensure stable inversions [79] [80] but these naturally compromise the 'perfect' tracking and convergence of the direct inverse. Even when a direct inversion is possible both $G(s)$ and $L(s)$ must be LTI for Equation (5.6) to hold. Real world systems can approximate LTI behaviour but are never truly linear or time invariant. Equation (5.6) also requires that the plant be capable of achieving the desired output. Take, for example, a square wave input. A feedback controller will do its best to approximate it and as long as it is stable once it will, barring disturbance, continue to be stable. However, an ILC that simply applies an inverse model to the error of the feedback system will continue to modify the input regardless of the fact that an infinite acceleration is beyond the ability of any real world system. This results can result in divergence. As a result of these limitations when inverse models are used in the learning functions modifications are made to the simple ILC scheme given in Figure 5-1.

Lee *et al* [81] used an inverse plant model in a cascade arrangement on chemical engineering batch processes. It was found that when an approximate plant model ($\bar{G}(i\omega)$) with a feedback controller ($H(i\omega)$) and a learning function (($L(i\omega)$

equal to the inverse of the approximate plant model was used then the convergence criterion is:

$$|1 - \frac{G(i\omega)}{\bar{G}(i\omega)}| < |1 + G(i\omega)H(i\omega)| \; for \; all \; \omega \in [0, \infty] \tag{5.7}$$

or that the relative error must be less than the return difference of the feedback loop. This again assumes that the inversion of the plant model is perfect even if the model itself isn't perfect. In order to allow for the inaccuracies in the inversion, which are likely to increase with frequency, Lee *et al* included a low pass filter $(Q(i\omega)$ into the forward path which modified the convergence criterion to be.

$$|1 - \frac{G(i\omega)}{\bar{G}(i\omega)}| < |\frac{1 + G(i\omega)H(i\omega)|}{|Q(i\omega)|} \; for \; all \; \omega \in [0, \infty] \tag{5.8}$$

Elci *et al* utilised a similar approach to control a discrete MIMO system with a zero-order low pass filter being placed at 18Hz - the confidence boundary of the inverse model [82].

5.2.2 H_∞ Type

Initially the field of H_∞ control appeared in ILC literature as a tool to examine learning functions that were derived heuristically [83] [84]. However, in 1996 de Roover published, what is believed to be, the first paper on the synthesis of a ILC learning function using H_∞ methods [85]. By reformulating the ILC problem into the 'standard plant' he showed it was possible to synthesise a H_∞ sub-optimal controller. This ability to include uncertainties in the formulation of the learning function enabled explicit decisions to be made with regards to the weighting of speed and quality of learning and robustness. The method outlined in this paper is applied to a wafer stage in [86]. De Roover suggested the use of a slightly modified and discrete time version of the update law in Equation (5.5) which includes a low pass filter Q(z):

$$u_{j+1}(t_k) = Q(z)(u_j(t_k) + L(z)e_j(t_k)) \tag{5.9}$$

$$L(z) = \underset{L \in H_\infty}{arg \; min} ||Q(z)(I - L(z)G(z)||_\infty \tag{5.10}$$

If the resulting controller meets the condition $||Q(z)(I - L(z)G(z)||_\infty < 1$, then the cut-off frequency of $Q(z)$ can be increased, if not then it must be decreased. The design process for $Q(z)$ and $L(z)$ are then repeated until the maximum acceptable cut-off value is found. Using this design method on an integrated circuit wafer stage motion control circuit, de Roover found that the magnitude of servo error after convergence was 5-10x smaller than for a heuristically designed system. Similar results could probably have been achieved with the heuristic system if a smaller learning gain was used, but at the cost of slower convergence.

5.2.3   Optimal Type

Unlike the other methods described thus far, quadratically optimal design can be used without requiring a model of the plant to be controlled, though the use of a plant can provide faster convergence and lower converged errors [87] [88]. Gunnarsson and Norrl of implemented quadratically optimal methods with a known plant to control the trajectory of a ABB IRB1410 robot [89]. He used the same update law as found in Equation (5.9) and for the LTI SISO discrete time system with feedback and feedforward control:

$$y_j(t) = T_r(q)y_d(t) + T_u(q)u_j(t) \tag{5.11}$$

where $T_r(q)$ and $T_u(q)$ are stable discrete time filters and q is the shift operator. Introducing the vectors:

$$\mathbf{Y_j} = [y_j(0), ..., y_j(N)]^T \tag{5.12}$$

$$\mathbf{Y_d} = [y_d(0), ..., y_d(N)]^T \tag{5.13}$$

$$\mathbf{U_j} = [u_j(0), ..., u_j(N)]^T \tag{5.14}$$

and therefore $\mathbf{E_j} = \mathbf{Y_d} - \mathbf{Y_j}$ where $t = 0, ..., N$ denote the sampling points. Using this notation the SISO LTI system becomes:

$$\mathbf{Y_j} = \mathbf{T_r}\mathbf{Y_d} + \mathbf{T_u}\mathbf{U_j} \tag{5.15}$$

83

where $\boldsymbol{T_r}$ is the matrix formed by the impulse response coefficients of the transfer operator $T_r(q)$ and is equal to:

$$\mathbf{T_r} = \mathbf{G(F_f + H)} \tag{5.16}$$

where $\boldsymbol{H}$ and $\boldsymbol{F_f}$ are the matrices corresponding to the feedback and feed-forward transfer operators. $\boldsymbol{T_u}$ is defined similarly and is equal to:

$$\mathbf{T_u} = \mathbf{GH} \tag{5.17}$$

Using this notation the problem can be posed as the minimisation of Equation 5.18.

$$\mathbf{J} = \mathbf{E_{j+1}^T W_e E_{j+1}} + \mathbf{U_{j+1}^T W_u U_{j+1}} \tag{5.18}$$

W_e and W_u are weight matrices which penalise the performance and input energy respectively, analogous to the Q and R matrices used in Chapter 4 to formulate the SVF controller. The optimal filter (Q) learning function (L) to minimise Equation 5.18 can be found from Equation 5.19 and 5.20 respectively.

$$\mathbf{Q} = (\mathbf{W_u} + \lambda \cdot \mathbf{I} + \mathbf{T_u^T W_e T_u})^{-1}(\lambda \cdot \mathbf{I} + \mathbf{T_u^T W_e T_u}) \tag{5.19}$$

$$\mathbf{L} = (\lambda \cdot \mathbf{I} + \mathbf{T_u^T W_e T_u})^{-1} \mathbf{T_u^T W_e} \tag{5.20}$$

The Lagrange multiplier, λ, is used as a design variable rather than computed explicitly. As when the optimal control techniques were used to formulate the feedback controller, the resulting controller will always be stable and convergent when the weighting matrices are positive and definite, assuming the plant model used is accurate. Using these equations and a first order model of one of the robot's actuators, Gunnarsson and Norr of [89] experimented with three different values of λ and then used the 'best fit' to the inverse model. When the resulting $\mathbf{Q}$ and $\mathbf{L}$ were used to control the robot a decrease in position error of over 90% was found in the first iteration with continuing decreases thereafter until the algorithm converged with a steady-state error. Further application of this method can be found in [90] and [91].

5.2.4 PD Type

The P-, D- and PD types of learning functions are the most commonly used and, indeed, Arimoto's original work utilised a simple D type learning function [92]. The popularity of PD-type functions arises largely from their ability to be tuned empirically with little or no knowledge of the plant and, in some cases, no knowledge of ILC. This particularly recommends them for use with non-linear systems, as methods based around linear models are naturally difficult to apply. Some of the non-linear systems they have been applied to include an injection moulding machine [93], magnetic bearings [94] and robot manipulators [95].

There is currently no widely accepted Zieger-Nichols analogue for PD type ILC, although numerous methods and design rules have been derived. A selection can be found in papers [96] [97] and [98]. In his paper entitled *'Iterative learning control and repetitive control for engineering practice'* [68] Longman elucidates what he believes to be the reasons for the lack of acceptance of ILC in the wider engineering community along with a method which aims to target these shortcomings. The aims he lays out for his method are:

- Use a linear formulation - This is based on the belief that the simplest tool to achieve the job is the correct one and results in [82] which show that a simple gain and compensator are able to produce 'perfect' tracking on a non-linear system.

- Create laws in discrete time - Given the need to store and process data in discrete time it is sensible to formulate controllers in discrete time too.

- Use existing feedback controllers - Given that many systems where ILC would reasonably be applied are already fitted with feedback controllers it is sensible to formulate a method which does not require the modification of these controllers but instead supplements them. Alternatively, a cascaded ILC, as mentioned above, may be suitable.

- Minimise the number of tunable variables - Despite the wealth of control techniques, the vast majority of controllers remain of the simple PID type or some combination thereof. This should inform the design of control laws which aim for practical acceptance rather than theoretical excellence.

- Require only basic control knowledge - Rather than achieving universal acceptance by making a universal controller that, theoretically, works on any system, make a unique controller that requires only basic knowledge to design. He limits this basic knowledge to the acquisition of, and a small amount of manipulating of, an experimental frequency response.

- Guarantee good learning transients - As important as the final error achieved using ILC is, it is also imperative the path taken is also sensible. More proverbially the ends does not justify the means. In order to qualify this statement whilst proving a point about universal controllers he applied an ILC with mathematically proven convergence to zero tracking and plotted its error against cycle number, Figure 5-2. The RMS error goes from 0.14 at iteration 7 to 1.2×10^{51} at around 6,000 iterations before finally converging to zero. Any real world system would saturate before 1.2×10^{51} RMS and thus violate the assumption of a linear plant that most universal controllers require.

- Guarantee long term stability - ILC can give the appearance of stability in the short term only for noise and other high frequency effects to eventually drive it unstable after thousands of iterations.
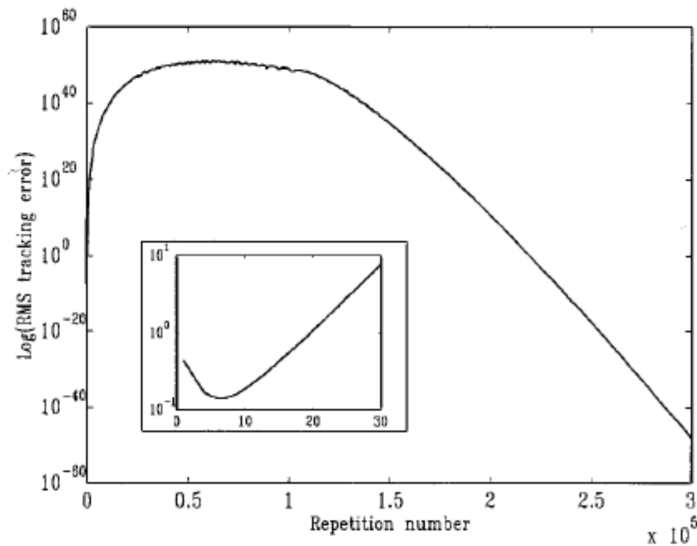
Figure 5-2: RMS tracking error of a universal controller (taken from [68])

In order to meet these aims, Longman lays out a three stage method based

86

on the update law given in Equation 5.21.

$$U_{j+1}(z) = Q(z)(U_j(z) + z^\gamma \Phi E_j(z)) \tag{5.21}$$

where Φ is the learning gain, Q is a filter which can take multiple forms and z^γ is a phase lead compensator or forward time shift. The first stage is to experimentally derive the frequency response of the plant to be controlled. This can then be plotted on a Nyquist plot in order to evaluate the bandwidth of ILC that can be provided by a simple P-type update law. To guarantee good learning transients, meaning monotonic converge of the 2-norm, and the convergence of the ILC the condition in Equation 5.22 must be met.

$$|1 - (e^{i\omega T})^\gamma \Phi G(e^{i\omega T})| < \frac{1}{|Q(e^{i\omega T}|)} \tag{5.22}$$

This can be checked visually by plotting a unit circle centred at $+1$ on the same axis as the measured frequency response. The frequency at which the Nyquist plot leaves this unit circle is the ω where the above condition is violated. The diagram in 5-3 can be used to infer the asymptotic stability criteria given in 5.22 for a given gain and lead. The diagram shows the measured response of the system $G(e^{i\omega T})$ transformed by the lead $(e^{i\omega T})^\gamma$ and multiplied by the gain ω. The frequency at which this plot leaves the unit circle therefore implies the frequency at which the condition in 5.22 is violated at thus the cross-over frequency for the low pass filter $Q(e^{i\omega})$ in order to guarantee convergence.

If this frequency is below the desired bandwidth then a phase lead compensator can be added. By multiplying the measured frequency response $G(e^{i\omega T})$ by the $(e^{i\omega T})^\gamma$ where γ is the number of time steps of lead, and then re-plotting, the new limit of ω can be found. Longman suggests an iterative approach, using the lowest value of γ which provides sufficient bandwidth. As part of this approach the value of Φ could also be tuned if desired, though it is suggested that this has little effect on bandwidth and should instead be chosen from the range of $0.25 \leq \Phi \leq 1$ to reflect the relative importance of convergence speed (high values) and lower final error (lower values). The final stage is the designing of the Q filter in order to guarantee long term stability. Multiple forms of filter are suggested including non-causal cliff filters or Butterworth IIR designs and more
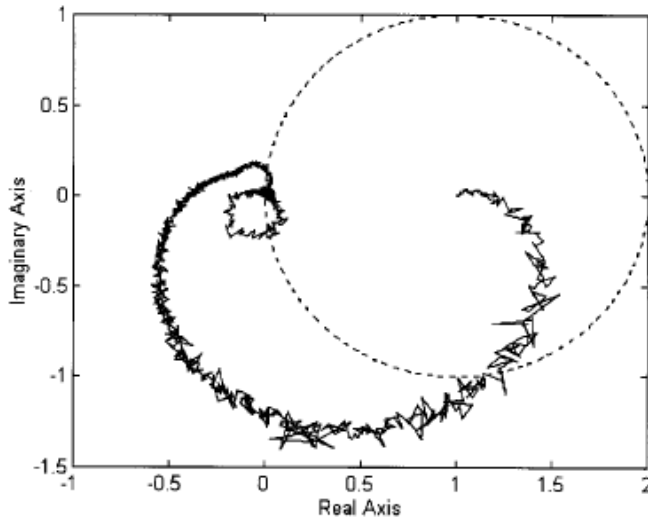
Figure 5-3: Nyquist diagram for evaluating Equation (5.22) (taken from [68])

simple causal designs with their inherent phase lag accommodated in the design of the compensator. The cut-off frequency of this filter is naturally implied from the control bandwidth found from the Nyquist diagram.

This method provides a neat, if somewhat conservative, solution to the ILC problem that can easily be applied, as well as some useful tools for evaluating other ILC control schemes.

5.2.5 Other Learning Functions

The forms of learning function covered above form the majority of the *prior art* but there are many other forms that have been investigated including, Fuzzy ILC [99] [100], neural networks [101] [102], adaptive control [103] [104] and blended multiple model ILC [105].

5.3 Learning Function Design

The large number of methods for designing ILC's makes selection of the most appropriate method challenging, with a trade-off between complexity and performance. A review of the response provided by the SVF system shows that the

closed loop system is a good approximation of a linear system and shows a clear input delay. This means that Longman's method is applicable and given the ease of use it was determined that this should form an initial stage in the controller design. A series of five 10s long white noise experiments were conducted and then averaged in the frequency domain in order to generate the Nyquist plot in Figure 5-4. Based on Longman's constraints for monotonic convergence a simple
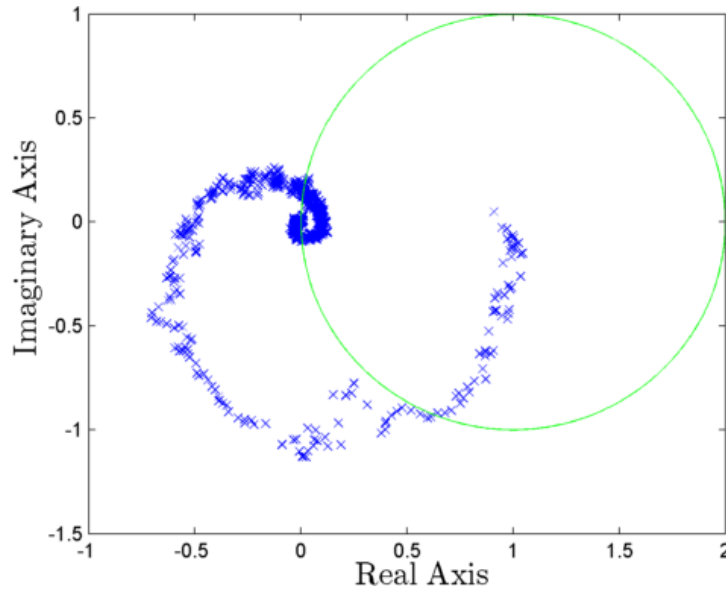
Figure 5-4: Nyquist plot of closed-loop system

proportional ILC law would be usable up to only 98Hz - significantly below the range that is desired. Longman suggests therefore that an iterative approach is used to find the number of samples of lead that would provide sufficient bandwidth. The addition of lead was achieved by treating the measured output of the previous cycle as:

$$y_j(t) = \tilde{y}_j(t + \tau) \tag{5.23}$$

$$where \; \tau = \gamma \cdot \Delta T \tag{5.24}$$

By applying the same delay to the reference signal before calculating the error and then reducing the cycle time by τ the output can be thought of as being advanced by τ. This is represented graphically in Figure 5-5 for the first iteration of the controller. Thus rather than shifting the calculated error forward in time as seen in $[70, 75, 76]$ the response can be considered as being shifted forward, within

the ILC circuit. It would be possible to utilise a similar method to actually bring the response forward but this was not done as the nature of the task at hand means that pure time delay is of no consequence. Shifting the response rather than the error will in general serve to reduce the initial RMS error and so convergence time, provided that the response in not shifted such that it leads the reference. Choosing γ must therefore have an extra condition to those posed by Longman and so a different method was devised. An interior point constrained non-linear optimisation algorithm [106] was used to minimise the average cycle error for a range of square waves between 1Hz and 125Hz to find the optimal value. This was found to be 11 samples. Therefore the value of γ could not exceed this value, Figure 5-6 shows the Nyquist plot generated using 10 and 11 samples. Ten samples of lead gave a bandwidth extended up to around 400Hz, whilst 11 samples provide a bandwidth of around 1000Hz, though the noise in the measurement means it could well be significantly higher. Reducing the learning gain from 1 to 0.25 is sufficient to increase the bandwidth at for ten beyond the point past which it was deemed sensible to drive the pilot valve (700Hz the beginning of its resonant peak) meaning 10 sample of delay or $\tau = 1ms$ was used. Figure 5-7 shows the reduction in error that was achieved by the addition of lead to the response. Naturally, shifting the error does not change the signal so the error calculated with $\tau = 0$ can be considered equal (excluding delay) to that which would be found using the lag compensation schemes given in [70, 75, 76].

The monotonic convergence guaranteed by Longman's algorithm is the convergence of the 2-norm, that is the sum of all the errors within a single cycle. It would therefore be possible the the infinity-norm (single largest error) to grow from cycle to cycle possibly resulting in the valve hitting the end stops. However given the intention to improve an already good response rather than drastically modify the valves tracking this is seen as an unlikely event. However the convergence of the infinity norm will be reported in order to confirm that this assumption is correct.

Taking heed of Park's warning [76] [75] concerning stability and convergence issues as a result of incorrect lag correction, a number of measures were implemented in order to protect the test rig and ensure good learning transients over and above Longman's guarantee of monotonic convergence.
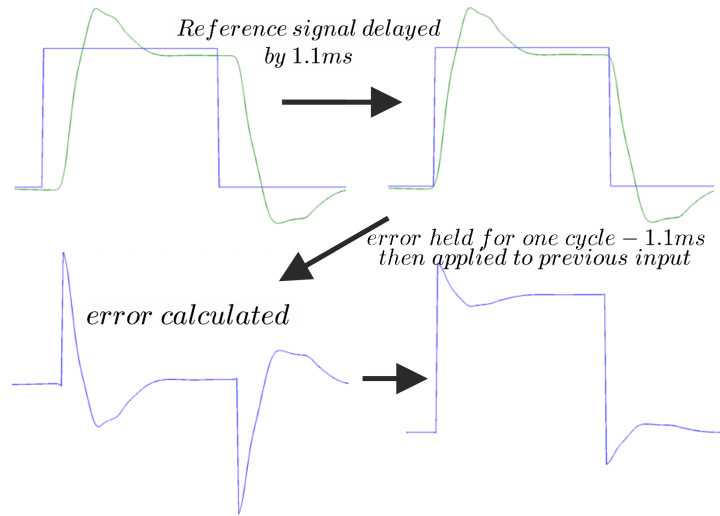
Figure 5-5: Addition of lead to ILC
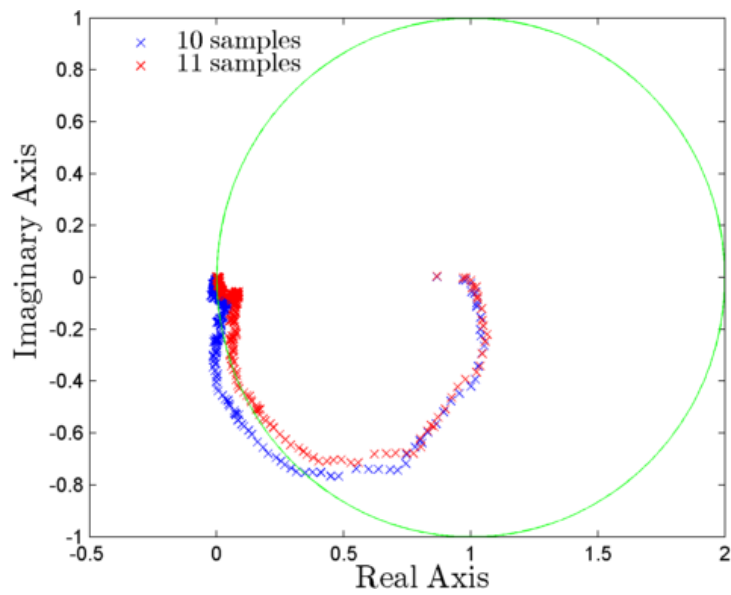
Figure 5-6: Nyquist plot of closed-loop system with lead

5.4 Stop Learning Conditions

These measures all manifest as logical tests which are conducted upon the various signals within the ILC and which have the ability to set $\Phi = 0$. These tests are conducted iteration by iteration rather than latching.

5.4.1 Sufficiency Criteria

The first, and perhaps most useful, of these conditions was termed the sufficiency criteria. That is, instead of comparing the measured response with the reference, a class of acceptable responses were defined and if the response, or any constituent part, met these conditions then no further improvements were made. In order to achieve this the response was divided into four constituent parts, rise, high hold, fall and low hold. An envelope of sufficiently good response was categorised for each part based upon the control aims stated in Chapter 4. Namely, that the rise and fall must happen in 1ms and that each of the holds must have an absolute value between 0.1 - 0.2mm respectively. This can be most easily appreciated graphically as in Figure 5-8. The use of this sufficiency condition begs the question as to how to now calculate error. There are arguments to be made for calculating the error from the ideal response, the closest acceptable response or some nominal response in the middle of the envelope. It was decided to use the closest acceptable response as this should also produce the lowest control effort and therefore acceleration, something that was beginning to become a concern and the subject of the next stop learning condition.

5.4.2 Acceleration Criteria

When the initial ILC experiments were undertaken it was noted that the response improved as expected and, correspondingly, acceleration increased. This started to become a concern as the acceleration began to approach the saturation point of the accelerometer. As the acceleration signal is used within the control system saturation would severely compromise results and could cause instability.
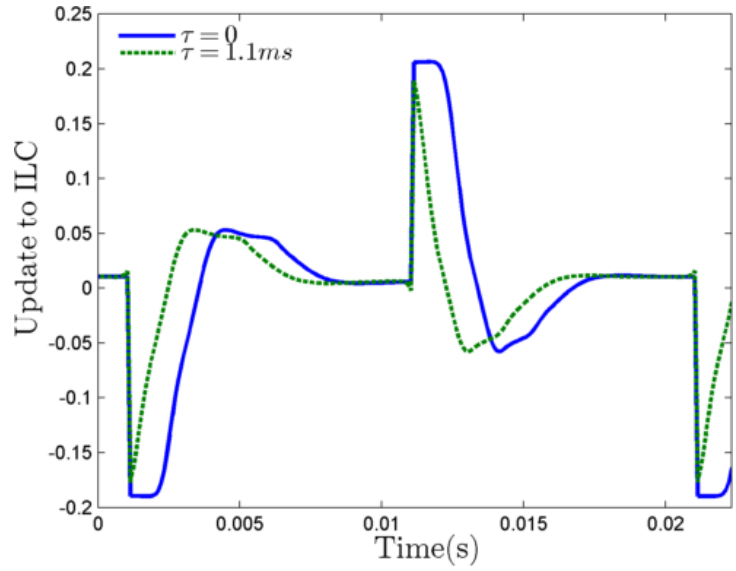
Figure 5-7: Calculated error with $\tau = 0$, $\tau = 1.1ms$
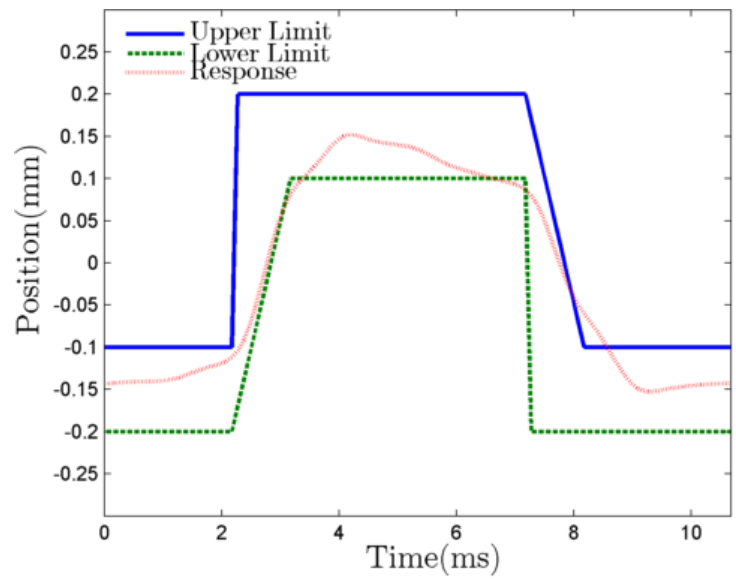
Figure 5-8: Envelope of sufficient responses

Therefore when the acceleration signal peaked above 85% of the accelerometer's limit no learning was conducted in the next iteration to avoid the change possibly causing saturation.

5.4.3   High Frequency Criteria

Whilst not truly a stop learning condition the use of a low pass filter will also be discussed here. As suggested by Longman [68] this filter was applied on the input to the feedback controller rather than just the error signal. Given that lag compensation was already being used it was decided that non-causal filtering offered little advantage and thus a second order Butterworth filter was used with its cut-off set to 700Hz in order to avoid the highly resonant peak of the pilot valve. By applying this filter to the SVF control input for the tests used to determine the optimal number of samples of lead, the delay it introduced was compensated for.

5.4.4   Effect on Convergence

As these stop learning conditions work by setting Φ equal to zero it can be seen that they violate the condition in 5.22 for convergence as when Φ is set equal to zero the equation reduces to:

$$|1 - e^{i\omega} G(e^{i\omega})| < \frac{1}{|Q(e^{i\omega})|}$$
$$|1 - 0| < \frac{1}{|Q(e^{i\omega})|}$$
$$and \quad |Q(e^{i\omega})| = 1 \quad for \ \omega < \omega_n$$
$$\therefore 1 = 1 \quad for \ all \ \omega < \omega_n \tag{5.25}$$

This is not surprising as if there is no learning taking place there can be no convergence. However, if 5.22 is modified slightly to be:

$$|1 - (e^{i\omega})^{\gamma} \Phi G(e^{i\omega T})| \leq \frac{1}{|Q(e^{i\omega T}|)} \tag{5.26}$$

94

it becomes a stability condition rather than a convergence condition and, as shown, this is met in all cases by the stop learning conditions. As expected these stop learning conditions stop convergence but guarantee stability of the ILC scheme.

5.4.5 Implementation

These stop learning conditions were implemented within the xPC system by using a series of subsystems which each housed the necessary logic for a single condition. If the signals did not meet the condition then they were passed to the next condition, if they did then the update signal was set to zero before being passed to the next condition. Each part of the cycle had a separate cascade for the sufficiency, the cycle being broken into four separate regions as seen in Figure 5-9. This was done so that if one part of the cycle met the sufficiency criteria then it
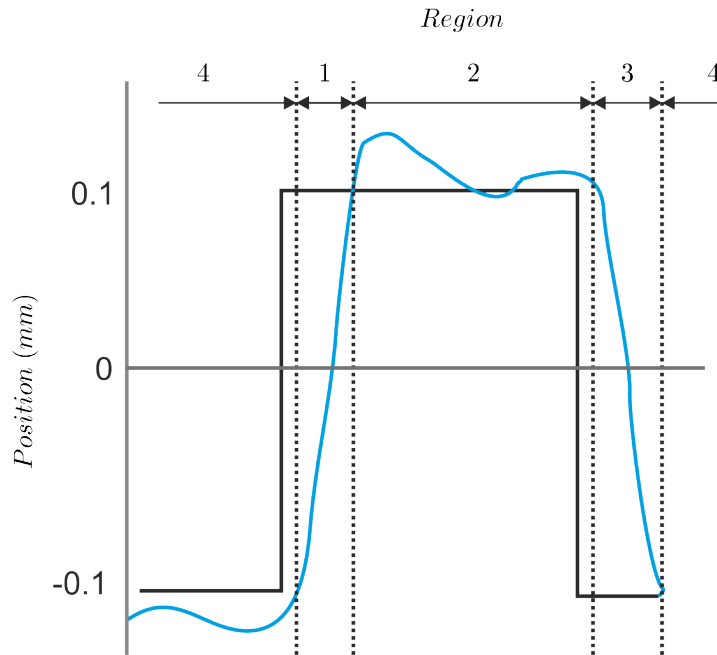
Figure 5-9: Division of cycle into separate regions

could be maintained rather than continuing to attempt to perfect it till all parts of the cycle were sufficient. The logical conditions that were used to split these regions up can be found in Table 5.1. The outputs of these four cascades were

Table 5.1: Logic for dividing cycle into regions

Region	Reference	Begins when Position Crossing	Reference	Ends when Position Crossing
1	>0mm	-0.1mm moving upwards	>0mm	+0.1mm moving upwards
2	>0mm	+0.1mm moving upwards	<0mm	+0.1mm moving downwards
3	<0mm	+0.1mm moving downwards	<0mm	-0.1mm moving downwards
4	<0mm	-0.1mm moving downwards	>0mm	-0.1mm moving upwards

then combined, passed to the acceleration criteria and then filtered, multiplied by Φ and then added to the output from the previous cycle. A block diagram illustrating this process can be seen in Figure 5-10.
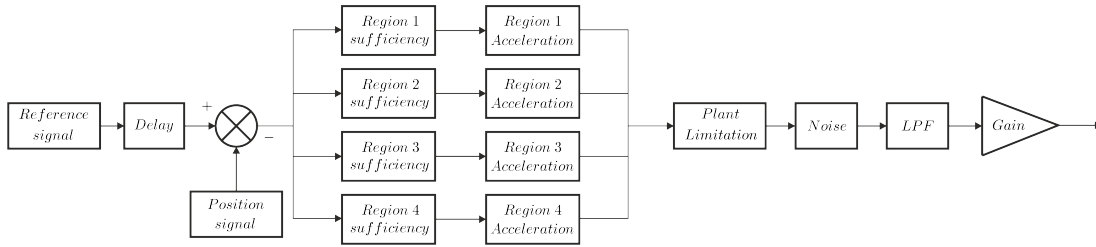
Figure 5-10: Implementation of stop learning conditions

5.5   Results

Using the ILC scheme laid out above significant improvements were obtained over the results shown for the SVF system in Chapter 4. A comparison of the two results at a range of frequencies can be seen in Figure 5-11 and some of the higher frequencies achievable as a result of the use of ILC can then be seen in Figure 5-12 with the corresponding outputs from the ILC and SVF controllers in Figure 5-13. The valve's response has been shifted forward in time by 1.1ms in order to provide a better comparison to the reference signal.

In all these cases the sufficiency condition was responsible for stopping the learning, demonstrating that the combination of ILC and SVF are able to meet the design requirements, even exceeding the required switching time in some cases. In Figure 5-11a a slight downturn can be seen in the ILC response this may be a result of non-perfect zero resetting discussed above. Figure 5-14 shows
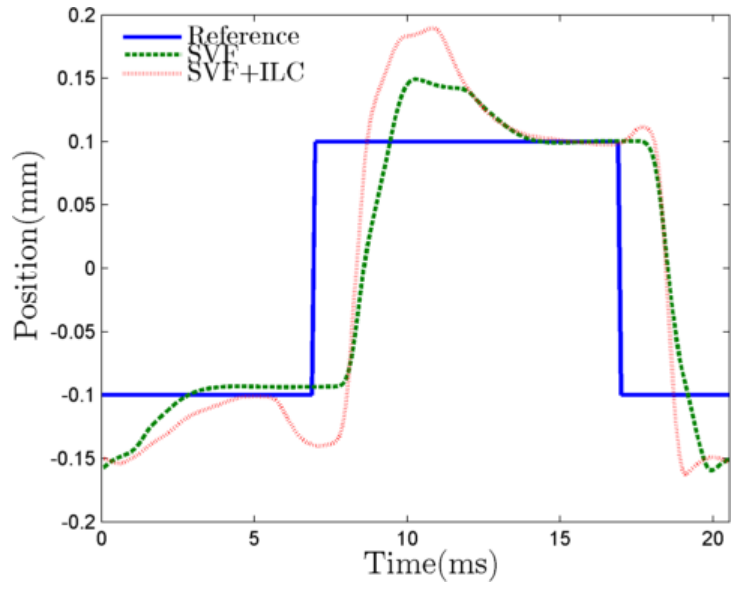
(a) 50Hz
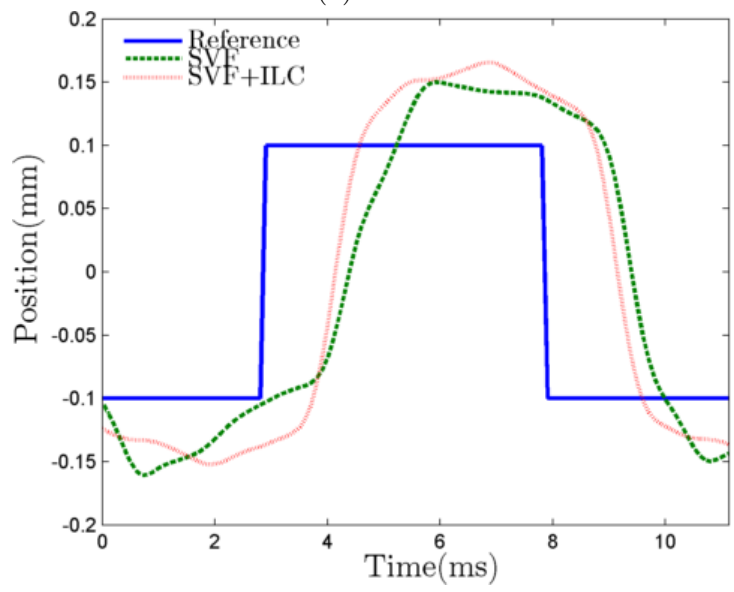
(b) 100Hz

Figure 5-11: Comparison of SVF control with and without ILC

97
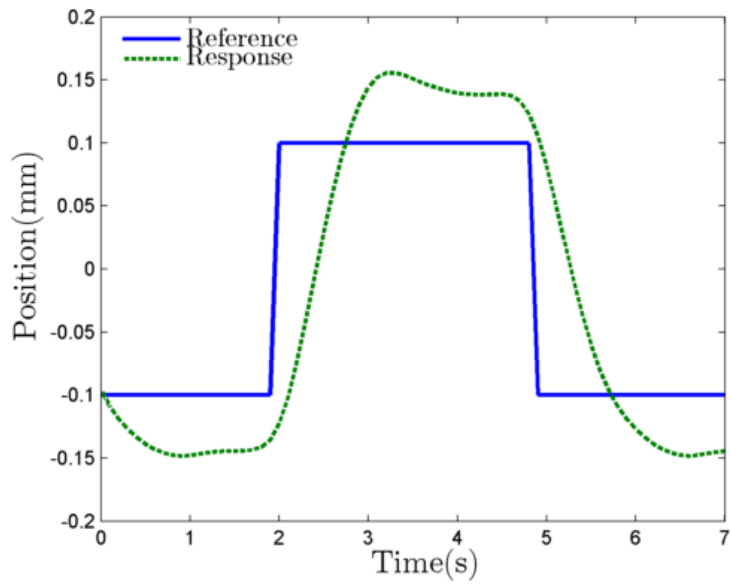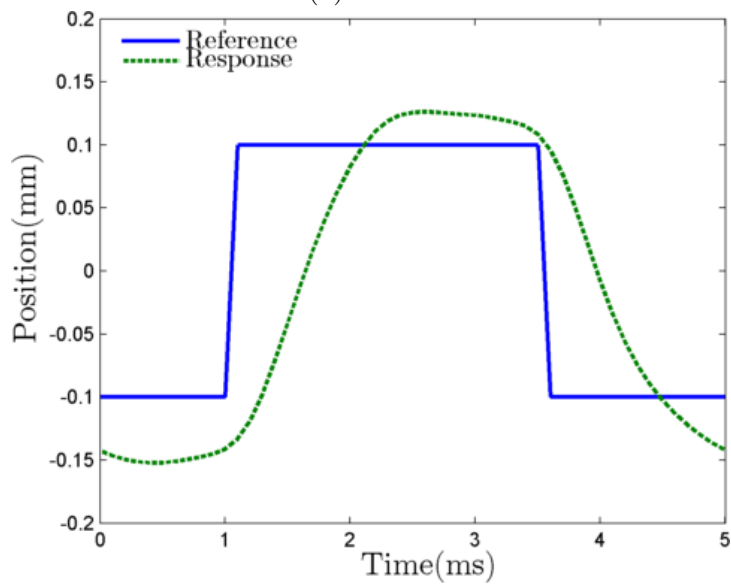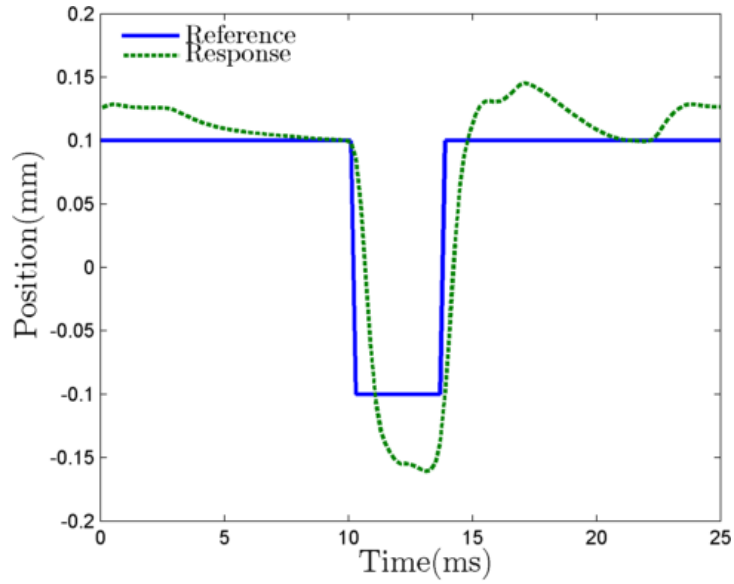
(a) 175Hz

(b) 200Hz

(c) 85% PWM at 45Hz

(d) 20% PWM at 77Hz

Figure 5-12: High frequency control using ILC

99

(a) 175Hz

(b) 200Hz

100
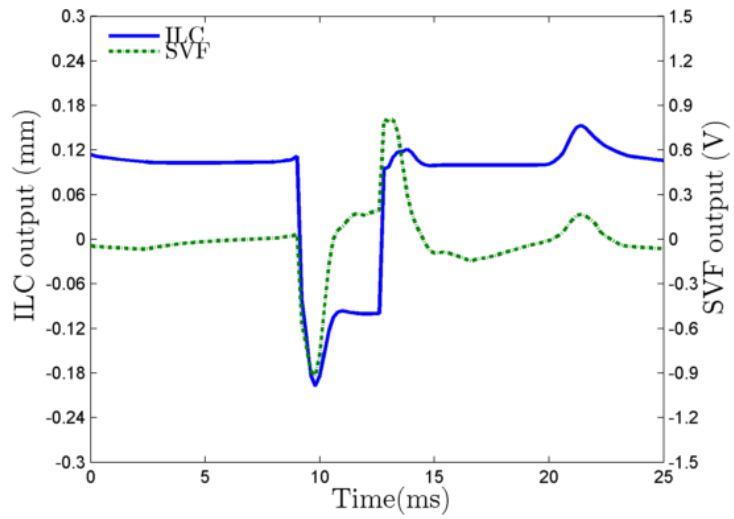
(c) 85% PWM at 45Hz
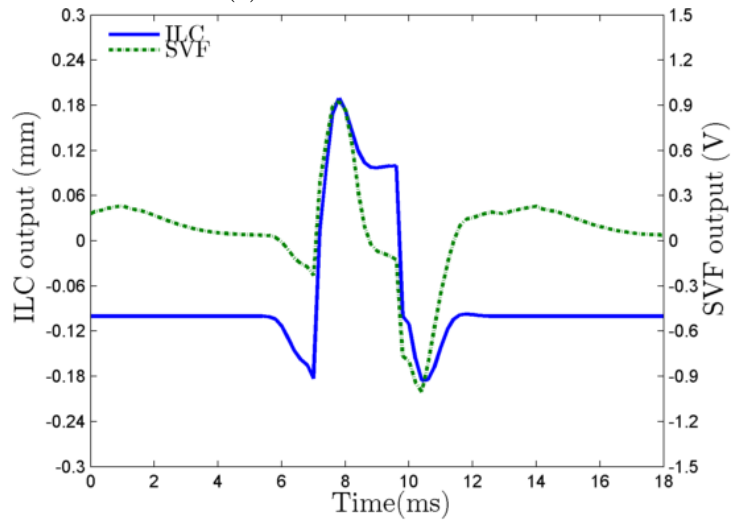
(d) 20% PWM at 77Hz

Figure 5-13: Control signals
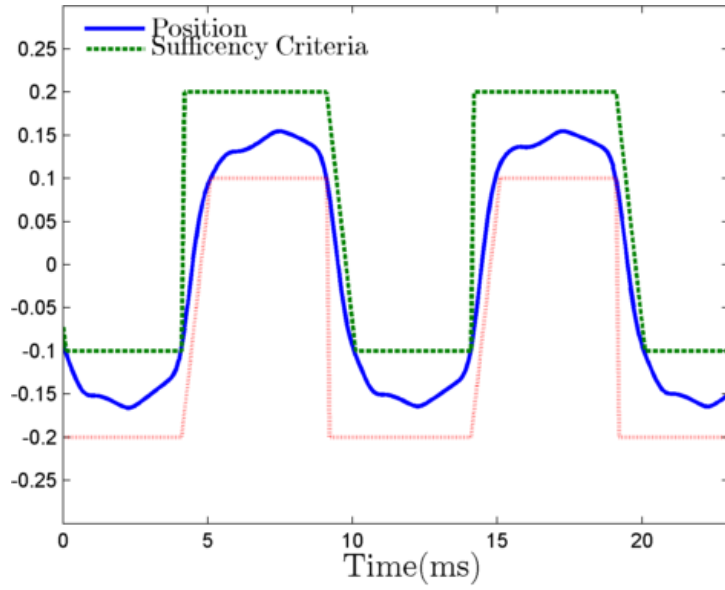
(a) Valve response and sufficiency envelope
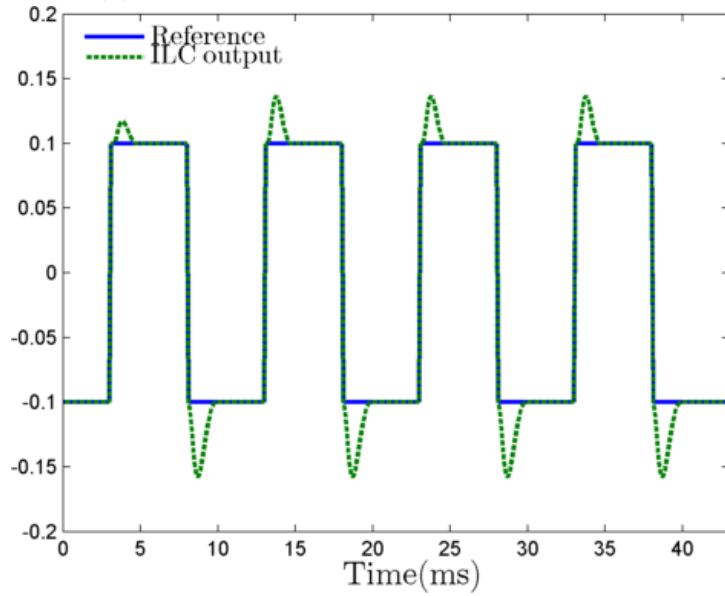
(b) Reference and output of ILC

Figure 5-14: Enacting of Sufficiency condition (100Hz)

the development of ILC output and valve response before and after the sufficiency condition was met for the 100Hz test. In can be seen in Figure 5-14a that the first iteration was not acceptable with the response not rising fast enough, though all other portions of that iteration were sufficient. Figure 5-14b shows the ILC over a slightly expanded time range to demonstrate that learning has stopped for the cycle following the sufficient cycle as the response were also sufficient.

In order to discover the limit of the valve's switching capabilities the sufficient rise time was set to zero and the acceleration criteria relaxed to be 95%, this meant there was a chance that the accelerometer would saturate but if it did the response would not be used to continue learning. It was determined that the largest accelerations accompanied the braking of the valve post switching, therefore the saturation should not stop the accurate representation of switching response. Figure 5-15 shows the converged results achieved using a 200Hz square wave. Figure 5-16 demonstrates the acceleration stop condition working. It can
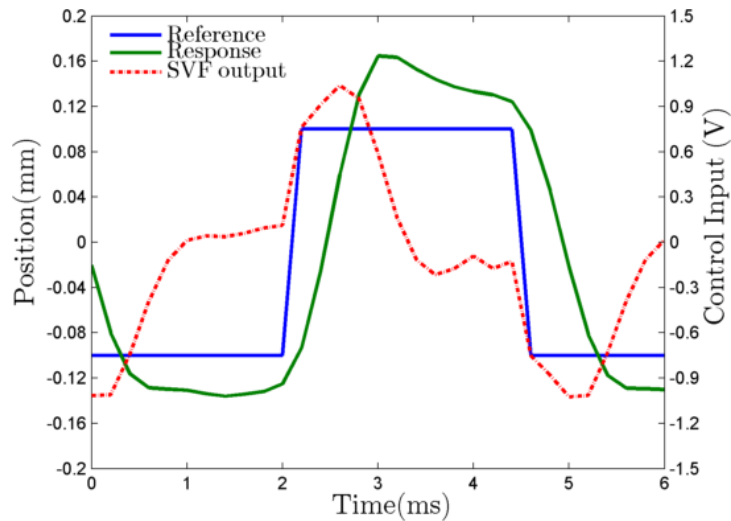
Figure 5-15: Fastest recorded switching time

clearly be seen that when the acceleration passes 95% the ILC stops updating as expected. It can also be seen that before this the correction applied by the ILC is becoming successively smaller as it reduces the error between the reference and response. Table 5.2 shows the fastest switching time recorded by each of the control methods mentioned in this report.

Although of lesser importance it can also be seen that the ILC converges quickly, Figure 5-17, and remains stable over long periods with over 5,000 cycles

103
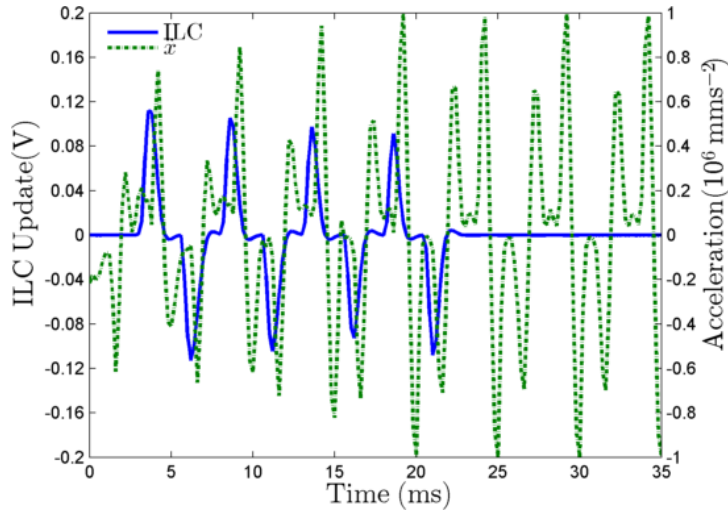
Figure 5-16: Comparison of valve acceleration and ILC update

Table 5.2: Minimum switching times for different control methods

Method	Fastest Rise Time (ms)
PID	1.5ms (Figure 4-7a)
SVF	1.0ms (Figure 4-11)
ILC	0.8ms (Figure 5-12b)
ILC (relaxed acceleration limit)	0.5ms (Figure 5-15)

at 100Hz being logged without any perceivable change from the converged result shown in Figure 5-11b. It should be noted that error is calculated as the total error with reference to the sufficiency conditions rather than the reference.

It can be seen that the convergence of both the 2-norm and the ∞-norm follow a similar pattern with most of the correction being made in the first cycle and full convergence happening after 20 iterations.

5.6   Conclusions

The combination of SVF and ILC was able to deliver the performance required in order to implement a Switched Inertance Hydraulic System of the form laid out in [24]. The fast convergence and stability of the proposed learning system

104

means that it will be easy to apply over a range of conditions with the conditions that the minimum pulse period be in excess of 2.5ms, equivalent to the period of the fastest square wave tested. Even though good convergence is shown the current control strategy is probably not acceptable when the SIHS is used as a control element for another system as the convergence time will significantly limit the bandwidth of control the SIHS can deliver. Current results show that the majority of convergence happens in the first iteration but unless this can be guaranteed it could pose a problem.
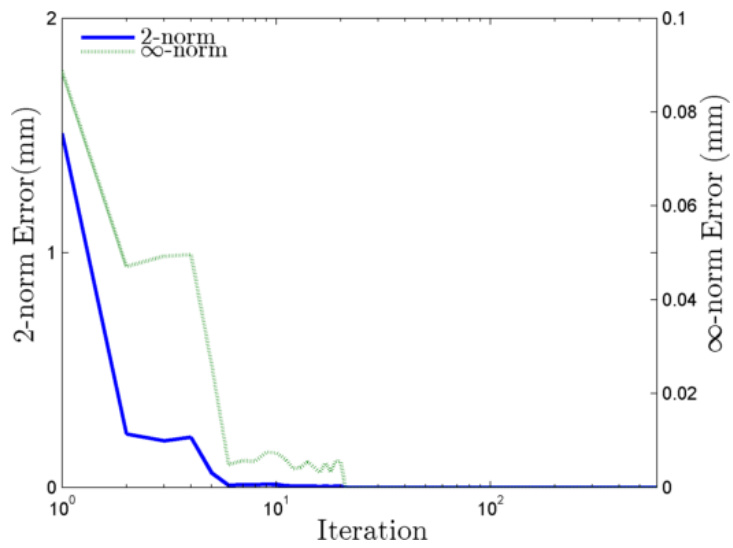
Figure 5-17: Convergence of ILC scheme for a 100Hz square wave

Chapter 6

Switched Inertance Hydraulic System

6.1 Introduction

At the outset it was clearly stated that the purpose of this report was to develop a valve that enabled the testing of Switched Inertance Hydraulic Systems. This chapter details the initial testing conducted in order to demonstrate the valve's suitability for this purpose.

6.2 Flow Loss Optimisation

The ideal frequency for each switching ratio should have the same minimum pulse width [24] which is related to the delay of pressure pulse reflection within the inertance tube. Therefore longer inertance tubes allow for slower switching times. If losses within the valve are neglected then a simple formula can be used to find the optimal switching frequency [24]:

$$f = \left\{ \begin{array}{ll} \frac{\alpha \cdot c}{2L} & 0 \leq \alpha \leq 0.5 \\ \frac{(1-\alpha)c}{2L} & 0.5 < \alpha \leq 1 \end{array} \right\} \tag{6.1}$$

where α is the switching ratio, c is the speed of sound (assumed to be 1350m/s) and L is the length of the tube, 1.6m. At α=0.5 therefore a switching frequency of 211Hz is required, this is believed to be in the range of the valve. This very simple model is based on lossless switching - something not present in the real world - and thus in order to find the minimum flow loss a bounded interior-point optimisation algorithm was used to minimise the flow loss, as defined in Chapter 1, over a range of pulse widths instead of simply calculating the flow loss with the suggested optimal switching frequencies. For the initial tests the HP line was held at 30bar and LP line at 20bar and the more simple SVF controller was used. The optimisation algorithm was bounded to have a minimum pulse length of 2.5ms: the shortest tested with the SVF (Figure 4-12a). Figure 6-1 shows the measured flow loss and efficiency of the SIHS over a range of pulse widths.

The flow loss was relatively constant until α=0.45 after which it increased greatly. It was found that the position sensor had slipped by -0.07mm within its holder and as a result the opening to HP was very small and resistance in this path correspondingly high. This naturally had more of an effect at higher switching ratios. The results from the lower switching ratios, however, are encouraging, showing a good efficiency over a considerable range of switching ratios. In order to confirm that the slippage in position sensor location was at fault another test was conducted at 100Hz and α=0.5 and an increased valve opening, this time using the ILC scheme. Figures 6-2 and 6-3 show the valve's response and the pressures within the SIHS under these conditions. The demanded square wave is clearly visible in the outlet pressure of Figure 6-3a, along with superimposed oscillations from the LP and HP ports. These oscillations do not appear to affect the mean HP and LP pressures as they are at higher frequencies. Figure 6-3b also shows that the pressure at the outlet of the inertance tube is almost equidistant from HP and LP as implied by the switching ratio of 0.5. After this confirmation that the SIHS was responding more as expected it was decided to modify the position sensor holder in order to reduce the risk of slippage in the future and as an attempt to reduce the noise in the position signal. However, the new holder broke during installation resulting in the valve needing to be disassembled and cleaned precluding further testing due to time restraints.
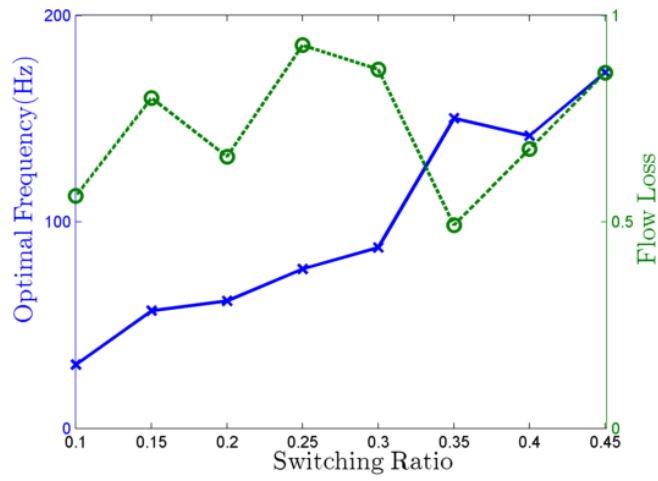
(a) Flow loss of the SIHS
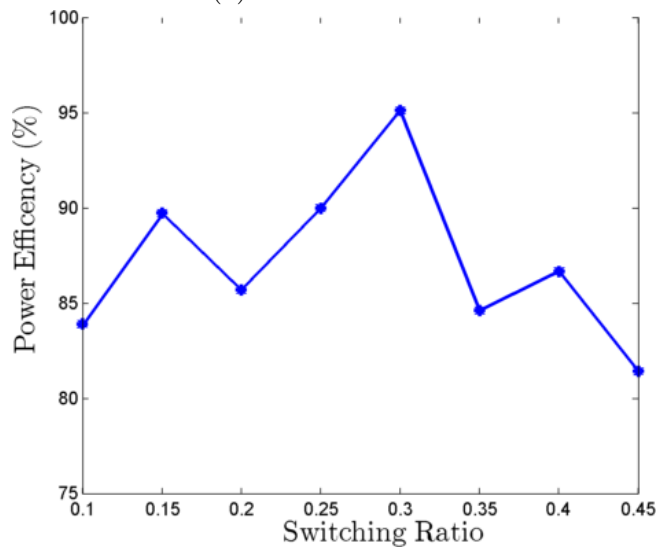
(b) Efficiency of SIHS

Figure 6-1: Performance of the SIHS at varying pulse widths
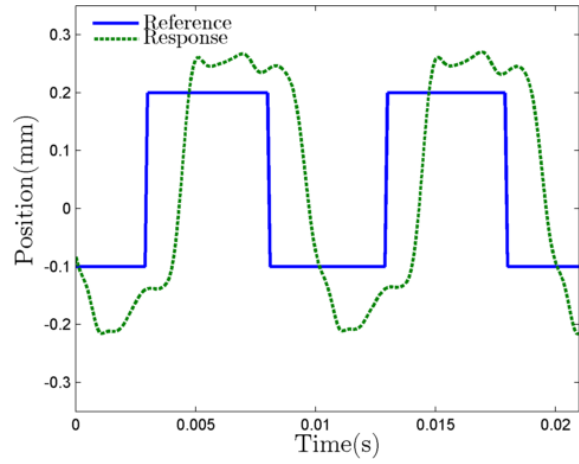
Figure 6-2: Response of valve with increased opening at 100Hz and α=0.5
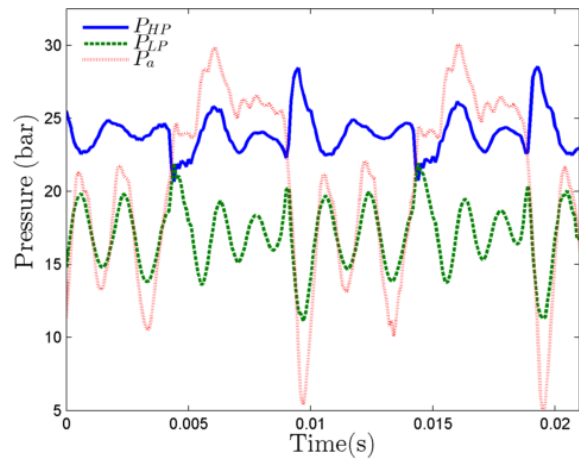
(a) Valve inlet and outlet pressures
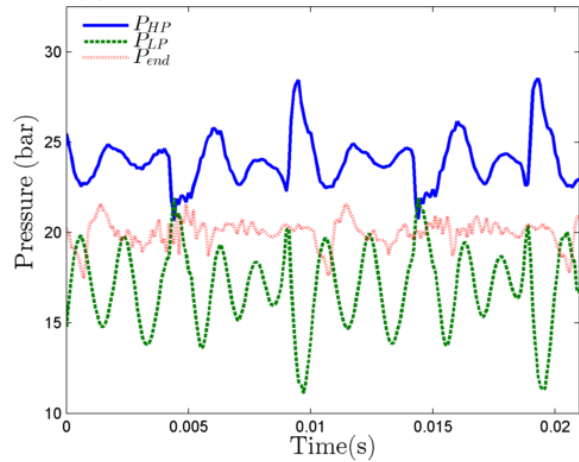
(b) Valve inlet and SIHS outlet pressure

Figure 6-3: Pressures in SIHS switching at 100Hz and α=0.5

6.3 Conclusion

Whilst only a small amount of data was gathered it is clear that at lower switching ratios the SIHS performs well and that the optimal switching frequencies estimated by the model in [25] were relatively accurate. It is necessary to repair the valve and conduct testing over a wider range of switching ratios as well as increased flow rates and pressure differences before any meaningful conclusions as the SIHS performance can be drawn.

Chapter 7

Discussion

Originally it was intended that the control design be a means to achieving the desired valve response. However, in the course of the controller design some results and methods worthy of discussion were generated. As a result this chapter is divided into three sections as, although there is an obvious overlap between the valve and the controller, each are worthy of consideration in isolation and a brief discussion is also given of the initial results found when using the valve in a SIHS.

7.1   Valve

As stated at the outset, the intention of this report is not to present a solution for the digital hydraulic valve problem but rather to chart the development of a digital hydraulic valve with a very specific purpose. Nonetheless it is worthwhile to compare the performance of the valve with other proposed designs. Lantela *et al* [45] provide in their recent paper a comparison of their valve, other digital hydraulic prototypes and two commercially available valves. Table 7.1 appends the performance of the valve in this paper to the list and adds a new metric, rate of change of flow, which looks at how much flow each valve is able to switch. As mentioned in Chapter 1 these figures are biased in favour of the small flow

Table 7.1: Comparison of digital hydraulic valves (modified from [45])

	Presented Valve	Valve from [45]	Valve from [41]	Valve from [46]	Valve from [47]	Hydac [45]	Parker [45]
Response Time (ms)	0.5-1	0.9-1.3	1.2-1.5	2	1.5-2	12	3.5
Max. Pressure (bar)	>200	>300	200	21	30	25	35
Flow(L/min@10bar)	50.5	4.7	0.3	3.3	15	17	21
Volume (cm^3)	26.4	4	2.4	7	88	73	559
Specific Flow $(L/min)/cm^3$	1.91	1.18	0.13	0.47	0.17	0.23	0.15
dQ/dt($\Delta L/mins^{-1}$)	101×10^3	52.2×10^3	250	1650	10×10^3	1416	6000

small volume prototypes. Therefore in order to give an accurate comparison with the greatest number of other prototype valves the volume used to calculate the specific flow of the valve presented in the report was that of the switching element. If the total volume of the valve is used then the flow density drops significantly, though it should be noted this is mainly due to the need to prototype the valve. The reported response times also differ in how they are derived. The 0.5ms stated for the presented valve is the time that the valve takes to switch from fully closed to fully open, this is achieved using a lag compensated ILC and so has an advantage in being able to pre-empt the demand signal, if the purely causal SVF controller were used then the response time would instead be closer to 2ms to include the lag and the switching time. Despite these reservations it can be seen that although not intentional the valve discussed here is actually quite competitive in the key metrics of flow density and response time. This can be attributed to two successful departures from the beaten path. Firstly the use of position control and secondly incorporating the actuation for multiple switching 'devices' into a single package. These also help the valve to come out on top in the appended metric, which is admittedly somewhat partisan. It provides a measure of fitness for the application of valves to SIHS where the two key considerations are fast switching and low flow resistance [24] and so favours the valve detailed here which was designed with this in mind but also highlights the success with which it achieves this aim.

No evidence of other position controlled digital valves could be found, with all other prototypes utilising a bang-bang arrangement with various actuation methods. The ability to position control the valve, along with the design of the grooves means that settling time can be replaced with the inherently faster switching time as the valve is effectively 'on' (connected to HP) from 0.1mm up to 0.3mm with the behaviour of the valve within this bound theoretically having no effect, other than possibly slowing down the next switch. The implementation

of a similar overlap in a bang-bang valve would necessarily come at the cost of the response time as the valve could not be returned to the 'just' fully open location (+0.1mm in this case) but must instead stay at its extreme. The other large advantage of position control with regards to SIHS is that the upper extremes of PWM SIHS becomes less efficient than throttling control, as the energy lost to throttling is less than the inefficiency of the SIHS. Therefore being able to take a hybrid approach where the most efficient control method is used can increase overall system efficiency. Another advantage which is realisable in almost all digital hydraulic systems is the ability to ease retrofitting. By being able to operate as a normal spool valve a failure of the digital control methodology doesn't leave machines unusable, and, for new test rigs it provides an easy method of comparing the two control methods. Finally, using position controlled devices instead of bang-bang devices removes some of the problems surrounding the robustness and wear within digital hydraulic valves. The valve is able to switch at frequencies in the region of 200Hz. This equates to almost a million collisions an hour if operating in a bang-bang mode and so the use of position control obviously provides a good way of increasing the robustness and reducing the wear of the the valve.

Most of the proposed digital hydraulic valves are self contained switching units intended to be used in parallel to generate high flow rates. There is one departure from this [42] which used a single actuator for multiple switching elements. This removes one of the advantages given from digital fluid power in [8]. With a common actuation stage a failure here will now cause the entire system to fail whereas the failure of a single paralleled valve results only in a lower flow rate or higher pressure drop. However, the advantage gained by this method is the cost difference and size difference between similar numbers of switching elements. For example in [42] sixteen switching elements were used but if eighteen or possibly twenty elements were desired there would be no increase in volume and a minimal increase in cost for the extra machining. However, with self contained valves there is a roughly linear relationship between number of switching elements and both cost and volume. They are therefore advantageous for smaller numbers of switching elements but at some point even the cost savings arising from standardisation mean that common actuation stages will be more cost and space efficient. Integrating the actuation of the switching elements also solves another problem, that of managing the timing of multiple valves opening and closing. By having a

single actuation module for all switching elements the relative opening and closing of the valves is determined by geometry rather than requiring careful control. This could possibly be a disadvantage as a change in relative switching could only be achieved in hardware, but no current digital hydraulic circuits currently require this ability to change relative switching. As well as simplifying the system level control, it simplifies the control infrastructure, with only a single electrical connection per block of switching units rather than one per valve. Four grooves were used to achieve the design flow rate of 65L/min at 10bar (closer to 50L/min in testing) it would be a fairly trivial exercise to add more grooves (within reason) when machining the spool and sleeve. This would require the controller design to be evaluated however as the valve dynamics would likely change, although it is unlikely that this would be sufficient to stop the current approach from being valid.

The valve has some obvious advantages and demonstrates that there is perhaps reason to once again consider position controlled valves, for the purposes of experimentation and development, even if bang-bang valves are more suitable for mass production. However, there remain a number of key challenges to be overcome with regards to valve design. The largest of these issues is actuation power supply. In Chapter 3 the actuation stage could be seen as being supplied from a dedicated power supply. This was expedient for testing purposes as it assured a consistent supply of fluid at 200bar. It is also, however, highly inefficient. Currently, most of the power generated is exhausted through a relief valve as the actuation stage requires <0.15L/min, significantly smaller than the power pack's rated flow. One possible solution would, of course, be to reduce the size of the pump considerably. The micro pump presented in [107] for example could theoretically meet the flow requirements of the actuation stage. Commercially available micropumps of the type produced by Hydroleduc could be utilised to manufacture a more suitably sized power pack. Further to this they are also bidirectional, meaning it may be possible to do away with the pilot valve and create a very small Electro Hydraulic Actuator (EHA) with a closed circuit. There is currently little information on the dynamic behaviour of these pumps, which could be limiting. Another alternative that is appealing is the idea of a recursive SIHS. Much in the same way that valves have multiple stages of progressively larger sizes it should be possible to have a small SIHS, whose valve could be ac-

tuated electronically, provide a constant pressure to the actuation stage by taking flow from the HP supply to the main stage of the valve and switching it to the 200bar required. Given the very small flow rates required the actuation SIHS could be fairly compact. A self enclosed SIHS is presented in [26] with a coiled inertance tube used to further minimise the volume. A similar approach, though with significantly smaller flow rates, could be adopted. It may be possible to use the SIHS as the control element as well as power source, removing the need for the pilot valve, depending on the bandwidth of the valve used in the pilot SIHS. Further study into this concept is needed before any definitive conclusions as to its applicability are made. The third actuation method under consideration is the use of a strain energy accumulator. Unlike the more common gas type accumulators strain energy accumulators, as documented in [108–110], theoretically produce constant pressure for almost the entire contraction of the accumulator. This makes them a very good pressure source and a 10L accumulator would be sufficient to run for over an hour. The accumulator charging could then either be built into the work cycle or done when the circuit was in idle. There are however a number of hurdles to overcome before strain accumulators are a viable technology including problems with manufacture, a disconnect between modelled and measured results and longevity concerns. If the strain accumulator route were to be pursued or if the SIHS was found to be of insufficient bandwidth to control the actuator directly then it would also be advantageous to replace the pilot valve with one of a smaller flow and larger bandwidth. As mentioned in Chapter 2 the valve has a significantly higher rated flow than required. The biggest control input used does not exceed 11% of the total range of the valve, a more suitably sized valve may therefore be able to produce even faster switching times.

The other key challenge lies with the control. Currently what appears to be a novel non-causal ILC is implemented in the forward path. Instead of delaying the error command to compensate for lag as is done in [70, 75, 76] the reference is delayed and the calculated error then moved forward in time when the correction is applied as documented in Chapter 5. By using this non-causal ILC in conjunction with a sub-optimal SVF controller it was possible to achieve switching times of 0.5ms and above whilst maintaining zero steady state error once converged. This is believed to be the fastest published 'settling' time, as switching is analogous to settling in bang-bang configurations. However, due to the non-causal nature

of the control system this can only realistically be achieved for repetitive inputs of the type used in the initial testing of SIHS. Once this testing at set points has been completed the next logical step is to attempt to use the SIHS as a control element. Therefore it cannot be assumed that the reference signal is repetitive, meaning the non-causal ILC must be replaced. Chapter 4 shows that the SVF alone is capable of achieving the desired switching time (1ms) but at low frequencies it exhibits steady state errors. The controller is known to be sub-optimal and thus it should be possible to improve the response by tuning the feedback gains. One possible way of maintaining the performance improvements of the converged ILC results whilst removing the requirement for repetitive reference signals is to move the ILC from a cascaded feedforward controller to an indirect tuning controller instead. By using a learning period of repetitive signals the ILC can be configured to modify the gains of the SVF. Once the ILC has converged it can then be switched off and straight feedback control undertaken using the tuned SVF controller. Another possibility would be to change the update law of the ILC for a casual update law, confirm the suitability of its converged performance and then use the equivalence of causal ILC and feedback control as stated in [111] to develop a feedback controller. However, this equivalence does not necessarily hold in real world systems [74], nor does it guarantee that the equivalent feedback controller is stable [112]. The final proposed solution is to attempt to fit a feedforward controller of suitable order to the converged ILC reference. Examining the converged ILC reveals a few common trends, such as an increase in the reference signal, sharpening of the initial response and a lack of symmetry that sees more controller effort being demanded to drive the valve down than up. There is, however, a marked difference between the slower and faster responses with changes made to the slower reference signals to correct the steady state error that is not present at higher frequencies. It is believed that at least one of these three methods should prove sufficient to meet the 1ms and no steady state error condition desired for the application in SIHS, if not surpassing it.

7.2 Control

The application of a State Variable Controller followed a well trodden path, iterative design based upon a nominal model. This process serves as a confirmation of Dutton's wisdom in naming his textbook 'The Art of Control Engineering' [52]. Control is generally considered a science. As such, much of what is published regarding control theory is done so with well reasoned mathematics and absolutes. However, these absolutes seem to blur when introduced to the real world, the hard science of control theory becoming the art of control engineering.

The mathematics remain useful but where a paper may promise stability or an 'optimal' result the reality is that design process remains iterative with the maths and theory giving a road map for this iteration rather than removing the need for it. The success of the SVF controller shows the applicability of this method and a debt is owed to Dutton and others like him who willingly admit that there exists a gulf between the theory and application of control. The control work outlined within this report has been based around this principle, so for this reason there is little of the pure maths associated with the techniques used as this is very well documented elsewhere. Instead focus has been given to the application of this theory and the hurdles this presented. It was the realisation that iterative design is nigh on impossible to avoid that led to an interest in learning controllers, where the task of the control engineer shifted from iterating a controller to providing the controller with the ability to iterate itself. The ILC did have many things that recommended it, particularly as a means of testing the limits of the valves ability, but in part its use was due to the allure of 'teaching' a controller rather than designing one. Aristotle is often misquoted as the source of the following:

'Those who know, do. Those who understand, teach'

Although the original author remains unknown, the argument is compelling and goes some way to explaining why ILC was used when a more conventional form of feedforward control may have been more applicable in the long term.

The formulation of the ILC update law and the application of stop learning conditions are somewhat more novel. This was not by design but rather a result of observations made whilst designing the ILC circuit, with the view to teaching a controller rather than designing one. The decision to include stop learning conditions was made after a review of the literature. Almost all advocates of ILC recommended the use of a low pass filter in order to ensure long term stability, effectively telling the controller to concentrate less on correcting errors above the cut-off and once performance below the cut-off is satisfactory to stop learning even though the response is not perfect. It provides a boundary for learning imposed by the control engineer, blinkers that keep it focused on the what the engineer wants it to do. Park applied a further stop learning condition, a saturation on the correction, [76], however no other evidence of stop learning conditions, or guides to learning could be found. However, there are other conditions that can be logically derived, as was done in Chapter 5. One of these is the saturation condition. This condition attempts to tell the ILC what it cannot correct with regards to the limitations of the plant. The majority of ILC derivation are based around linear models, [74], but all real world plants are non-linear: they have limits. When an ILC is used to maximise the performance of a plant invariably the operation will be approaching, or at, these limits. If no allowance is made for this then there is a real risk of long term stability issues arising from the ILC trying to push the plant past its limits in pursuit of the optimal result. In the specific case of this report the limitation proved to be with the instrumentation rather than the physical plant and thus this limit was explicitly known and was managed by the acceleration criteria. However, if the limiting factor was unknown then by adding a feedback loop within the corrective arm of the ILC it is possible to infer whether the changes being made are having any effect. Comparing the correction from the last cycle and the proposed correction for the current cycle will show whether the previous correction had any effect on the error. If the two corrections are the same (or similar to some degree) then the ILC can be told to stop butting its head against the proverbial brick wall. The other obvious time to stop learning is when the results are good enough. This was of particular importance in this report as the reference signals used were unobtainable square waves. It is hard, mathematically, to prove the effect these conditions had, and any attempt to do so will be left to greater minds, but a good case can be built

logically to support the use of the stop learning conditions mentioned in Chapter 5 in ILC systems that utilise linear update rules. For non-linear update laws some of the assumptions start to break down, though with minor modification most could still be made applicable. ILC is a highly capable but wholly unintelligent tool and by providing guidelines for it the extremes of the valve's ability could be charted, with the bandwidth of the accelerometer providing the ceiling to switching performance, though the fastest switching time of 0.5ms achieved is still of note.

7.3   Conclusion

As with most research as many questions as answers have been posed by the work presented in this document. A more formal and structured further work section detailing these questions and the paths down which it is suggested answers be sought can be found in the next chapter. An attempt will also be made to summarise what has been discovered.

Chapter 8

Conclusion

8.1   Conclusions

The primary aim of this project was to develop a fast switching linear valve to enable the testing of Switched Inertance Hydraulic Systems (SIHS). The requirements for SIHS were derived from the collective work of [5, 24, 49] as being the ability to switch and settle from HP to LP in 1ms whilst reproducing a range of PWM signals and provide a high flow rate (>50L/min at a 10bar pressure drop). A welcome consequence of this aim was to hopefully contribute to the commonwealth of knowledge with regards to digital hydraulic valves and Iterative Learning Control.

The valve's design, like most proposed designs, used multiple small switching elements in order to achieve the high flow rates and fast switching rates required. In this case multiple grooves were machined onto a single spool, centralising the actuation of the spool and eliminating problems with controlling opening and closing timings. However, it differed from the norm by using position control instead of bang-bang actuation. This was significantly easier to implement with centralised actuation as it needed be done only once for the four grooves rather than being done individually which would add complexity to the timing problem. This was done to bolster the robustness of the valve in the face of the high

number of cycles expected, however there was a positive upshot. Namely, that settling time requirements could be replaced with switching time requirements as the design of the spool means that at ±0.1mm it is theoretically fully open and remains so until ±0.3mm meaning that as long as the spool remains between these two extremes it can be considered to be settled.

In order to enable the prototype manufacture of the valve some compromises were necessary in the design. Foremost of these was the use of a too large servo-valve for the pilot stage. The Moog E050-899 used as a pilot stage has a rated flow of 29.5L/min at 65bar whilst a flow of less than 1L/min at 200bar was actually required. This in itself is not a problem. However, the Moog valves dropped off above 300Hz and had a resonant peak in its response at 1kHz, effectively providing a limit on the control bandwidth. Other compromises included an overly large main stage housing, which, whilst not affecting the valve's performance could later cause problems with fitting the valve into a test rig and also the use of o-rings as seals which is likely to increase the break-away force somewhat. An attempt was made to include all these effects in the non-linear model developed of the valve. It was found that using this model and a Zieger-Nichols tuned PID controller it was possible to achieve a switching time of around 2ms. When tested on the actual valve PID control performs a little better giving a minimum switching time of 1.5ms.

A test rig was created which had the full functionality required to begin SIHS testing. For the majority of the control tests the main stage had little or no pressure difference across it, meaning it acted as a lubricating flow rather than a SIHS, though as the spool is pressure balanced this should make little difference. The HP and LP ports of the main stage were both supplied from the same power pack via a pair of relief valves. This caused some problems with pressure pulsations but was workable. What was untenable in the long run is the supplying of actuation pressure from a separate power pack as was done for testing. Initial steady state tests showed that for a 10bar pressure drop the valve flowed 50.5L/min at 30℃ and rather than being zero-lapped as intended, had an overlap of around 0.15mm giving rise to some leakage between stages when switching.

Through the use of a State Variable Feedback (SVF) controller the switching time was reduced to 1ms. This controller was designed using quadratically optimal methods and an identified model of the valve. It was possible to measure the position and acceleration of the valve's central shaft using the instrumentation on the valve and from these calculate velocity giving access to all the states in the model allowing full state feedback. The data from the position sensor and accelerometer were combined using complementary filters in order to extend the bandwidth of all the state measurements to 0Hz-5kHz with the upper limit being dictated by sampling frequency of 10kHz. The optimal method was used iteratively with changing weights on the various states and controller effort until a suitable response was found when testing on the linear model. It was found that this method produced responses that were too damped, giving slow switching times and very small overshoots unless very large gains were used. This was likely a result of the design method used being optimal for regulators rather than position tracking with the natural integrative action of a hydraulic cylinder proving insufficient to overcome this sub-optimality. The knowledge gained from this iterative process was applied to empirically tuning the controller gains. The empirically tuned controller produced a switching time of 1.2ms when applied to the valve model and 1ms when applied to the actual valve whilst utilising only 9% of the input range. At low frequencies the valve struggled to hold a high position, possibly due to leakage between the second and third stages. Given this fact and the amount of remaining input range it was determined that a better response could be achieved, it was decide to use a learning feedforward controller to do this.

The reasons for using a learning controller were twofold. Firstly, given the repetitive nature of the demand signals used in SIHS testing, an Iterative Learning Controller (ILC) provided a means of exploring the limits of the valve capabilities. By providing guidelines that told the ILC when it was approaching the limits of the valve it was possible to repeatedly make it attempt to achieve faster switching until it reached the limits. This was achieved using a simple proportional update rule coupled with a non-causal lag compensation technique in which when the reference signal is followed is not deemed important but rather how closely it is followed. Therefore the reference signal has lag added to it in order to calculate the error in the response without any lag, the update calculated

from this error is then shifted forward in time by applying it one cycle minus the lag compensation later. In order to keep the controller stable and heading in the correct direction a set of stop learning conditions were derived. The first of these is the sufficiency condition. This relaxes the convergence target of the ILC from being a perfect response to being a response which meets certain performance targets. The other stop learning condition monitored the acceleration signal to ensure it didn't exceed 85% as saturation could easily lead to instability. Further to these two logical conditions a low pass filter with it's cut-off at 700Hz was also used in order to avoid the resonant peak in the pilot valves response. Using the ILC it was found that the performance criteria given for the valve were easily met and that by relaxing the saturation margin on the accelerometer a switching time of 0.5ms could be achieved. This switching or, by analogy, settling, time is believed to be the fastest of any digital hydraulic valve reported and could likely be improved if the accelerometer had a greater range. The second reason was, in all honesty, curiosity. The prospect of a controller that is taught rather than designed is certainly intriguing and the creation of stop learning conditions helps to provide some guidelines for this learning, some reasoned boundaries which the unintelligent ILC is unable to provide for itself.

Some initial testing was conducted on SIHS using the valve. This showed promising results at low pulse widths but was cut short due to the failure of the position sensor holder. There were however sufficient results to be happy concluding that the valve was suitable for use in SIHS.

In Chapter 1 four objectives were outlined, below is an evaluation of these objectives.

1. **To further the development of the valve first proposed in Kudzma et al [43]** - The steady state performance reported in Chapter 3 exceeds that reported in [43]. It showed a flow rate more than 3 times greater for a 10bar pressure drop and effectively no leakage outside the transition area, though there was a higher leakage during transition. Modifications were made to the tolerances of multiple components in order to reduce the friction within the valve, allowing for easier actuation.

124

2. **To develop a control system for said valve which is capable of meeting the requirements of operating in a SIHS, namely that it switch in 1ms or less and minimise flow resistance. These requirements are derived from the literature in Chapter 2** - The required switching time was achieved using a SVF controller which was designed iteratively, the response was further improved by the addition of a ILC feedforward controller. This featured a novel lag compensation scheme which involved shifting the reference signal before calculating the error. It also utilised two new stop learning conditions in conjunction with a low pass filter. These additions allowed the valve to switch in 0.5ms and removed all undershoot at a range of frequencies and pulse widths, thus minimising flow resistance.

3. **To benchmark the valves performance against those presented in Lantela *et al*** - When benchmarked against commercial and prototype valves in Chapter 7 the valve discussed in this thesis was shown to be highly competitive on the key metric of specific flow and to have the fastest response time all of the valves reported.

4. **To apply the valve to an experimental SIHS in order to show its applicability** - The valve was used to conduct some initial SIHS tests. These showed promising results at low pulse widths but due to slippage in the position sensor the higher pulse widths results were unrepresentative. Whilst attempting to remove the problem of slippage the position sensor holder broke suspending further testing. The results gained suggest the the valve is well suited to use in SIHS but wider ranging tests would need to be conducted in order to confirm this.

8.2   Further Work

A structured and succinct list detailing the suggested areas of further study can be found below. This is intended as a rough guide rather than a detailed map and as such contains some supposition and many divergent possibilities.

8.2.1 Valve Design

The use of position control proved to offer some interesting advantages and is worthy of further consideration. However, it would be possible to use a similar spool design with bang-bang actuation in order to take advantage of the difference between switching time and settling time. The valve design proved successful for SIHS on a test rig but a complete redesign of the position sensor holder is advised in order to stop creepage and reduce noise if possible. If it continues to exist in its current form then a pilot valve with greater bandwidth would also be advantageous.

8.2.2 Valve Actuation

A large hurdle to the valve ever leaving the test bed is the need to supply consistent 200bar flow to the pilot stage. In Chapter 7 a range of alternative hydraulic actuation methods were discussed they are listed below for completeness.

- Recursive SIHS either as pressure source and control element or as a pressure source with separate control element.

- Strain relief accumulator as pressure source.

- Micro pump either directly driving the second stage or providing pressurised fluid to the pilot stage in a closed loop.

All the methods proposed have much to recommend them though the most appealing is perhaps the recursive SIHS. Careful consideration should also be given to electrical means of actuation such as piezoelectrics, solenoids and voice coil actuators. These were dismissed in the original valve design for multiple reasons but there has been marked development since then and a careful study should be conducted before going down the path of hydraulic actuation.

8.2.3   Valve Control

The other hurdle to the valve leaving the test bed is replacing the ILC with one capable of operating without repetitive reference signals. The intention was to fit a simple linear model to the converged ILC outputs thus turning ILC into a design method for feedforward controllers. This was cut short by the failure of the position sensor holder however. The other proposed avenue of exploration would be to use an ILC to tune the SVF controller over a range of references before the ILC controller is stopped, it could then be run periodically to ensure the valve's performance remained satisfactory in the face of wear and changing conditions.

8.2.4   Iterative Learning Control

There are likely a number of other stop learning conditions that could be constructed over and above those given in this report. There is also more investigation that could be done with the stop learning conditions presented here. The most intriguing avenue of research would be with regards to the sufficiency criteria. Currently the error is calculated with respect to the nominal reference but it could be referenced to the closest sufficient response or an arbitrary sufficient response. This could reduce the cycle to cycle modification, possibly increasing stability and convergence time. It may also be possible to use the stop learning conditions to increase the learning gain and thus reduce the convergence time but a fuller study would be required.

8.2.5   Switched Inertance Hydraulic Systems

The focus of this report was never on SIHS themselves. However, it was hoped that some information would be gleaned in the testing of the valve within a SIHS. Sadly this testing was cut short, leaving many questions to be answered. It was shown that the SIHS is viable and, more importantly perhaps, a test bed exists upon which this testing can continue with a valve capable of providing enough bandwidth for extending testing past single conditions to a control application.

8.3 Final Remarks

The intentions outlined at the beginning of this thesis have been met but sadly the aspirations of it remain tantalised but unfulfilled. Hopefully though, the commonwealth of both digital hydraulics and iterative learning control have been left a littler richer for its passing through.

References

[1] P. Achten. Convicted to innovation in fluid power. *Proc. Institution of Mechanical Engineers, Part I: Journal of Systems and Control Engineering*, 224(6):619–621, 2010.

[2] K. Stelson. Presentation on "the centre for compact & efficient fluid power". Scandinavian International Conference on Fluid Power, 2013.

[3] T. O. Deppen, A. G. Alleyne, K. A. Stelson, and J.J. Meyer. Optimal energy use in a light weight hydraulic hybrid passenger vehicle. *Journal of Dynamic Systems, Measurement, and Control*, 134(4), 2012.

[4] R. Henderson. Design, simulation, and testing of a novel hydraulic power take-off system for the pelamis wave energy converter. *Renewable Energy*, 31(2):271 – 283, 2006.

[5] D.N. Johnston. A switched inertance device for efficient control of pressure and flow. In *Proc. ASME Dynamic Systems and Control Conference*, pages 589–596, 2009.

[6] T.A. Minav, P. Sainio, and M. Pietola. Direct-driven hydraulic drive without conventional oil tank. In *Proc. ASME/Bath Sym. on Fluid Power & Motion Control*, 2014.

[7] Peter A.J. Achten. The hydrid transmission. Technical report, SAE Technical Paper, 2007.

[8] R. Scheidl, M. Linjama, and S. Schmidt. Is the future of fluid power digital? *Proc. Institution of Mechanical Engineers, Part I: Journal of Systems and Control Engineering*, 226(6):721–723, 2012.

[9] M. Linjama and J. Tammisto. New alternative for digital pump-motor-transformer. In *Second Workshop on Digital Fluid Power*, 2009.

[10] W.H. Rampden. Gearless transmission of large wind turbines-the history and future of hydraulic drives. Technical report, Artemis IP Ltd, 2006.

[11] J. Taylor, W. H. S. Rampen, A. Roberson, and N. Caldwell. Digital displacement hydraulic hybrids. In *Presented at the JSAE Annual Congress*, 2011.

[12] G. S. Payne, A. E. Kiprakis, M. Ehsan, W. H. S. Rampen, J. P. Chick, and A. R. Wallace. Efficiency and dynamic performance of digital displacement hydraulic transmission in tidal current energy converters. *Proc. Institution of Mechanical Engineers, Part A: Journal of Power and Energy*, 221(2):207–218, 2007.

[13] S. Heitzig, S. Sgro, and H. Theissen. Energy efficiency of hydraulic systems with shared digital pumps. *International Journal of Fluid Power*, 13(3):49–57, 2012.

[14] M. Heikkil, J. Tammisto, M. Huova, K. Huhtala, and M. Linjama. Experimental evaluation of a piston-type digital pump-motor-transformer with two independent outlets. In *Third Worshop on Digital Fluid Power*, 2010.

[15] K. J. Merrill, F. Y. Breidi, and J. Lumkes. Simulation based design and optimization of digital pump/motors. In *Proc. ASME/Bath Sym. on Fluid Power & Motion Control*, 2013.

[16] M. D. Ehsan, W. H. S. Rampen, and S. H. Salter. Modeling of digital-displacement pump-motors and their application as hydraulic drives for nonuniform loads. *Journal of Dynamic Systems, Measurement and Control*, 122(1):210–215, 1997.

[17] A. Dell'Amico, M. Carlsson, E. Norlin, and M. Sethson. Investigation of a digital hydraulic actuation system on an excavator arm. In *Proc. Scandinavian International Conference on Fluid Power*, 2013.

[18] K. Pettersson and S. Tikkanen. Secondary control in construction machinery: Design and evaluation of an excavator swing drive. In *Proc. Scandinavian International Conference on Fluid Power*, volume 9, pages 2–4, 2009.

[19] M. Linjama. Energy saving digital hydraulics. In *The Second Worshop on Digital Fluid Power*, pages 5–22, 2009.

[20] M. Huova, A. Laamanen, and M. Linjama. Energy efficiency of three-chamber cylinder with digital valve system. *International Journal of Fluid Power*, 11(3):15–22, 2010.

[21] T. H. Ho and A. Kyoung-Kwan. Saving energy control of cylinder drive using hydraulic transformer combined with an assisted hydraulic circuit. In *ICCAS-SICE, 2009*, pages 2115–2120, 2009.

[22] F. T. Brown. Switched reactance hydraulics: a new way to control fluid power. In *Proc. National Conference on Fluid Power*, pages 25–33, 1987.

[23] F. T. Brown, S. C. Tentarelli, and S. Ramachandran. A hydraulic rotary switched-inertance servo-transformer. *Journal of Dynamic Systems Measurement and Control-Transactions of the ASME*, 110(2):144–150, 1988.

[24] M Pan, D.N. Johnston, A. Plummer, S. Kudzma, and A. Hillis. Theoretical and experimental studies of a switched inertance hydraulic system. *Proc. Institution of Mechanical Engineers, Part I: Journal of Systems and Control Engineering*, 228(1):12–25, 2014.

[25] M. Pan, J. Robertson, N. Johnston, Plummer A., and A. Hillis. Experimental inverstigation of a switched inertance hydraulic system. In *Proc. ASME/Bath Sym. on Fluid Power & Motion Control*, 2014.

[26] H. Kogler, R. Scheidl, M. Ehrentraut, E. Guglielmino, C. Semini, and D. G. Caldwell. A compact hydraulic switching converter for robotic applications. In *Proc. ASME/Bath Sym. on Fluid Power & Motion Control*, pages 56–68, 2010.

[27] E. D. Bishop. Digital hydraulic transformer-approaching theoretical perfection in hydraulic drive efficiency. In *Proc. Scandinavian International Conference on Fluid Power*, 2009.

[28] M. Heikkil and M. Linjama. Displacement control of a mobile crane using a digital hydraulic power management system. *Mechatronics*, 23(4):452–461, 2013.

[29] M. Linjama and K. Huhtala. Digital hydraulic power management system-towards loseless hydraulics. In *Third Workshop on Digital Fluid Power*, 2009.

[30] H. C. Tu, M. B. Rannow, J. D. Van de Ven, M. Wang, P. Y. Li, and T. R. Chase. High speed rotary pulse width modulated on/off valve. In *ASME International Mechanical Engineering Congress and Exposition*, pages 89–102, 2007.

[31] H. C. Tu, M. B. Rannow, M. Wang, P. Y. Li, and T. R. Chase. Modeling and validation of a high speed rotary pwm on/off valve. In *ASME Dynamic Systems and Control Conference*, pages 629–636. American Society of Mechanical Engineers, 2009.

[32] M. Wang, H. C. Tu, M. B. Rannow, P. Y. Li, and T. R. Chase. Cfd analysis of a novel high speed rotary on/off valve. In *Proc.6th FPNI PhD Symposium*, 2011.

[33] H. C. Tu, M. B. Rannow, M. Wang, P. Y. Li, T. R. Chase, and K. Cheong. High-speed 4-way rotary on/off valve for virtually variable displacement pump/motor applications. In *Proc. ASME/Bath Sym. on Fluid Power & Motion Control*, pages 201–208.

[34] A. A. Katz and J. D. Van de Ven. Design of a high-speed on-off valve. In *ASME International Mechanical Engineering Congress and Exposition*, pages 237–246, 2009.

[35] J. D. Van de Ven and A. Katz. Phase-shift high-speed valve for switch-mode control. *Journal of Dynamic Systems, Measurement, and Control*, 133(1):011003, 2011.

[36] J. D. Van de Ven. On fluid compressibility in switch-mode hydraulic circuitspart i: Modeling and analysis. *Journal of Dynamic Systems, Measurement, and Control*, 135(2), 2013.

[37] J. D. Van de Ven. On fluid compressibility in switch-mode hydraulic circuitspart ii: Experimental results. *Journal of Dynamic Systems, Measurement, and Control*, 135(2):021014, 2013.

[38] S. Yokota. A fast-acting electro-hydraulic digital transducer: a poppet-type on-off valve using a multilayered piezoelectric device. *JSME International Journal. Series 1, Solid mechanics, strength of materials*, 34(4):489, 1991.

[39] H. Zhang and T. Haran. A new type of digital valve actuated by piezoelectric ultrasonic motor. In *The Second Workshop on Digital Fluid Power*, pages 21–32, 2009.

[40] M. Karvonen, M. Juhola, V. Ahola, L. Sderlund, and M. Linjama. A miniture needle valve. In *Third Worshop on Digital Fluid Power*, pages 61–78, 2010.

[41] M. Karvonen, M. Ketonen, M. Linjama, and V. Puumala. Recent advances in miniture valve development. In *Fourth Workshop on Digital Fluid Power*, pages 90–103, 2011.

[42] B. Winkler, A. Pl'oeckinger, and R. Scheidl. A novel piloted fast switching multi poppet valve. *International Journal of Fluid Power*, 11(3):7–14, 2010.

[43] S. Kudzma, D. N. Johnston, A. Plummer, N. P. Sell, A. Hillis, and M. Pan. A high flow fast switching valve for digital hydraulic systems. In *Fifth Workshop on Digital Fluid Power*, page 175, 2012.

[44] N. P. Sell, D. N. Johnston, A. R. Plummer, and S. Kudzma. Control of a fast switching valve for digital hydraulics. In *Proc. Scandinavian International Conference on Fluid Power*. University of Bath, 2013.

[45] T. Lantela, J. Kajaste, and M. Pietola. Pilot operated miniature valve with fast response and high flow capacity. *International Journal of Fluid Power*, 15(1):11–18, 2014.

[46] J-P. Uusitalo, V. Ahola, L. Soederlund, M. Linjama, M. Juhola, and L. Kettunen. Novel bistable hammer valve for digital hydraulics. *International Journal of Fluid Power*, 11(3):35–44, 2010.

[47] A. Plöeckinger, B. Winkler, and R. Scheidl. Development and prototyping of a compact, fast 3/2 way switching valve with integrated onboard electronics. In *Proc.Scandinavian International Conference on Fluid Power*, 2009.

[48] F Breidi, T.r Helmus, M.l Holland, and J. Lumkes. The impact of peak-and-hold and reverse current driving strategies on the dynamic performance of commercial cartridge valves. In *Proc. ASME/Bath 2014 Sym. on Fluid Power & Motion Control*, 2014.

[49] V.J. De Negri, P. Wang, A. Plummer, and D.N. Johnston. Behavioural prediction of hydraulic step-up switching converters. *International Journal of Fluid Power*, 15(1):1–9, 2014.

[50] Parker Hannafin Corp. Fluid power seal design guide. `www.parker.com/literature/Engineered%20Polymer%20Systems/5370.pdf`. Last Accessed On 25/10/14.

[51] A.R Plummer. A detailed dynamic model of a six-axis shaking table. *Journal of Earthquake Engineering*, 12(4):631–662, 2008.

[52] K. Dutton, S. Thompson, and B. Barraclough. *The Art of Control Engineering*. Addison Wesley, 1997.

[53] D.P. Stoten. Fusion of kinetic data using composite filters. *Proc.Institution of Mechanical Engineers, Part I: Journal of Systems and Control Engineering*, 215(5):483–497, 2001.

[54] A.R. Plummer. Optimal complementary filters and their application in motion measurement. *Journal of Systems & Control Engineering*, 220(6), 2006.

[55] T.F. Coleman and Y. Li. An interior trust region approach for nonlinear minimization subject to bounds. *SIAM Journal on optimization*, 6(2), 1996.

[56] T.F. Coleman and Y. Li. On the convergence of reflective newton methods for large-scale nonlinear minimization subject to bounds. *Mathematical Programming*, 67(2), 1994.

[57] C.-Y. Su and Y. Stepanenko. Adaptive control of a class of nonlinear systems with fuzzy logic. *IEEE Transactions on Fuzzy Systems*, 2(4):285–294, 1994.

[58] S. Sastry. *Nonlinear systems: analysis, stability, and control*, volume 10. Springer New York, 1999.

[59] The MathWorks Inc. Prediction error estimate for linear and nonlinear model. `http://uk.mathworks.com/help/ident/ref/pem.html`. Last Accessed On 26/05/15.

[60] P. Young and A. Jakeman. Refined instrumental variable methods of recursive time-series analysis part iii. extensions. *International Journal of Control*, 31(4), 1980.

[61] B. Friedland. *Control system design: an introduction to state-space methods*. McGraw-Hill, 1986.

[62] G. F. Franklin, J. D. Powell, and A. Emami-Naeini. *Feedback control of dynamic systems*. Pearson, 6 edition, 2009.

[63] B.D Anderson and J.B. Moore. *Optimal control: linear quadratic methods*. Courier Dover Publications, 1989.

[64] W. L. Brogan. *Modern control theory, 3rd*, chapter An Introduction to Optimal Control Theory. Prentice Hall, 1991.

[65] Y. Wang and F.J. Gao, F. Doyle. Survey on iterative learning control, repetitive control, and run-to-run control. *Journal of Process Control*, 19(10):1589 – 1600, 2009.

[66] J.-X. Xu and R. Yan. On initial conditions in iterative learning control. *IEEE Transactions on Automatic Control*, 50(9):1349–1354, 2005.

[67] H.-S. Lee and Z Bien. Study on robustness of iterative learning control with non-zero initial error. *International Journal of Control*, 64(3):345–359, 1996.

[68] R.W. Longman. Iterative learning control and repetitive control for engineering practice. *International Journal of Control*, 73(10):930–954, 2000.

[69] J. Xu, T. Heng Lee, and H. Zhang. Analysis and comparison of iterative learning control schemes. *Engineering Applications of Artificial Intelligence*, 17(6):675–686, 2004.

[70] C.-K. Chen and W.-C. Zeng. The iterative learning control for the position tracking of the hydraulic cylinder. *JSME International Journal Series C*, 46(2):720–726, 2003.

[71] K.S. Lee, I.-S. Chin, H.J. Lee, and J.H. Lee. Model predictive control technique combined with iterative learning for batch processes. *AIChE Journal*, 45(10):2175–2187, 1999.

[72] Y. Hu and J. Li. Iterative learning control based pid controller parameter tuning scheme design and stability analysis. In *Proc. Control and Decision Conference*, pages 2361–2365. IEEE, 2010.

[73] E.J. Solcz and R. W. Longman. Disturbance rejection in repetitive controllers. 76:2111–2130, 1992.

[74] D.A. Bristow, M. Tharayil, and A.G. Alleyne. A survey of iterative learning control. *IEEE Control Systems Magazine*, 26(3):96–114, June 2006.

[75] K.-H. Park, Z. Bien, and D.-H. Hwang. Design of an iterative learning controller for a class of linear dynamic systems with time delay. *Proc. IEEE Control Theory and Applications*, 145(6):507–512, Nov 1998.

[76] K. Park and Z Bien. A study on robustness of iterative learning controller with input saturation against time-delay. In *Proc. 3rd Asian Control Conf.*, 2002.

[77] H. Elci, R.W. Longman, M.Q. Phan, J-N. Juang, and R. Ugoletti. Simple learning control made practical by zero-phase filtering: Applications

to robotics. *IEEE Transactions on Circuits and Systems I: Fundamental Theory and Applications*, 49(6):753–767, 2002.

[78] M.H.A Verwoerd, G. Meinsma, and T.J.A de Vries. On the use of noncausal lti operators in iterative learning control. In *Proc.41st IEEE Conference on Decision and Control*, volume 3, pages 3362–3366, 2002.

[79] D. Chen and B. Paden. Stable inversion of nonlinear non-minimum phase systems. *International Journal of Control*, 64(1):81–97, 1996.

[80] X. Wang and D. Chen. Causal inversion of nonminimum phase systems. In *Proc.40th IEEE Conference on Decision and Control*, volume 1, pages 73–78, 2001.

[81] K.S. Lee, Bang S.H., and K.S. Chang. Feedback-assisted iterative learning control based on an inverse process model. *Journal of Process Control*, 4(2):77 – 89, 1994.

[82] H. Elci, R.W. Longman, M. Phan, J.-N. Juang, and R. Ugoletti. Discrete frequency based learning control for precision motion control. In *Proc. IEEE International Conference on Systems, Man, and Cybernetics*, volume 3, pages 2767–2773, 1994.

[83] Y.-J. Liang and D.P. Looze. Performance and robustness issues in iterative learning control. In *Proc.32nd IEEE Conference on Decision and Control*, pages 1990–1995, Dec 1993.

[84] F. Padieu and R. Su. An H_∞ approach to learning control systems. *International Journal of Adaptive Control and Signal Processing*, 4(6):465–474, 1990.

[85] D. de Roover. Synthesis of a robust iterative learning controller using an H_∞; approach. In *Proc.35th IEEE Conference on Decision and Control*, volume 3, pages 3044–3049, Dec 1996.

[86] D. De Roover and O.H. Bosgra. Synthesis of robust multivariable iterative learning controllers with application to a wafer stage motion system. *International Journal of Control*, 73(10):968–979, 2000.

[87] M.Q. Phan and J.A. Frueh. Model reference adaptive learning control with basis functions. In *Proc.38th IEEE Conference on Decision and Control*, volume 1, pages 251–257, 1999.

[88] J.A. Frueh and M.Q. Phan. Linear quadratic optimal learning control (lql). *International Journal of Control*, 73(10):832–839, 2000.

[89] S. Gunnarsson and M. Norrlöf. On the design of ilc algorithms using optimization. *Automatica*, 37(12):2011–2016, 2001.

[90] N. Amann, D.H. Owens, and E. Rogers. Iterative learning control using optimal feedback and feedforward actions. *International Journal of Control*, 65(2):277–293, 1996.

[91] N. Amann, D.H. Owens, and E. Rogers. Predictive optimal iterative learning control. *International Journal of Control*, 69(2):203–226, 1998.

[92] S. Arimoto, S. Kawamura, and F. Miyazaki. Bettering operation of robots by learning. *Journal of Robotic systems*, 1(2):123–140, 1984.

[93] H. Havlicsek and A. Alleyne. Nonlinear control of an electrohydraulic injection molding machine via iterative adaptive learning. *IEEE/ASME Transactions on Mechatronics*, 4(3):312–323, Sep 1999.

[94] H.G. Chiacchiarini and P.S. Mandolesi. Unbalance compensation for active magnetic bearings using ilc. In *Proc. IEEE International Conference on Control Applications*, pages 58–63, 2001.

[95] H. Elci, M. Phan, R.W. Longman, J.-N. Juang, and R. Ugoletti. Experiments in the use of learning control for maximum precision robot trajectory tracking. In *Proc. Conference on Information Sciences and Systems*, pages 951–958, 1994.

[96] K.L. Moore. An observation about monotonic convergence in discrete-time, p-type iterative learning control. In *Proc. IEEE International Symposium on Intelligent Control*, pages 45–49, 2001.

[97] H-S. Lee and Z. Bien. Robustness and convergence of a pd-type iterative learning controller. In *Iterative Learning Control*, pages 39–55. 1998.

[98] Y.Q. Chen and K.L. Moore. An optimal design of pd-type iterative learning control with monotonic convergence. In *Proc. IEEE International Symposium on Intelligent Control*, pages 55–60, 2002.

[99] C-J Chien, C-T Hsu, and C-Y Yao. Fuzzy system-based adaptive iterative learning control for nonlinear plants with initial state errors. *IEEE Transactions on Fuzzy Systems*, 12(5):724–732, 2004.

[100] P. Albertos, M. Olivares, and A. Sala. Fuzzy logic based look-up table controller with generalization. In *Proc. American Control Conference*, volume 3, pages 1949–1953, 2000.

[101] Chien C. and Fu L. A neural network based learning controller for robot manipulators. In *Proc.39th IEEE Conference on Decision and Control*, volume 2, pages 1748–1753, 2000.

[102] T.W.S. Chow and Yong F. A recurrent neural-network-based real-time learning control strategy applying to nonlinear systems with unknown dynamics. *IEEE Transactions on Industrial Electronics*, 45(1):151–161, Feb 1998.

[103] A. Tayebi. Adaptive iterative learning control for robot manipulators. *Automatica*, 40(7):1195–1203, 2004.

[104] D. Sun and J.K Mills. High-accuracy trajectory tracking of industrial robot manipulator using adaptive-learning scheme. In *Proc. American Control Conference*, volume 3, pages 1935–1939, 1999.

[105] A. Tayebi and M. B. Zaremba. Iterative learning control for non-linear systems described by a blended multiple model representation. *International Journal of Control*, 75(16-17):1376–1384, 2002.

[106] The MathWorks Inc. Constrained nonlinear optimization algorithms. `http://uk.mathworks.com/help/optim/ug/constrained-nonlinear-optimization-algorithms.html`. Last Accessed On 23/02/15.

[107] J. Kim, S. Yokota, M. Satoh, and K Edamura. Ecf mircopump-integrated micro hand by mems technology. In *Proc. ASME/Bath 2014 Sym. on Fluid Power & Motion Control*, 2014.

[108] J.M. Tucker and E.J. Barth. Design, fabrication, and evaluation of a distributed piston strain-energy accumulator. *International Journal of Fluid Power*, 14(1):47–56, 2013.

[109] A. Pedchenko and E. J. Barth. Design and validation of a high energy density elastic accumulator using polyurethane. In *ASME Dynamic Systems and Control Conference*, pages 283–290. American Society of Mechanical Engineers, 2009.

[110] E.J. Barth and A Pedchenko. Elastic hydraulic accumulator/reservoir system, May 2013. US Patent 8,434,524.

[111] P.B. Goldsmith. On the equivalence of causal lti iterative learning control and feedback control. *Automatica*, 38(4):703 – 708, 2002.

[112] E. Owens, D.H .and Rogers. Comments onon the equivalence of causal lti iterative learning control and feedback control. *Automatica*, 40(5):895–898, 2004.

Appendices

Appendix A

Published Works

A.1 Published

N.P. Sell, D.N. Johnston, A.R. Plummer, S. Kudzma and Pan, M. A linear valve actuated switched inertance hydraulic transformer. *Proc. Scandinavian International Conference on Fluid Power*, 2015.

N.P. Sell, D.N. Johnston, A.R. Plummer and S. Kudzma. Control of a fast switching valve for digital hydraulics. *Proc. Scandinavian International Conference on Fluid Power*, 2013.

S. Kudzma, D.N. Johnston, A.R. Plummer and N.P. Sell. A high flow fast switching valve for digital hydraulics. *The Fifth Workshop on Digital Fluid Power*, 2012.

A.2 In Process

N.P. Sell, D.N. Johnston, A.R. Plummer, S. Kudzma and Pan, M. Development of a fast switching valve for digital hydraulics. *Proc. ASME/Bath Sym. on Fluid Power & Motion Control*, 2015.

Appendix B

Valve Drawings

SECTION B-B

120,55

248,3
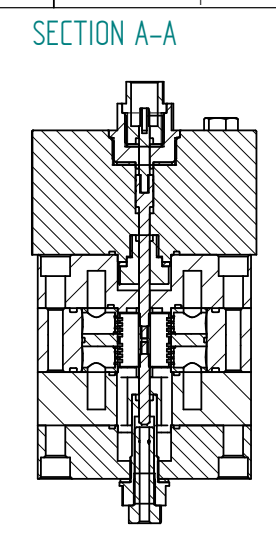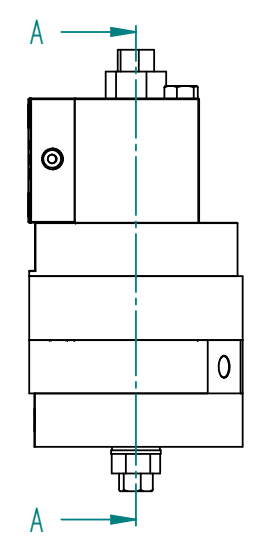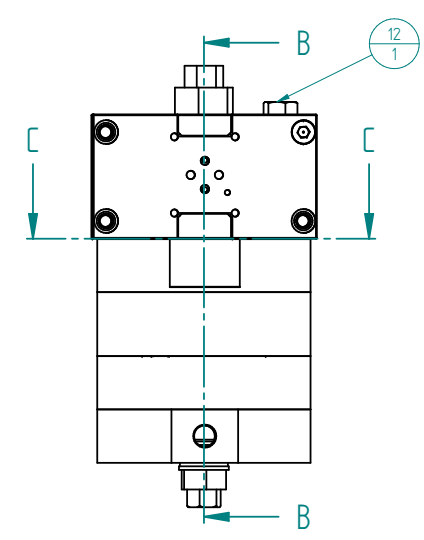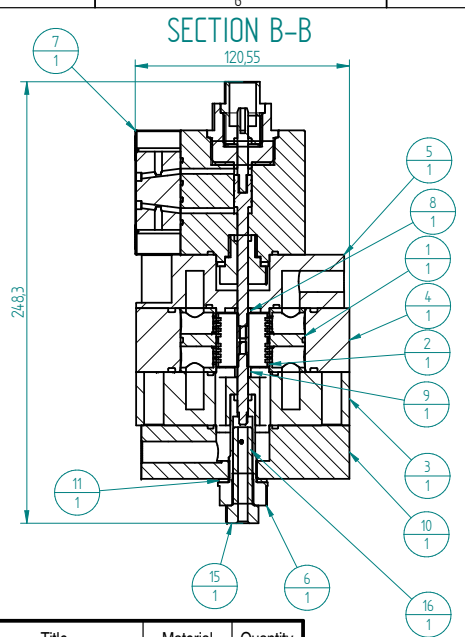
SECTION A-A

SECTION C-C
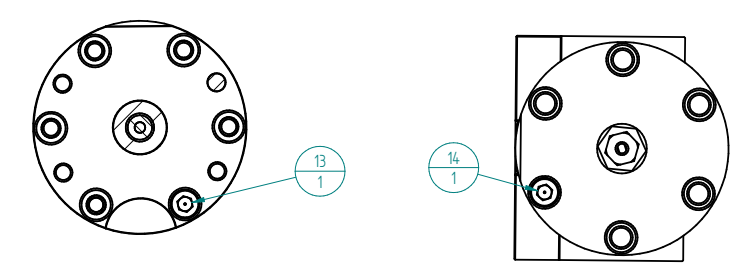
Item Number	Document Number	Title	Material	Quantity
11		Bonded Washer		1
1	01-01	Sleeve	Stainless Steel, 304	1
2	01-02	Spool	Stainless Steel, 304	1
3	01-03	Cover no.1 bottom	Stainless Steel, 304	1
4	01-04	Housing	Stainless Steel, 304	1
5	01-05	Cover top	Stainless Steel, 304	1
6	01-06	Screw Bottom	Stainless Steel, 304	1
7	01-07	Actuation Module	see drawing	1
8	01-08	Bush Top	Stainless Steel, 304	1
9	01-09	Bush Bottom	Stainless Steel, 304	1
10	01-10	Cover no.2 bottom	Stainless Steel, 304	1
12*	01-12	M10 x 96mm Hex	Steel	4
13*	01-13	M10 x 32mm Cap	Steel	6
14*	01-14	M8 x 23mm Cap	Steel	6
15	01-15	Screw no.2 bottom	Stainless Steel, 304	1
17*	01-16	Spool Rod	Mild Steel	1

DO NOT TAKE MEASUREMENTS FROM DRAWING PRINTS. IF IN DOUBT: ASK.

2	25/1/13	NPS		Changed to reflect modified parts and assembly
ISSUE	DATE	DRAWN	APPROVED	DETAILS OF CHANGES

REVISION HISTORY

MATERIAL

PROTECTIVE FINISH

DIMENSIONS IN MM | SCALE AT A2 SIZE:
DRAWN IN ACCORDANCE WITH BS8888
TOLERANCES UNLESS OTHERWISE STATED
LINEAR ±
ANGULAR ±
SURFACE TEXTURE
REMOVE ALL BURRS AND SHARP EDGES
0.5 MAX. RADIUS OR 45°CHAMFER

UNIVERSITY OF BATH
DEPARTMENT OF MECHANICAL ENGINEERING
THIS DOCUMENT IS COPYRIGHT AND THE PROPERTY OF THE UNIVERSITY OF BATH. IT MUST NOT BE COPIED IN WHOLE OR IN PART NOR DISCLOSED TO ANY THIRD PARTY WITHOUT PRIOR PERMISSION FROM THE UNIVERSITY.
© UNIVERSITY OF BATH 2008

PROJECT
Valve

ACTIVITY	NAME	DATE	TITLE
DRAWN	Sylwester Kudzma	2011/04/15	
CHECKED			Valve 01
APPROVED			

THIRD ANGLE PROJECTION

SIZE A2
594mm x 420mm

DRAWING NUMBER
01-00

SHEET No.
OF

ISSUE

SECTION A-A

B

1,45 $_{-0.05}^{0}$

8,5

16,65

19

36 $_{0}^{-0.02}$

2,7

2 x 0.25 x 45°

A

Ra 0.32

ϕ 30 $_{0}^{+0.003}$

ϕ 70 f7 $\left(_{-0.060}^{-0.030}\right)$

Ra 1.6

0.002

0.015 | A

Make a mark to distinguish a spool orientation

ϕ 54

A

A

ϕ 70

8 holes x ϕ 12
18.5 deep
as shown

8 holes x ϕ 10

DETAIL B

2 x 0.25 x 45°

8 grooves x 1 ±0.02

0.005 | A

5,5 $_{-0.005}^{0}$

8,5 $_{-0.005}^{0}$

11,5 $_{-0.005}^{0}$

14,5 $_{-0.005}^{0}$

21,5 $_{0}^{+0.005}$

24,5 $_{-0.005}^{0}$

27,5 $_{0}^{+0.005}$

30,5 $_{0}^{-0.005}$

ϕ 35 $_{0}^{+0.1}$
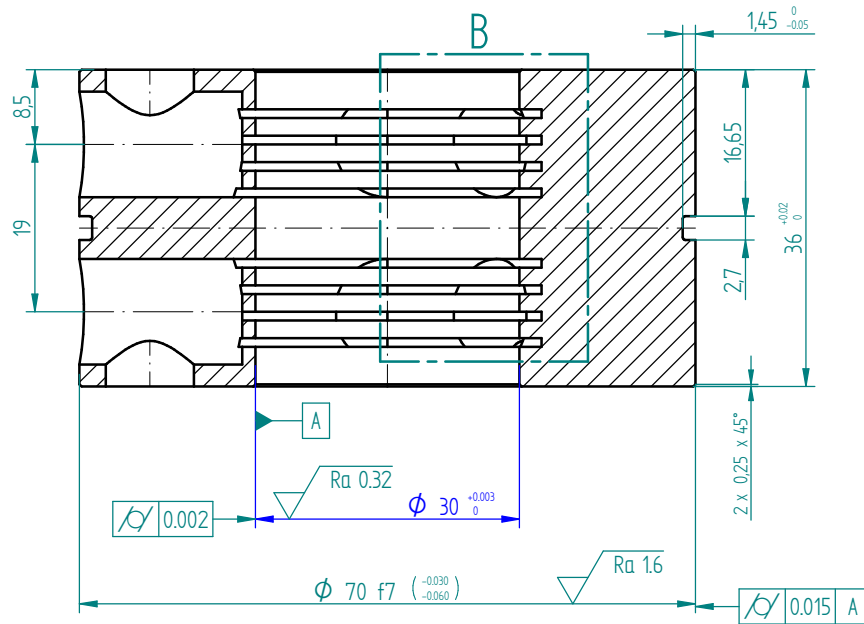
Technical requirement
Assembling relationship: spool has to match the sleeve with the smallest possible radial clearance but enable slight movement

Harden and Temper to min. HRC 55%

Material: Stainless steel
AISI Type 440C

Ra 1.25

sealing groove flanks, groove diameter

Bottom edges of O-ring groove round R 0.3

Unspecified roughness Ra 2.5

Unspecified tolerances ± 0.05

drawn: Sylwester Kudzma
date: 04/03/2013
project: valve
University of Bath

title: Sleeve
Drawing No 01-01

SECTION A-A

A

A

VIEW B

B

A
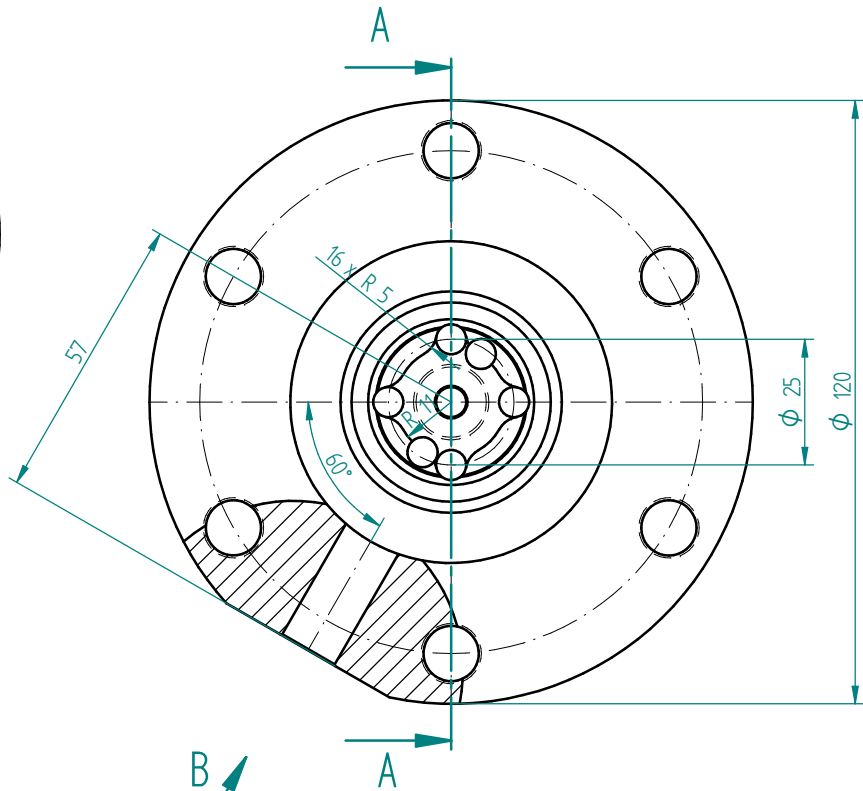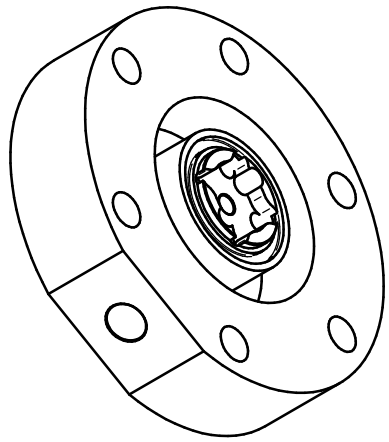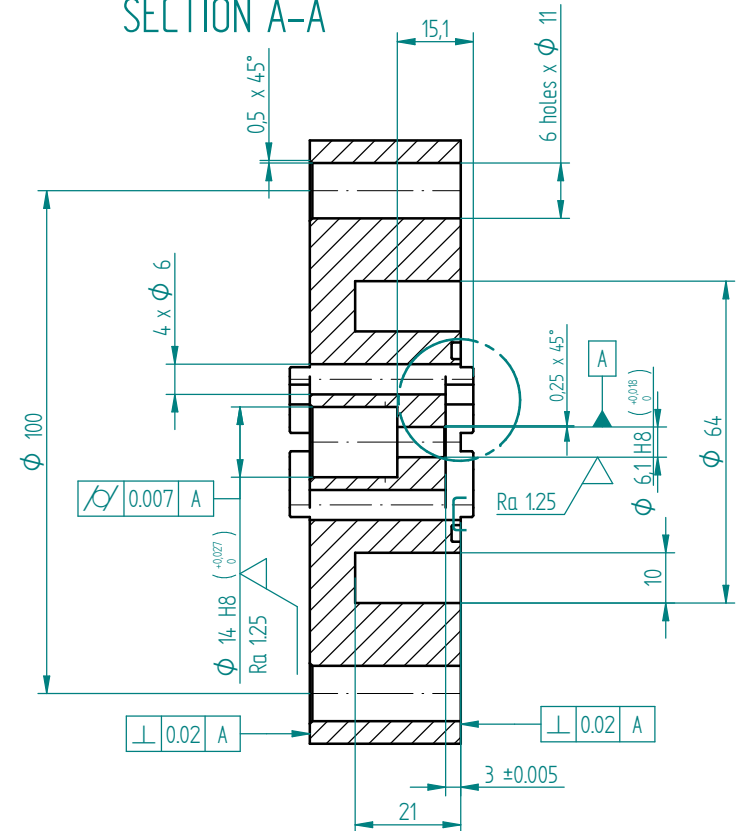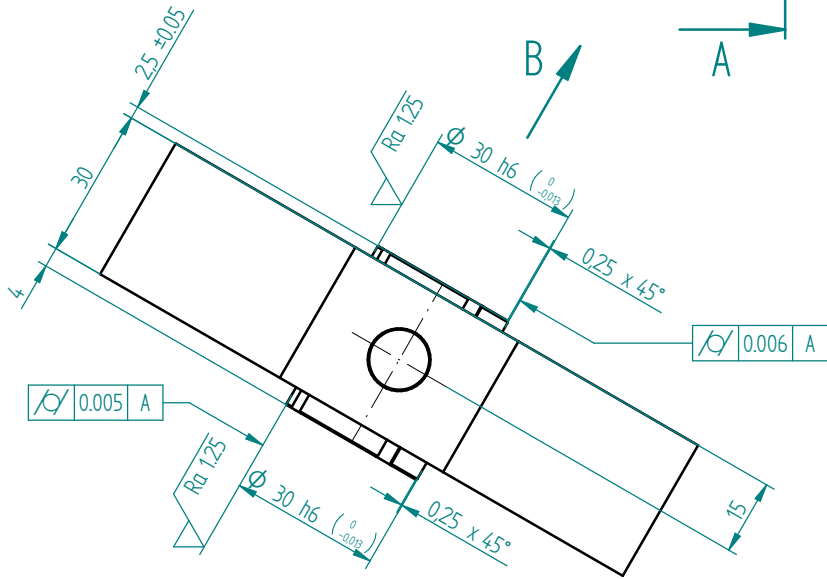
DETAIL C

Unspecified roughness ∇ Ra 2.5

Unspecified tolerances ± 0.05

ϕ 120
ϕ 25
57
16 x R 5
60°

ϕ 100
0.5 x 45°
4 x ϕ 6
ϕ 14 H8 $\binom{-0.027}{0}$
Ra 1.25
$\perp$ 0.02 A
21
3 ±0.005
15,1
6 holes x ϕ 11
0.25 x 45°
A
ϕ 6.1 H8 $\binom{+0.018}{0}$
ϕ 64
Ra 1.25
10
$\perp$ 0.02 A
$\oslash$ 0.007 A

25 ±0.05
30
4
Ra 1.25
ϕ 30 h6 $\binom{0}{-0.013}$
0.25 x 45°
$\oslash$ 0.006 A
$\oslash$ 0.005 A
Ra 1.25
ϕ 30 h6 $\binom{0}{-0.013}$
0.25 x 45°
15

1,8 $\binom{0}{-0.1}$
3,3 $\binom{+0.1}{0}$
ϕ 39,6 $\binom{+0.096}{-0.008}$

sealing grooves flanks, grooves diameter ∇ Ra 1.6

Bottom edges of O-ring grooves round R 0.3

SECTION A-A

A

⌀ 100

⌀ 120

◎ 0.01 | A

6 holes x M 10 both sides

36 $^{+0.02}_{0}$

15

15

2 grooves 4 $^{-0.1}_{0}$ both sides

⌀ 0.023

A

2.3 $^{0}_{-0.1}$

⌀ 70 H8 ($^{+0.046}_{0}$)

⌀ 84 $^{-0.645}_{-0.210}$

⊥ 0.01 | A

2 X 20°

2 X 20°

Ra 1.25

1 X 45°

1 X 45°
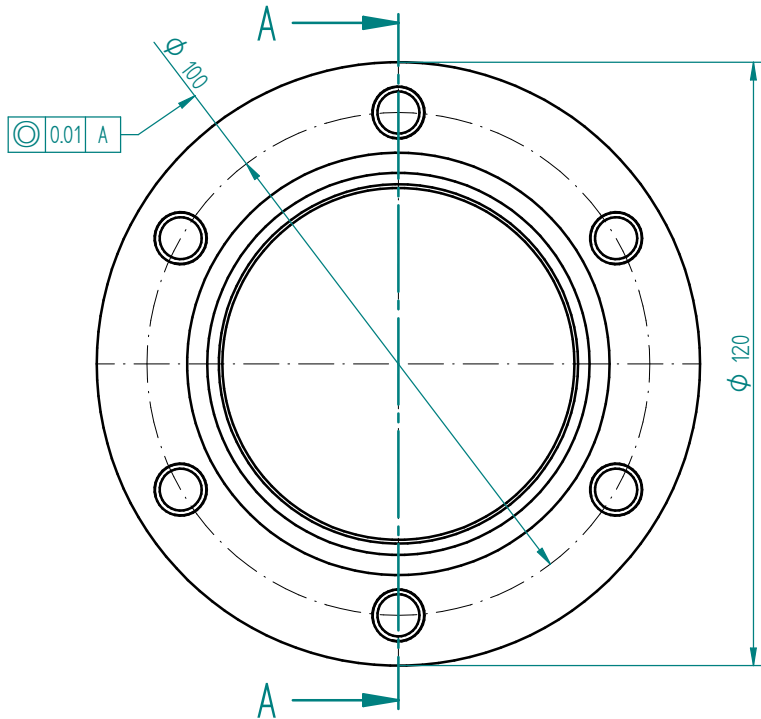
⊥ 0.01 | A
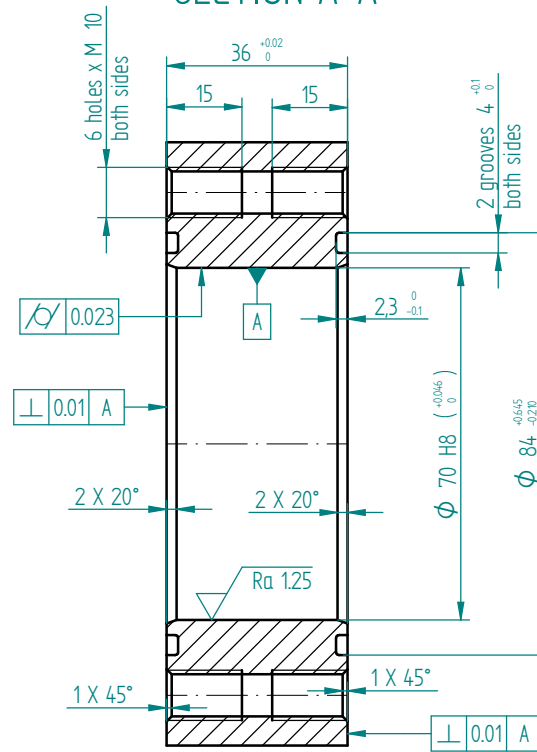
Bottom edges of O-ring grooves round R 0.6

O-ring groove flanks, groove diameter — Ra 1.6

Unspecified roughness — Ra 2.5

Unspecified tolerances ± 0.05

DO NOT TAKE MEASUREMENTS FROM DRAWING PRINTS. IF IN DOUBT: ASK.

MATERIAL		
Material: Stainless steel AISI Type 304		
PROTECTIVE FINISH		

DIMENSIONS IN MM | SCALE AT A3 SIZE:

DRAWN IN ACCORDANCE WITH BS8888

TOLERANCES UNLESS OTHERWISE STATED
LINEAR ±
ANGULAR ±
SURFACE TEXTURE ✓

REMOVE ALL BURRS AND SHARP EDGES
0.5 MAX. RADIUS OR 45°CHAMFER

UNIVERSITY OF BATH
DEPARTMENT OF MECHANICAL ENGINEERING

PROJECT: valve

ACTIVITY	NAME	DATE
DRAWN	Sylwester Kudzma	2011/04/15
CHECKED		
APPROVED		

TITLE: Housing

THIRD ANGLE PROJECTION

SIZE A3
420mm x 297mm

DRAWING NUMBER: 01-04

SHEET No. OF

ISSUE

SECTION B-B

SECTION A-A

SECTION B-B

3/8 BSP

0.25 X 45°

Ra 25

Ra 1.6

Ra 1.25

Ra 1.6

$\perp$ 0.005 A

$\perp$ 0.005 A

0.25 X 45°

Ø 30 H7

15

1.85

34

20

10

3

21

30

57

Ø 64

Ø 34.4

6 equidistant Ø 11
Ø16.5 x 12 deep
positioned as shown

30° 30°

30°

Ra 1.25

Ø 100

R 20.25

SECTION A-A

2.5

1 X 45°

4 holes M 10

Ra 1.25

Ø 6 H7 ($^{-0.002}_{0}$)

A

Ø 120

Ø 30 h6

Ø 20

0.25 x 45°

2.5

Ra 1.25

$\oslash$ 0.005 A

$\oslash$ 0.005 A

1 x 45°

12

Bottom edges of O-ring grooves round R 0.3

O-ring groove flanks, groove diameter   Ra 1.6

Unspecified roughness   Ra 2.5

Unspecified tolerances ± 0.05

ISSUE	DATE	DRAWN	APPROVED	DETAILS OF CHANGES
2	2014/01/16	NPS		Inner diameter increased by 0.1mm
				REVISION HISTORY

DO NOT TAKE MEASUREMENTS FROM DRAWING PRINTS. IF IN DOUBT: ASK.

MATERIAL				
Stainless steel AISI Type 304	DIMENSIONS IN MM	SCALE AT A3 SIZE:		

DRAWN IN ACCORDANCE WITH BS8888

TOLERANCES UNLESS OTHERWISE STATED
LINEAR ±
ANGULAR ±
SURFACE TEXTURE

PROTECTIVE FINISH

REMOVE ALL BURRS AND SHARP EDGES
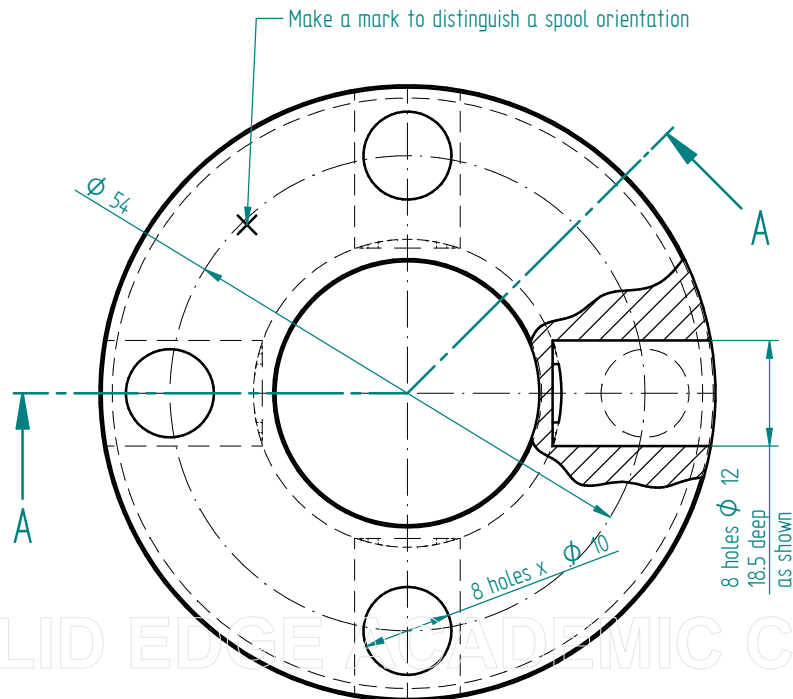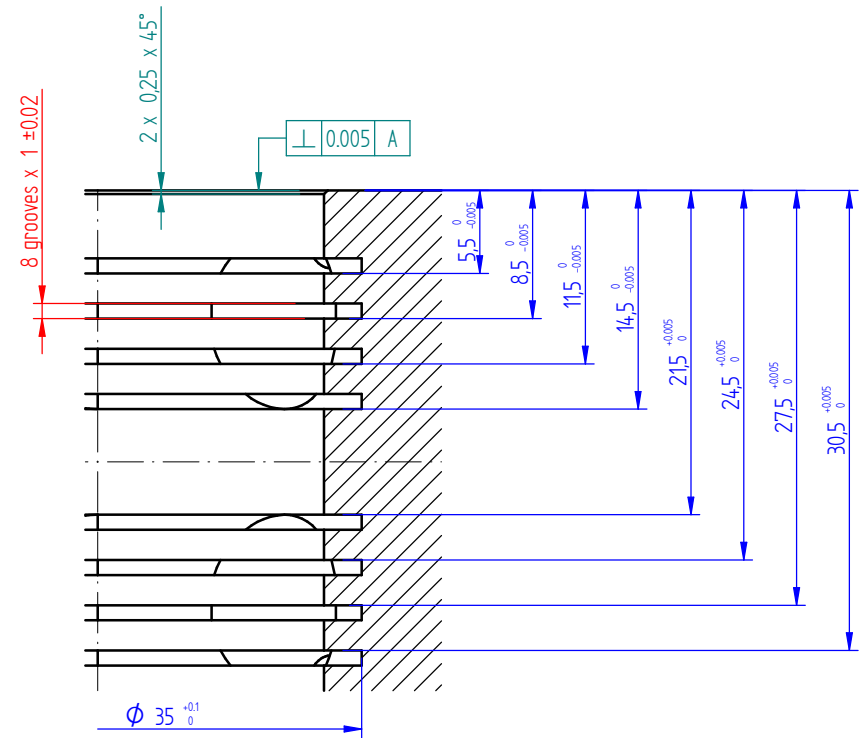0.5 MAX. RADIUS OR 45°CHAMFER

UNIVERSITY OF BATH
DEPARTMENT OF MECHANICAL ENGINEERING

THIS DOCUMENT IS COPYRIGHT AND THE PROPERTY OF
THE UNIVERSITY OF BATH. IT MUST NOT BE COPIED IN
WHOLE OR IN PART NOR DISCLOSED TO ANY THIRD PARTY
WITHOUT PRIOR PERMISSION FROM THE UNIVERSITY.
© UNIVERSITY OF BATH 2008

ACTIVITY	NAME	DATE	PROJECT: Valve
DRAWN	Sylwester Kudzma	15/04/2011	TITLE
CHECKED			Cover top
APPROVED			

THIRD ANGLE PROJECTION

SIZE **A3**
420mm x 297mm

DRAWING NUMBER
01-05

SHEET No.   OF

ISSUE
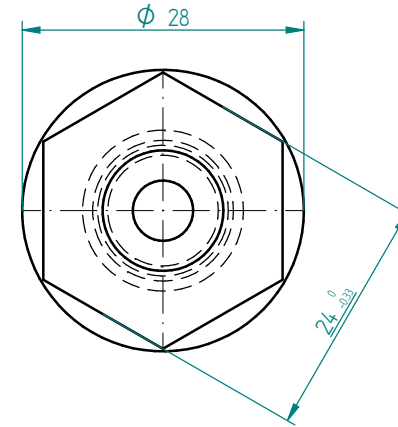
SECTION A-A

Unspecified roughness ∇ Ra 2.5

Unspecified tolerances ± 0.05

DO NOT TAKE MEASUREMENTS FROM DRAWING PRINTS. IF IN DOUBT: ASK.

2	2014/01/16	NPS		Inner diameter increased by 0.1mm
ISSUE	DATE	DRAWN	APPROVED	DETAILS OF CHANGES

REVISION HISTORY

MATERIAL
Stainless steel
AISI Type 304

PROTECTIVE FINISH

DIMENSIONS IN MM | SCALE AT A3 SIZE:
DRAWN IN ACCORDANCE WITH BS8888
TOLERANCES UNLESS OTHERWISE STATED
LINEAR ±
ANGULAR ±
SURFACE TEXTURE ✓
REMOVE ALL BURRS AND SHARP EDGES
0.5 MAX. RADIUS OR 45°CHAMFER

UNIVERSITY OF BATH
DEPARTMENT OF MECHANICAL ENGINEERING

PROJECT	Valve
ACTIVITY	NAME	DATE
DRAWN	Sylwester Kudzma	2011/04/15
CHECKED		
APPROVED		

TITLE
Screw bottom

THIRD ANGLE PROJECTION

SIZE **A3**
420mm x 297mm

DRAWING NUMBER
01-06

SHEET No.
OF

ISSUE

SECTION A-A
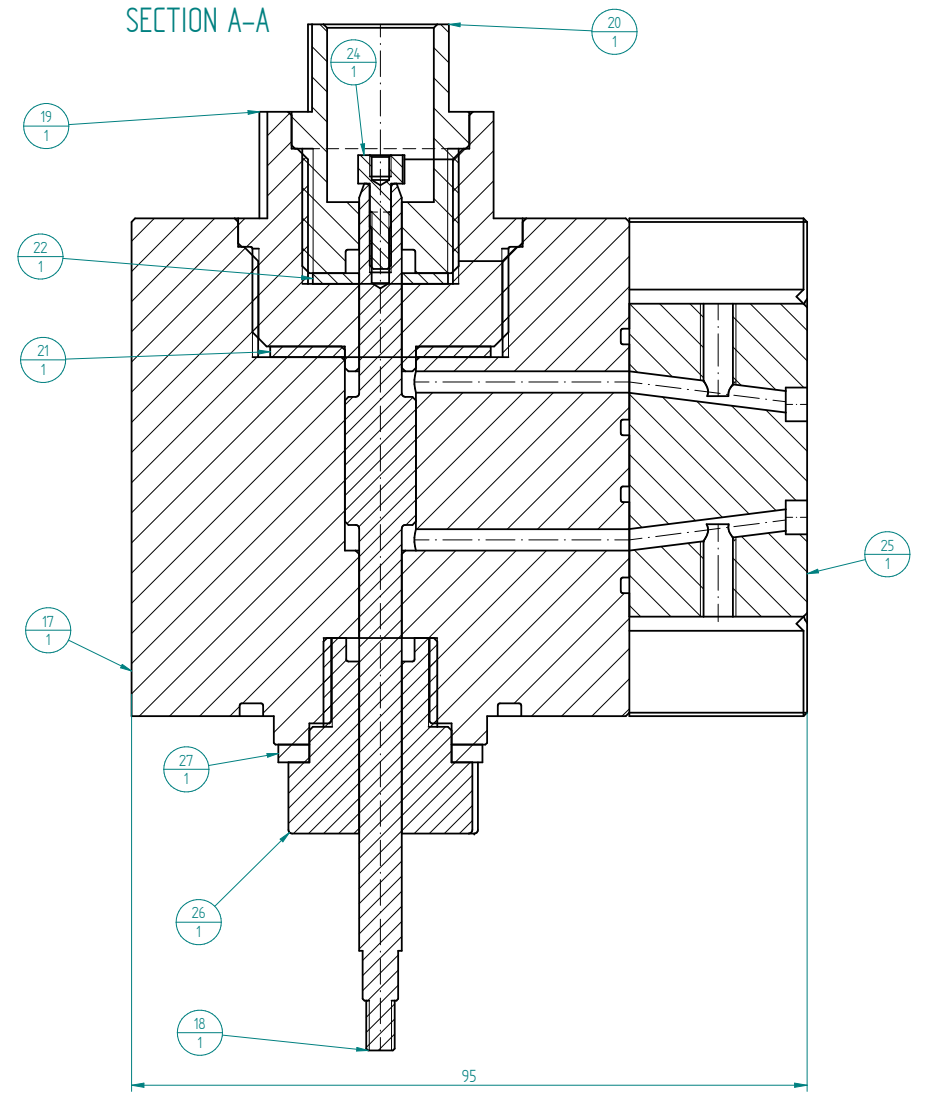
Item Number	Document Number	Title	Material	Quantity
17	01-17	block		1
18	01-18	piston	Stainless Steel, 304	1
19	01-19	Screw no 2 top		1
20	01-20	Screw no 1 top		1
21	01-21	fiber washer no 2 top		1
22	01-22	fibre washer no 1 top	(None)	1
23	01-23	Bolt no 3	Steel, structural	1
24	01-24	Screw for accelerometer	Stainless Steel, 304	1
25	01-25	manifold block		1
26	01-26	Screw bottom	Steel, structural	1
27	01-27	Bounded washer		1

144.3

95

DO NOT TAKE MEASUREMENTS FROM DRAWING PRINTS. IF IN DOUBT: ASK.

MATERIAL

PROTECTIVE FINISH

DIMENSIONS IN MM   SCALE AT A2 SIZE:
DRAWN IN ACCORDANCE WITH BS8888
TOLERANCES UNLESS OTHERWISE STATED
LINEAR ±
ANGULAR ±
SURFACE TEXTURE
REMOVE ALL BURRS AND SHARP EDGES
0.5 MAX. RADIUS OR 45°CHAMFER

UNIVERSITY OF BATH
DEPARTMENT OF MECHANICAL ENGINEERING

ISSUE	DATE	DRAWN	APPROVED	DETAILS OF CHANGES

REVISION HISTORY

PROJECT   Valve

ACTIVITY	NAME	DATE	TITLE
DRAWN	Sylwester Kudzma	2012/07/31	
CHECKED			Valve 02
APPROVED			

THIRD ANGLE PROJECTION

SIZE **A2** 594mm x 420mm

DRAWING NUMBER 01-07

SHEET No. OF

ISSUE

SECTION A-A

70

0,5 X 45°

ϕ 40 H7 $\binom{+0,025}{0}$

0,5 X 45°

$\boxed{/\!/} \; 0.012 \; A$

Ra 1.25

M 36 x 1.5

4 $\binom{+0,1}{0}$

2 holes x ϕ 3 through

1,2 $\binom{0}{-0,05}$

15,5

B

27,2

70

ϕ 15 $\binom{+0,047}{-0,006}$

2 grooves x 2,2 $\binom{+0,1}{0}$

C

4

0,25 X 45°

$\boxed{/\!/} \; 0.006$

A

ϕ 0,5 X 45°

ϕ 6 H7 $\binom{+0,012}{0}$

Ra 1.25

DETAIL B

0,5 X 45°

$\boxed{/\!/} \; 0.007 \; A$

Ra 1.25

ϕ 10 H7 $\binom{+0,015}{0}$

126

111

A

0,5 X 45°

2 X 45°

0,5 X 45°

23

22,2

50

10

Ra 1.25

7,5

4 holes ϕ 11 through positioned as shown

Ra 1.25

A

ϕ 30 h6 $\binom{0}{-0,013}$

$\boxed{/\!/} \; 0.006 \; A$

DETAIL C

1,8 $\binom{0}{-0,1}$

0,25 X 45°

15

3,3 $\binom{+0,1}{0}$

3

3/8 BSP

ϕ 20 H7 $\binom{+0,021}{0}$

ϕ 39,6 $\binom{+0,396}{-0,008}$

4 holes x M 8 positioned as shown

19,7

86,6

10

28

32

70

50

35

7

63

Ra 1.25

sealing grooves flanks, grooves diameter

Bottom edges of O-ring grooves round R 0.3

Ra 2.5

Unspecified roughness

Unspecified tolerances ± 0.05

Material: Stainless steel
AISI Type 304

Drawn: Sylwester Kudzma   Date: 15/04/2011

University of Bath

project: Valve
title: block
Drawing No. 01-17

0,5 x45°

0,5 x45°

⌀ 0.06 A

A

Ra 0.63

14

12,5

0,25 x45°

M 4

0,25 x45°

⌀ 5 h7

⌀ 6 g7

R 0.5

⌀ 0.04

⌀ 10 h6

R 0.5

M 3 x 0.5

⌀ 6 g7

2 x20°

rounded, polished

⌀ 0.09 A

74

18

37,5

0,75 Flats

7

7

2,75 5,5   5,5 2,75

10

0,25   0,5   0,5   0,5

Note: Edges of grooves to be rounded

1:1

DO NOT TAKE MEASUREMENTS FROM DRAWING PRINTS. IF IN DOUBT: ASK.

MATERIAL			
Mild Steel			

DIMENSIONS IN MM   SCALE AT A3 SIZE: 3:1
DRAWN IN ACCORDANCE WITH BS8888
TOLERANCES UNLESS OTHERWISE STATED
LINEAR ±0.05
ANGULAR ±
SURFACE TEXTURE   √Ra 1.25

PROTECTIVE FINISH

REMOVE ALL BURRS AND SHARP EDGES
0.5 MAX. RADIUS OR 45°CHAMFER

ISSUE	DATE	DRAWN	APPROVED	DETAILS OF CHANGES

REVISION HISTORY

PROJECT
Linear Fast Switching Valve

ACTIVITY	NAME	DATE
DRAWN	Nathan Sell	28/01/2014
CHECKED		
APPROVED		

TITLE
Piston

THIRD ANGLE PROJECTION

SIZE A3
420mm x 297mm

DRAWING NUMBER
01-18

SHEET No.
1 OF 1

ISSUE
2

19 $^{0}_{-0.33}$

ϕ 25 h6 $\left(^{0}_{-0.08}\right)$

Ra 1.25

A

$\varnothing$ 0.006

A

A

0.5 X 45°

1 X 45°

5.2

35

17.5

M 22

SECTION A-A

15

25

ϕ 6 H8 $\left(^{+0.018}_{0}\right)$

$\varnothing$ 0.009 A

R 0.15

ϕ 11.3 $^{+0.2}_{0}$

2.2 $^{+0.2}_{0}$

Ra 2.5

Unspecified roughness

Unspecified tolerances ± 0.05

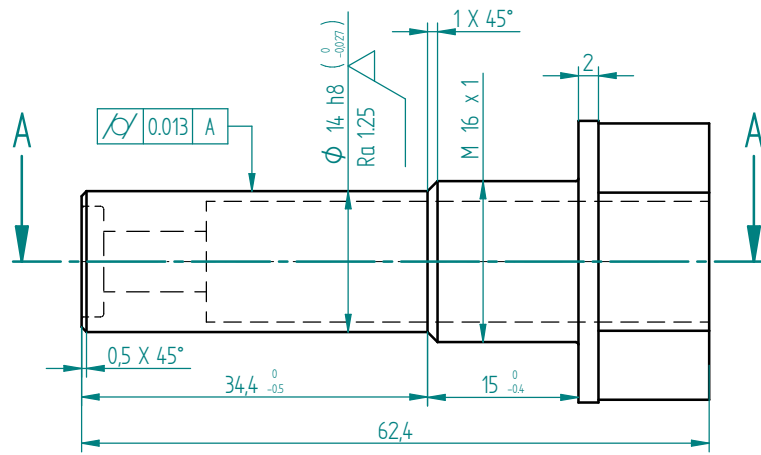DO NOT TAKE MEASUREMENTS FROM DRAWING PRINTS. IF IN DOUBT: ASK.

2	2014/01/16	NPS		Inner diameter increased by 0.1mm
ISSUE	DATE	DRAWN	APPROVED	DETAILS OF CHANGES

REVISION HISTORY

MATERIAL		
Stainless steel AISI Type 304		
PROTECTIVE FINISH		

DIMENSIONS IN MM   SCALE AT A3 SIZE:

DRAWN IN ACCORDANCE WITH BS8888

TOLERANCES UNLESS OTHERWISE STATED
LINEAR ±
ANGULAR ±
SURFACE TEXTURE ✓

REMOVE ALL BURRS AND SHARP EDGES
0.5 MAX. RADIUS OR 45°CHAMFER

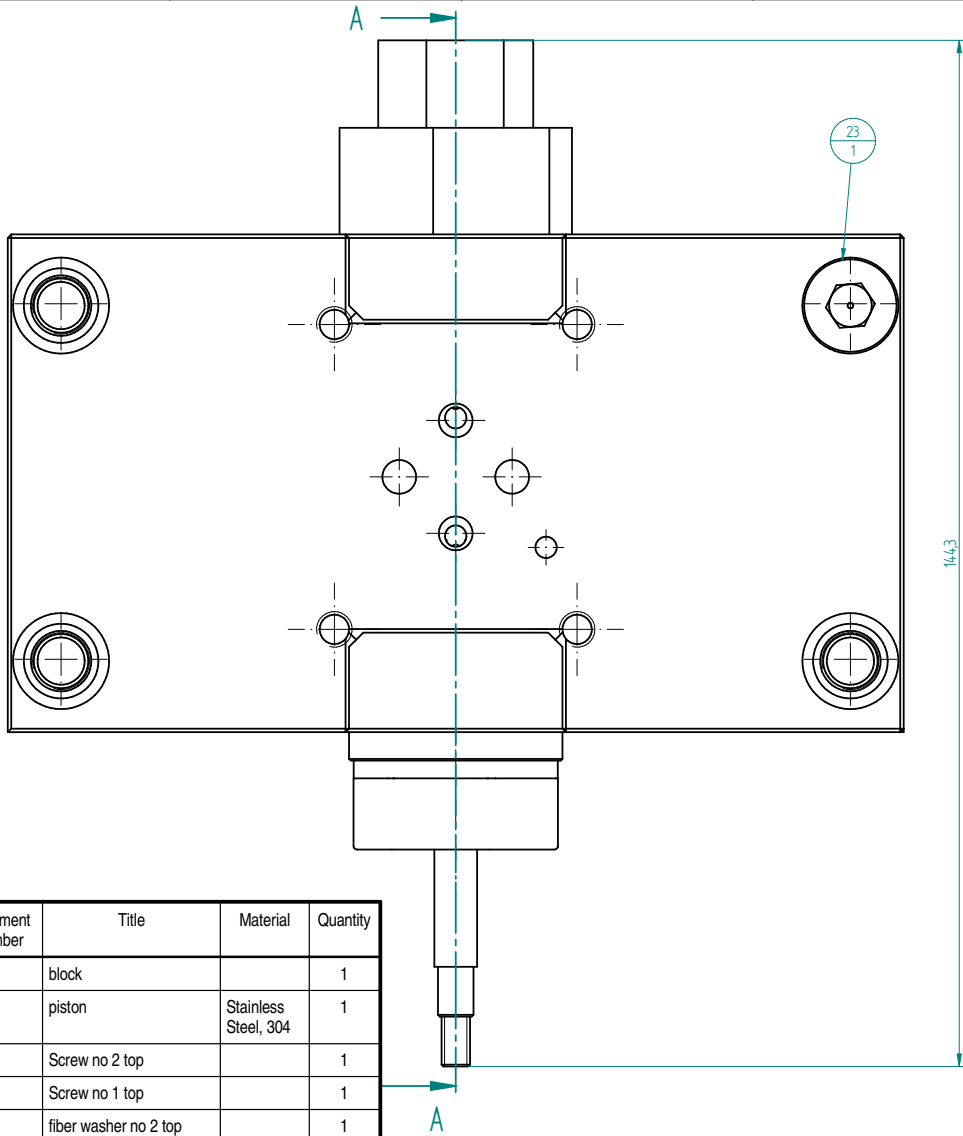## UNIVERSITY OF BATH
DEPARTMENT OF MECHANICAL ENGINEERING

PROJECT

ACTIVITY	NAME	DATE
DRAWN	Sylwester Kudzma	15/04/2011
CHECKED		
APPROVED		

TITLE

Screw No 2 top

THIRD ANGLE PROJECTION

SIZE A3
420mm x 297mm

DRAWING NUMBER
01-21

SHEET No.
OF

ISSUE

SECTION A-A

A

Ra 1.25

33

14 $^{+0.3}_{0}$ 4

3,5

0.5 X 45°

⌖ | 0,011 | A

Ra 1.25

1,5 X 45°

ϕ 40 h6 $\left(^{0}_{-0.016}\right)$

M 36 x 1,5

ϕ 6,1 H8 $\left(^{-0.018}_{0}\right)$

M 22 x 1,5

25 H7 $\left(^{+0.021}_{0}\right)$

B

⌖ | 0,09 | A

Ra 2.5

5,2

⌖ | 0,008

2 X 45°   0,5 X 45°

24,2

A   A

30 $^{0}_{-0.33}$

DETAIL B

0,5 X 45°

ϕ 10 g6 $\left(^{-0.005}_{-0.014}\right)$

Ra 1.25

0,5 X 45°

⌖ | 0,01 | A

Unspecified roughness   √ Ra 2.5   Unspecified tolerances ± 0.05

2	2014/01/16	NPS		Inner diameter increased by 0.1mm
ISSUE	DATE	DRAWN	APPROVED	DETAILS OF CHANGES

REVISION HISTORY

DO NOT TAKE MEASUREMENTS FROM DRAWING PRINTS. IF IN DOUBT: ASK.

MATERIAL			
Material: Stainless steel AISI Type 304	DIMENSIONS IN MM	SCALE AT A3 SIZE:	
	DRAWN IN ACCORDANCE WITH BS8888		
	TOLERANCES UNLESS OTHERWISE STATED LINEAR ± ANGULAR ± SURFACE TEXTURE ✓		
PROTECTIVE FINISH			
	REMOVE ALL BURRS AND SHARP EDGES 0.5 MAX. RADIUS OR 45°CHAMFER		

UNIVERSITY OF BATH
DEPARTMENT OF MECHANICAL ENGINEERING

PROJECT	valve		
ACTIVITY	NAME	DATE	
DRAWN	Sylwester Kudzma	2011/04/15	TITLE
CHECKED			Screw No1 top
APPROVED			

THIRD ANGLE PROJECTION ⊕ ⊲

SIZE **A3** 420mm x 297mm

DRAWING NUMBER 01-20	SHEET No. OF	ISSUE

16

3,5

12

8

M 3

M 3

0,25 X 45°

0,5 X 45°

3

6 0 / −0.12

DO NOT TAKE MEASUREMENTS FROM DRAWING PRINTS. IF IN DOUBT: ASK.

ISSUE	DATE	DRAWN	APPROVED	DETAILS OF CHANGES

REVISION HISTORY

MATERIAL		TOLERANCES UNLESS OTHERWISE STATED	ACTIVITY	NAME	DATE
304		LINEAR ±	DRAWN	Sylwester Kudzma	2011/04/14
		ANGULAR ±			
		SURFACE TEXTURE ✓	CHECKED		
PROTECTIVE FINISH		DRAWN IN ACCORDANCE WITH BS8888	APPROVED		
		REMOVE ALL BURRS AND SHARP EDGES 0.5 MAX. RADIUS OR 45°CHAMFER	PROJECT	Valve	

SCALE AT A4 SIZE:		TITLE		
SIZE A4	DIMENSIONS IN MM	screw for accelerometer		
297mm x 210mm				
THIRD ANGLE PROJECTION		DRAWING NUMBER 01-25	SHEET No. OF	ISSUE

SECTION C-C

4 holes φ 8.5 through 8.5
φ 13.5 x 9 deep

50
70

0.02

SECTION B-B

Ra 1.25
Ra 1.25
Ra 1.25
Ra 1.25

12,5
3
12
83° ±1
22,2
φ 4,75
φ 3
2 holes
4
2 holes M5

30
25
12,5
63
0,5 X 45°
126

111
2 x 45°
both sides

B
C
A
A
C
B

1.8
1.7
1.3
1.4
1.2
1.1
1.9
1.5
1.6

35,9
10
7,5
63

SECTION A-A

57,44
φ 5
3/8 BSP
2 holes
12,5
15
2,62 X 45°
20
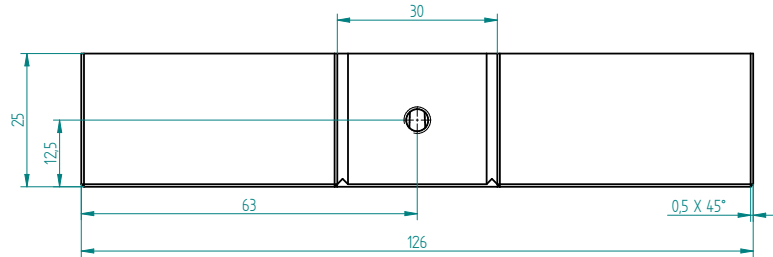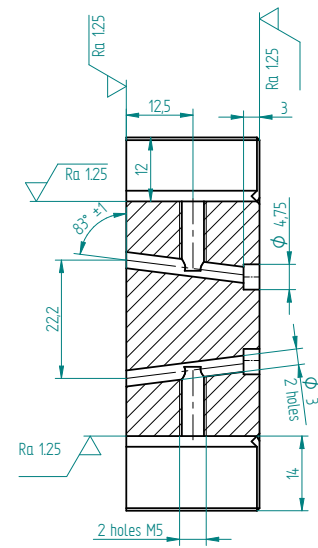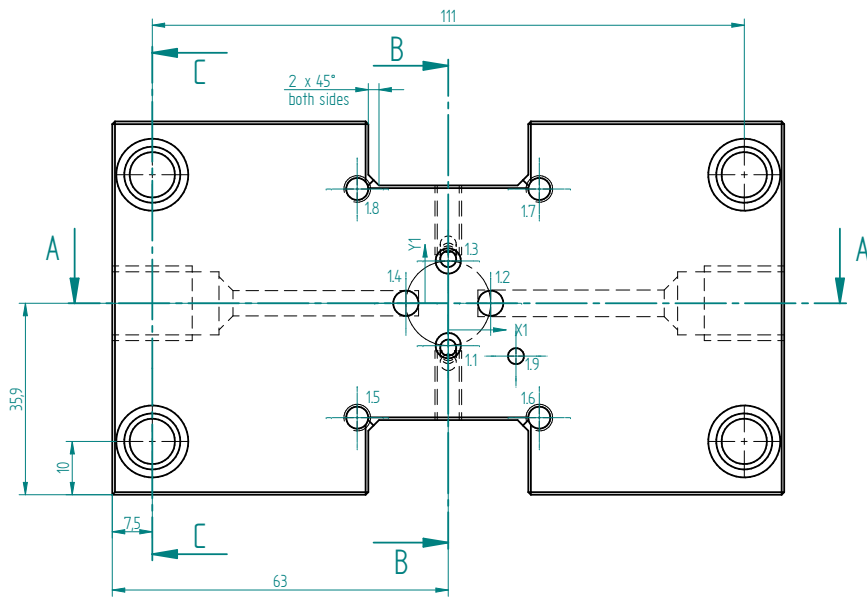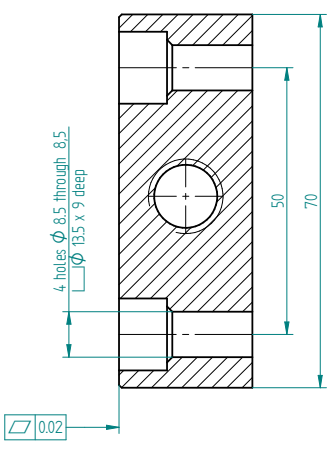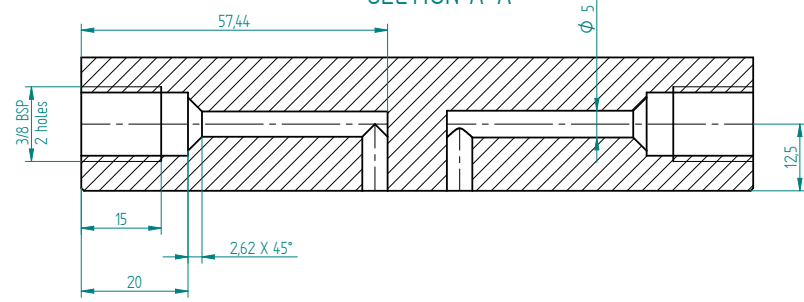
Unspecified roughness Ra 2.5

Unspecified tolerances ± 0.05

Hole Table

Hole	X	Y	Size	Type	Callout	depth
1.1	0	−7,94	φ 4,75	Simple		through
1.2	7,94	0	φ 4,75	Simple		15
1.3	0	7,94	φ 4,75	Simple		through
1.4	−7,94	0	φ 4,75	Simple		15
1.5	−17,07	−21,44	φ 5	Simple Threaded	M5	through
1.6	17,07	−21,44	φ 5	Simple Threaded	M5	through
1.7	17,07	21,44	φ 5	Simple Threaded	M5	through
1.8	−17,07	21,44	φ 5	Simple Threaded	M5	through
1.9	12,7	−9,91	φ 3	Simple		2.5

DO NOT TAKE MEASUREMENTS FROM DRAWING PRINTS. IF IN DOUBT: ASK.

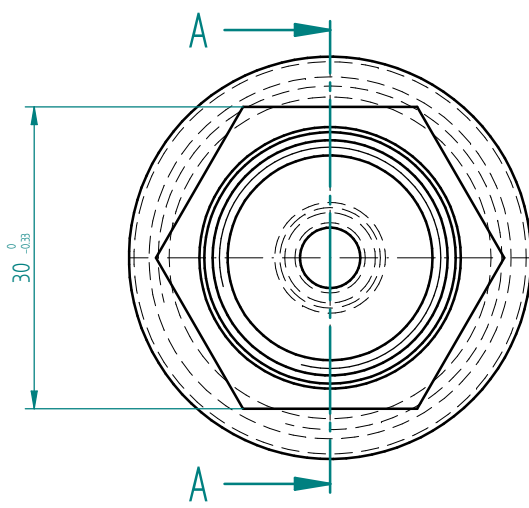| MATERIAL	DIMENSIONS IN MM	SCALE AT A2 SIZE:				

MATERIAL
Stainless steel
AISI Type 304

PROTECTIVE FINISH

DIMENSIONS IN MM | SCALE AT A2 SIZE:
DRAWN IN ACCORDANCE WITH BS8888
TOLERANCES UNLESS OTHERWISE STATED
LINEAR ±
ANGULAR ±
SURFACE TEXTURE
REMOVE ALL BURRS AND SHARP EDGES
0.5 MAX. RADIUS OR 45°CHAMFER

UNIVERSITY OF BATH
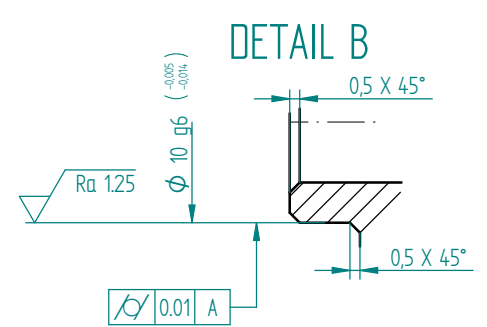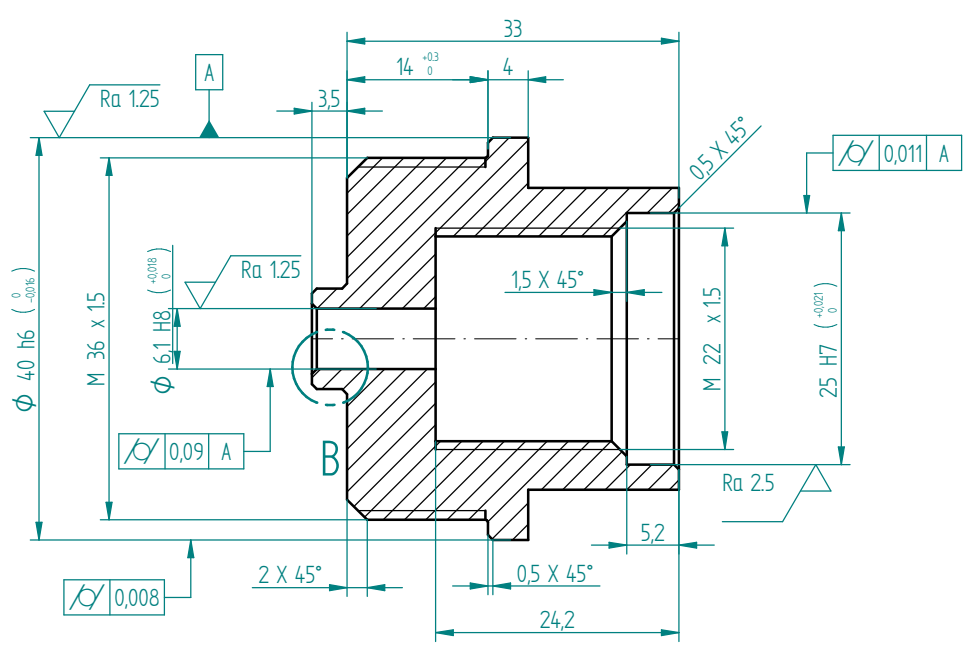### DEPARTMENT OF MECHANICAL ENGINEERING

ISSUE	DATE	DRAWN	APPROVED	DETAILS OF CHANGES

REVISION HISTORY

PROJECT valve

ACTIVITY	NAME	DATE
DRAWN	Sylwester Kudzma	09/06/2011
CHECKED		
APPROVED		

TITLE
Manifold block 01

THIRD ANGLE PROJECTION

SIZE A2
594mm x 420mm

DRAWING NUMBER
01-19a

SHEET No.
OF

ISSUE

Ra0.63

2,2 +0.2 / 0

⌀ 0.05 A

11,3 +0.2 / 0

⌖ 0.006   A

⌀ 6,1 FG7 (+0.018 / -0.006)

Ra0.63

SECTION A-A

29,14

A

25,5

A

R.05

5 0 / -0.1

⌀ 0.05 A

3/8 BSP

20 h6 (0 / -0.013)

17,5 0 / -0.1

27,5

Unspecified roughnes: Ra1.25

Unspecified tolerances ± 0.05

2	2014/01/16	NPS		Inner diameter increased by 0.1mm
ISSUE	DATE	DRAWN	APPROVED	DETAILS OF CHANGES

REVISION HISTORY

DO NOT TAKE MEASUREMENTS FROM DRAWING PRINTS. IF IN DOUBT: ASK.

PROJECT
linear valve

MATERIAL				
Structural steel S355 (50A)	DIMENSIONS IN MM	SCALE AT A3 SIZE:		
	DRAWN IN ACCORDANCE WITH BS8888			
	TOLERANCES UNLESS OTHERWISE STATED LINEAR ± ANGULAR ± SURFACE TEXTURE ✓			
PROTECTIVE FINISH	REMOVE ALL BURRS AND SHARP EDGES 0.5 MAX. RADIUS OR 45°CHAMFER			

UNIVERSITY OF BATH
DEPARTMENT OF MECHANICAL ENGINEERING

THIS DOCUMENT IS COPYRIGHT AND THE PROPERTY OF THE UNIVERSITY OF BATH. IT MUST NOT BE COPIED IN WHOLE OR IN PART NOR DISCLOSED TO ANY THIRD PARTY WITHOUT PRIOR PERMISSION FROM THE UNIVERSITY.
© UNIVERSITY OF BATH 2011

ACTIVITY	NAME	DATE
DRAWN	Sylwester Kudzma	2012/07/31
CHECKED		
APPROVED		

TITLE
Screw bottom

THIRD ANGLE PROJECTION

SIZE A3
420mm x 297mm

DRAWING NUMBER

SHEET No.   OF

ISSUE

2,7 ±0.005

ϕ 9

ϕ 6 H11 $\left(^{+0.075}_{0}\right)$

0,25 X 45°

0,25 X 45°

Unspecified roughness — Ra 1.25

Unspecified tolerances ± 0.1

DO NOT TAKE MEASUREMENTS FROM DRAWING PRINTS. IF IN DOUBT: ASK.

ISSUE	DATE	DRAWN	APPROVED	DETAILS OF CHANGES

REVISION HISTORY

MATERIAL Stainless steel AISI Type 304	TOLERANCES UNLESS OTHERWISE STATED LINEAR ± ANGULAR ± SURFACE TEXTURE ✓	ACTIVITY	NAME	DATE
		DRAWN	Sylwester Kudzma	15/04/2011
		CHECKED		
PROTECTIVE FINISH	DRAWN IN ACCORDANCE WITH BS8888	APPROVED		

REMOVE ALL BURRS AND SHARP EDGES 0.5 MAX. RADIUS OR 45°CHAMFER

PROJECT

valve

SCALE AT A4 SIZE:

SIZE A4   DIMENSIONS IN MM

297mm x 210mm

THIRD ANGLE PROJECTION

TITLE

bush top

DRAWING NUMBER	SHEET No.	ISSUE
01-08	OF	

5,7 ±0.005

9

0,25 X 45°

0,25 X 45°

ϕ 6 H11 $\left(^{+0.075}_{0}\right)$
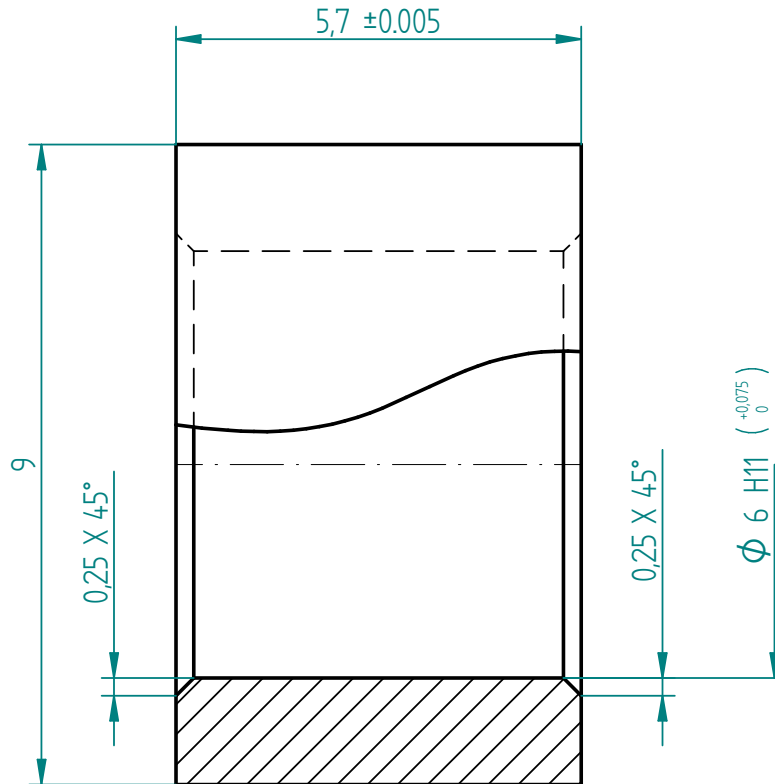
Unspecified tolerances ± 0.1

Unspecified roughness ▽ Ra 1.25

DO NOT TAKE MEASUREMENTS FROM DRAWING PRINTS. IF IN DOUBT: ASK.

MATERIAL Stainless steel AISI Type 304	TOLERANCES UNLESS OTHERWISE STATED LINEAR ± ANGULAR ± SURFACE TEXTURE ✓	ACTIVITY	NAME	DATE
		DRAWN	Sylwester Kudzma	15/04/2011
		CHECKED		
PROTECTIVE FINISH	DRAWN IN ACCORDANCE WITH BS8888	APPROVED		
	REMOVE ALL BURRS AND SHARP EDGES 0.5 MAX. RADIUS OR 45°CHAMFER	PROJECT valve		

UNIVERSITY OF BATH
DEPARTMENT OF MECHANICAL ENGINEERING

SCALE AT A4 SIZE:		TITLE bush bottom		
SIZE A4 297mm x 210mm	DIMENSIONS IN MM			
THIRD ANGLE PROJECTION		DRAWING NUMBER 01-09	SHEET No. OF	ISSUE

SECTION B-B

1 X 45°
1 X 45°

6 equidistant holes φ φ 11
φ 16.5 x 12 deep

⌀ 0.009

Ra 2.5

B

VIEW A

30
15

φ 120

A

15

0.5 X 45°

3/8 BSP

117

B

$\phi\ 39.6\ ^{+0.396}_{-0.008}$
$\phi\ 30\ H7\ ^{(-0.021}_{\ 0}$
$33\ ^{+0.1}_{\ 0}$
M 16 x 1
$1.8\ ^{0}_{-0.1}$
20

Unspecified roughness   Ra 2.5   Unspecified tolerances ± 0.05

Bottom edges of O-ring groove round R 0.3

O-ring groove flanks, groove diameter   Ra 1.6

DO NOT TAKE MEASUREMENTS FROM DRAWING PRINTS. IF IN DOUBT: ASK.

ISSUE	DATE	DRAWN	APPROVED	DETAILS OF CHANGES

REVISION HISTORY

MATERIAL			
Material: Stainless steel AISI Type 304	DIMENSIONS IN MM SCALE AT A3 SIZE:		
	DRAWN IN ACCORDANCE WITH BS8888		
	TOLERANCES UNLESS OTHERWISE STATED LINEAR ± ANGULAR ± SURFACE TEXTURE ✓		
PROTECTIVE FINISH			
	REMOVE ALL BURRS AND SHARP EDGES 0.5 MAX. RADIUS OR 45°CHAMFER		

UNIVERSITY OF BATH
DEPARTMENT OF MECHANICAL ENGINEERING

THIS DOCUMENT IS COPYRIGHT AND THE PROPERTY OF THE UNIVERSITY OF BATH. IT MUST NOT BE COPIED IN WHOLE OR IN PART NOR DISCLOSED TO ANY THIRD PARTY WITHOUT PRIOR PERMISSION FROM THE UNIVERSITY.
© UNIVERSITY OF BATH 2010

				PROJECT
				Valve
ACTIVITY	NAME	DATE		
DRAWN	Sylwester Kudzma	15/04/2011		TITLE
CHECKED				cover No 2 bottom
APPROVED				

THIRD ANGLE PROJECTION
SIZE A3
420mm x 297mm
DRAWING NUMBER
01-10
SHEET No.
OF
ISSUE

SOLID EDGE ACADEMIC COPY

M 12 x 1

ϕ 10,92 h8 $\left(^{0}_{-0.027}\right)$

M 2 x 0.25

$17\ ^{0}_{-0.27}$

R 05

0,5 X 45°

8

ϕ 5,4 $^{+0.1}_{0}$ through

15

29

54

DO NOT TAKE MEASUREMENTS FROM DRAWING PRINTS. IF IN DOUBT: ASK.

ISSUE	DATE	DRAWN	APPROVED	DETAILS OF CHANGES

REVISION HISTORY

MATERIAL				ACTIVITY	NAME	DATE
304	TOLERANCES UNLESS OTHERWISE STATED					
	LINEAR ±			DRAWN	Sylwester Kudzma	2011/04/15
	ANGULAR ±					
	SURFACE TEXTURE	✓		CHECKED		

PROTECTIVE FINISH	DRAWN IN ACCORDANCE WITH BS8888	APPROVED	

	REMOVE ALL BURRS AND SHARP EDGES 0.5 MAX. RADIUS OR 45°CHAMFER	PROJECT
		Valve

SCALE AT A4 SIZE:

SIZE **A4** 297mm x 210mm DIMENSIONS IN MM

THIRD ANGLE PROJECTION

TITLE

Screw No. 2 bottom

DRAWING NUMBER 01-15

SHEET No. OF

ISSUE

Appendix C

Pilot Valve Data

MOOG

MOOG Controls Limited , Aschurch , Tewkesbury , Glos. GL20 8NA   TEL: (0684) 29660   FAX: (0684) 296760

```
    DATE OF TEST              :      26-08-2011  09:14:18
    OPERATOR                  :      al

    VALVE    MODEL   NUMBER   :      e050_899
    VALVE    SERIAL  NUMBER   :      e101

    PILOTE   MODEL   NUMBER   :
    PILOTE   SERIAL  NUMBER   :

    CUSTOMER         NAME     :
    ORDER            NUMBER   :
```

```
================================================================================
|          N E W              |       p r o d u c t     a c c e p t a n c e      t e s t      |
--------------------------------------------------------------------------------
|       O P E R A T I O N     | UNIT |     SPEC      |      SPEC      |     RESULT   |STATUS|
--------------------------------------------------------------------------------
|   FLUSH VALVE               | sec  |               |     15.00      |     DONE     |      |
|   TEMPERATURE               | deg  |     32.00     |     45.00      |     39       |      |
|   FLOW GAIN                 | cis  |     13.50     |     16.50      |     16.34    |      |
|   FLOW GAIN                 | cis  |     13.50     |     16.50      |     16.27    |      |
|   POLARITY TEST             | ---  |  at 4000 psi  |     +,LH       |     +,LH     |      |
|   NULL BIAS                 | mA   |  at 4000 psi  |     0.50       |     0.00     |      |
|   HYSTERESE                 | mA   |  at 4000 psi  |     0.75       |     0.22     |      |
|   NULL PRESSURE             | psi  |      0        |     4000       |     1351     |      |
|   PRS NUL SHIFT             | mA   |  4400 ... 2400|     1.00       |     0.09     |      |
|   THRESHOLD                 | mA   |  at 4000 psi  |     0.12       |     0.02     |      |
|   INTERNAL LEAKAGE          | cis  |  at 4000 psi  |     1.95       |     1.02     |      |
|   TARE     LEAKAGE          | cis  |  at 4000 psi  |     1.50       |     0.73     |      |
--------------------------------------------------------------------------------
|   T E S T    P A R A M E T E R    |                                                        |
--------------------------------------------------------------------------------
|   PILOTE   supply           | ---  |   i n t e r n  |              |              |      |
|   PILOTE   return           | ---  |   i n t e r n  |              |              |      |
|   LEAKAGE  spec             | ---  |     n e w      |              |              |      |
|   LEAKAGE  pres             | psi  |                |              |              |      |
|   EXTERN   pres             | psi  |                |              |              |      |
|   OPTIONS                   | ---  |                |              |              |      |
--------------------------------------------------------------------------------
```

Connector PC06 E8-45   Size 8 4pl

FEC 147-6632   £43-04

Certificate of Conformity
It is hereby certified that the equipment described within this data package has been manufactured,
inspected, tested and found to be conform under all aspects to the requirements of the applicable
specification

                                                    Released by   _____/_____

model nr.   : e050_899   serial nr.   : e101   date   : 26-08-2011 09:22:05

⊚FLOW PLOT :   EXPANDED

system pres. : 4000   psi   extern pres   :   0   psi   el. connect   : Q->D   M->E
command signal : ->   scale   : 1.60   mA / div
flow   : ↑   scale   : 2.00   cis / div

MOOG

MOOG Controls Limited , Aschurch , Tewkesbury , Glos. GL20 8NA   TEL: (0684) 29660   FAX: (0684) 296760
----

model nr.   : e050_899   serial nr.   : e101   date   : 26-08-2011 09:23:41

⊚FLOW PLOT :   4__W A Y

system pres.   : 1000   psi   extern pres   :   0   psi   el. connect   : Q->D   M->E
command signal : ->   scale   : 8.00   mA / div
flow   : ↑   scale   : 5.00   cis / div

moog semi valvetest   version nr : 1.50   parameter set nr   testrigg nr. :   4

Moog Controls Ltd., Aschurch, Tewkesbury, Glos. GL20 8NA UK **Tel:** +44 (0)1684 296600 **Fax:** +44 (0)1684 296760

© Moog Proprietary and/or Confidential Data

MOOG

MOOG Controls Limited , Aschurch , Tewkesbury , Glos. GL20 8NA   TEL: (0684) 29660   FAX: (0684) 296760

----

model nr.   : e050_899   serial nr.   : e101   date   : 26-08-2011 09:24:38

©FLOW PLOT :   LEAKAGE

system pres.   : 4000   psi   extern pres   :   0   psi   el. connect   : Q->D   M->E
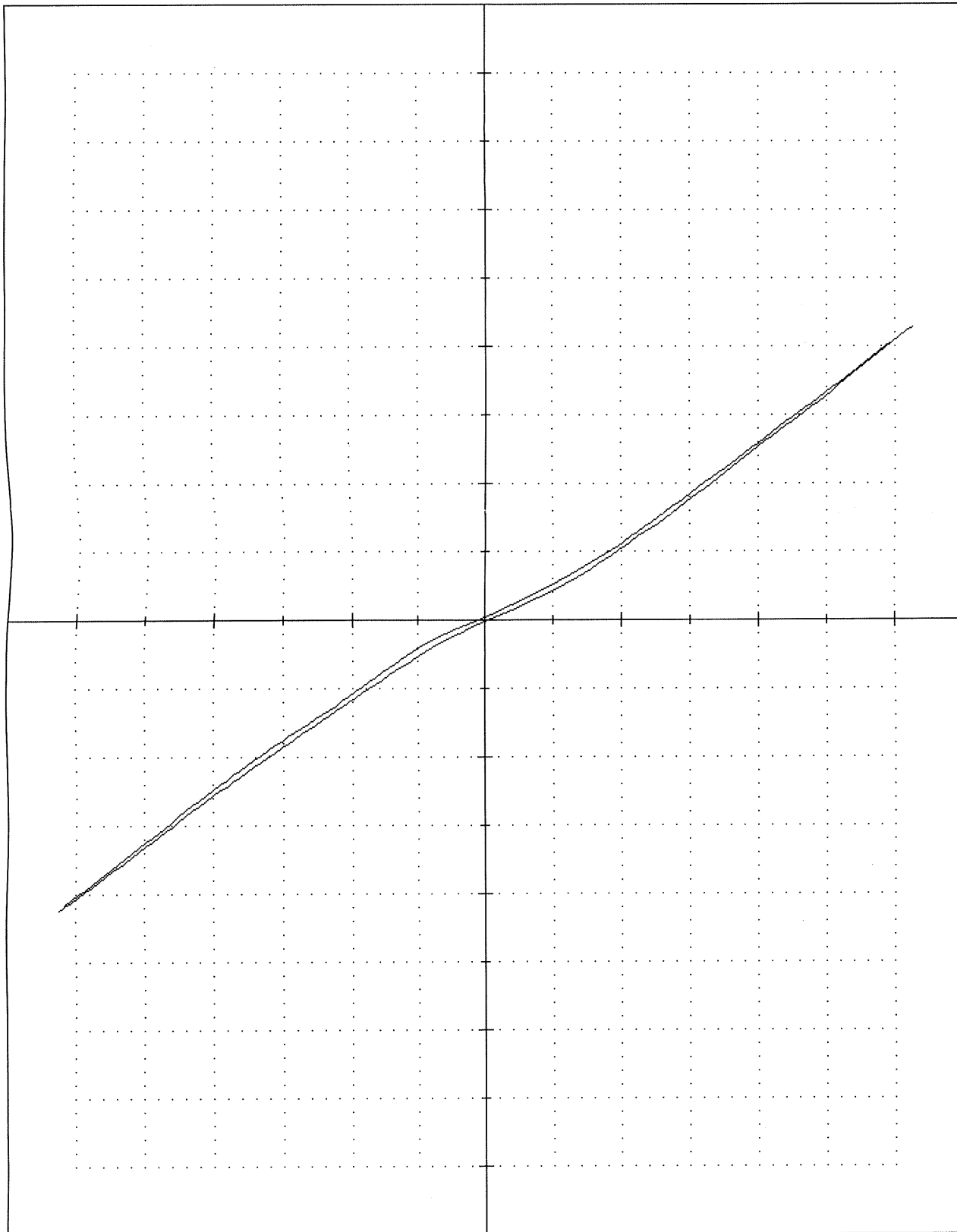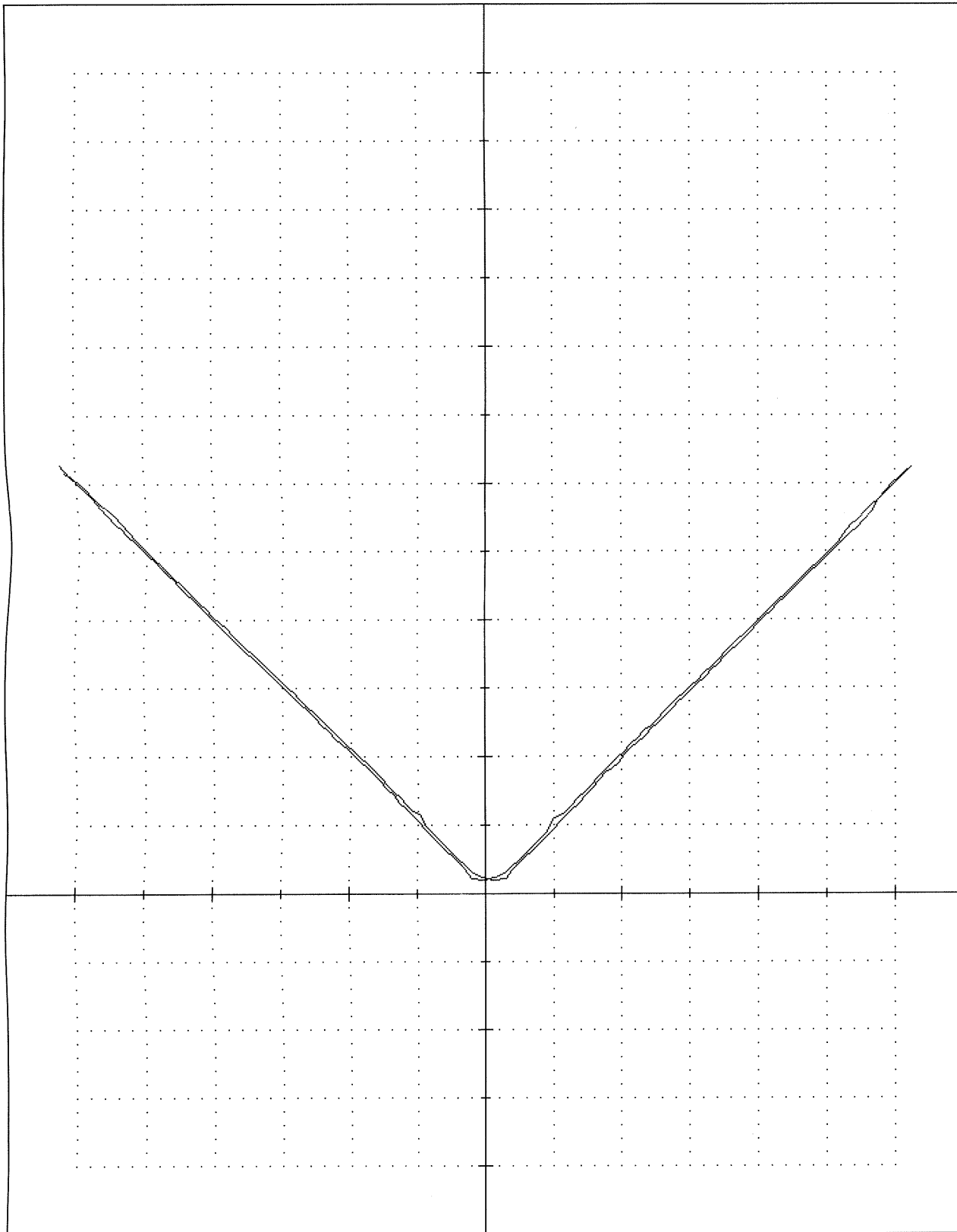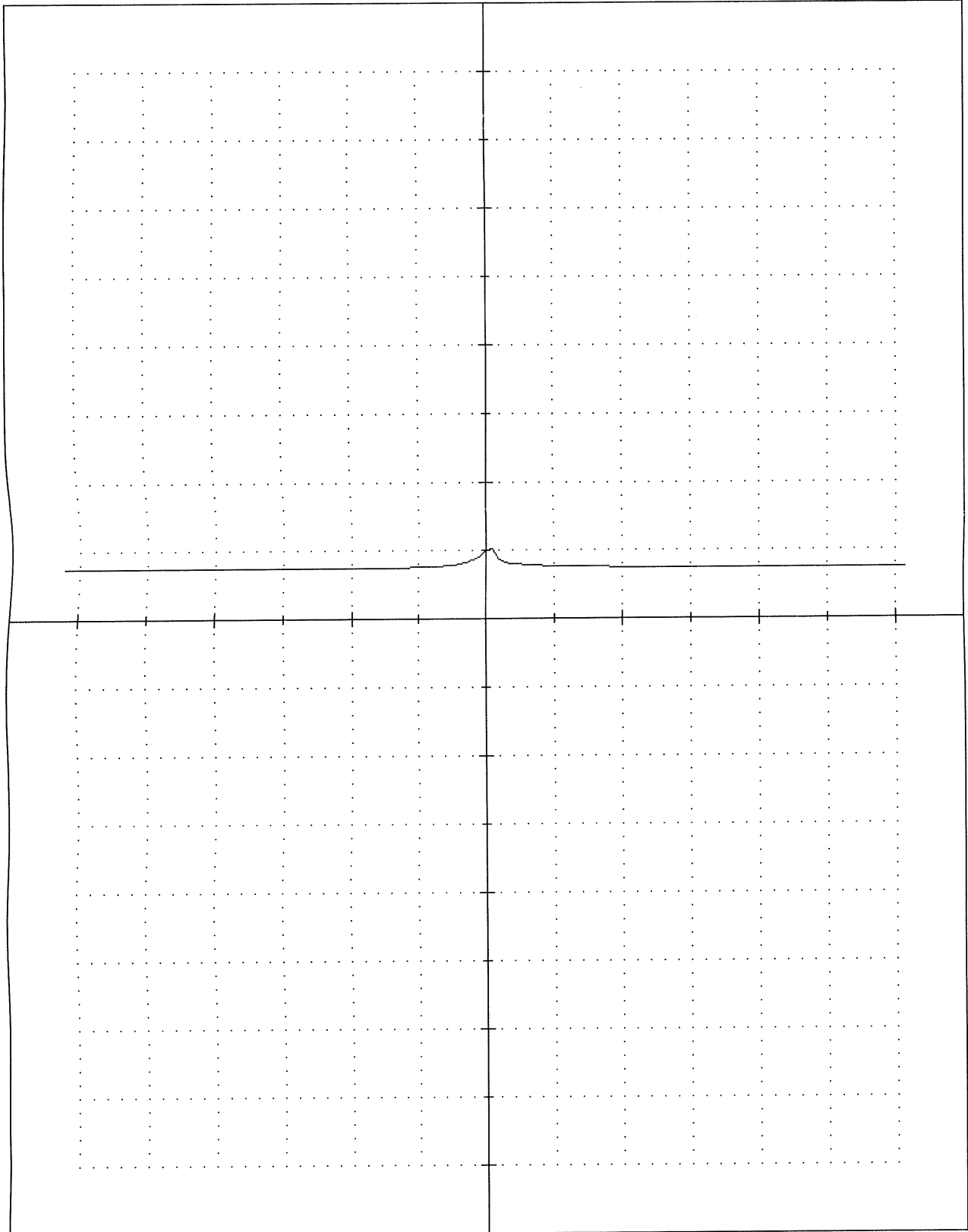command signal : ->   scale   : 8.00   mA / div
flow   : ↑   scale   : 2.00   cis / div

Frequency Response Test Results

Test Date	26/08/2011		Time	09:44
Model No.	E050-899	Serial No. E101	Operator	AL
System Pressure	4000 psi	Input Signal 10.00 mA pk-pk	Bias 0.00	mA
Rev/Date	NC/ 24 - 02- 03		Temp 32.0	deg C
-3dBs 249.8 Hzs		-90 degs 300.6 Hzs	Peaking 0.00	dBs

Notes:

Frequency (Hz)	Magnitude (dBs)	Phase Angle (Degs)
10.0	-0.16	-9.26
10.5	-0.13	-9.04
11.1	-0.17	-9.40
11.7	-0.19	-9.12
12.4	-0.22	-9.70
13.0	-0.20	-9.47
13.7	-0.26	-10.08
14.5	-0.26	-9.78
15.3	-0.27	-10.39
16.1	-0.30	-10.82
17.0	-0.33	-11.11
17.9	-0.35	-11.43
18.9	-0.35	-11.32
19.9	-0.38	-11.59
21.0	-0.41	-12.12
22.1	-0.40	-12.82
23.3	-0.41	-13.06
24.6	-0.42	-13.74
26.0	-0.45	-14.01
27.4	-0.47	-14.40
28.9	-0.48	-14.85
30.4	-0.49	-15.60
32.1	-0.50	-16.45
33.8	-0.52	-17.07
35.7	-0.54	-17.80
37.6	-0.58	-18.31
39.7	-0.61	-19.25
41.8	-0.63	-19.79
44.1	-0.64	-20.60
46.5	-0.68	-21.65
49.0	-0.70	-22.33
51.7	-0.73	-23.43
54.5	-0.77	-24.05
57.5	-0.79	-25.65
60.6	-0.86	-26.55
63.9	-0.87	-27.62
67.4	-0.89	-28.68
71.0	-0.94	-30.08
74.9	-0.97	-31.21
79.0	-0.99	-32.43
83.3	-1.05	-33.92
87.8	-1.11	-35.24
92.6	-1.15	-36.69
97.6	-1.23	-38.31
102.9	-1.28	-39.63
108.5	-1.34	-41.29
114.4	-1.42	-42.95
120.6	-1.47	-44.97
127.2	-1.44	-47.18
134.1	-1.54	-49.57
141.4	-1.65	-51.72
149.1	-1.63	-53.38
157.2	-1.78	-56.21
165.8	-1.80	-57.65
174.8	-2.05	-60.86
184.3	-2.09	-63.36
194.3	-2.29	-66.14
204.9	-2.44	-69.41
216.1	-2.40	-70.91
227.8	-2.56	-72.98
240.2	-2.78	-75.96
253.3	-3.08	-79.96
267.1	-3.36	-83.41
281.6	-3.59	-86.88
296.9	-3.65	-89.39
313.1	-3.80	-92.08
330.1	-3.90	-95.39
348.1	-4.37	-99.93
367.0	-4.45	-103.09
387.0	-4.51	-106.76
408.1	-4.54	-110.49
430.3	-5.02	-115.68
453.7	-5.71	-119.86
478.4	-5.72	-122.25
504.4	-5.65	-126.43
531.8	-5.80	-130.82
560.8	-6.24	-136.73
591.3	-6.08	-140.94
623.5	-6.04	-146.24
657.4	-5.92	-151.46
693.1	-5.78	-157.15
730.9	-5.42	-163.80
770.6	-4.79	-172.40
812.6	-5.68	170.90
856.8	-4.07	159.24
903.4	-2.16	139.45
952.5	-0.73	125.44
1004.4	-1.32	103.71
1059.0	-2.61	50.05
1116.6	-6.73	70.42
1177.4	-8.52	55.97
1241.5	-12.24	36.86
1309.0	-13.34	30.06
1380.3	-16.57	11.89
1455.4	-20.93	-7.40
1534.5	-22.50	-6.62
1618.0	-25.85	-5.92
1706.1	-28.07	-27.07
1798.9	-27.54	-36.12
1896.8	-28.45	-45.46
2000.0	-28.05	-55.06

Frequency Response Test Results

Model Number	E050-899	Serial No.	E101	Date	26/08/2011
-3dBs	249.8 Hzs	-90 degs	300.6 Hzs	Peaking	0.00 dBs

Magnitude (dB) vs Frequency (Hz), Phase Angle
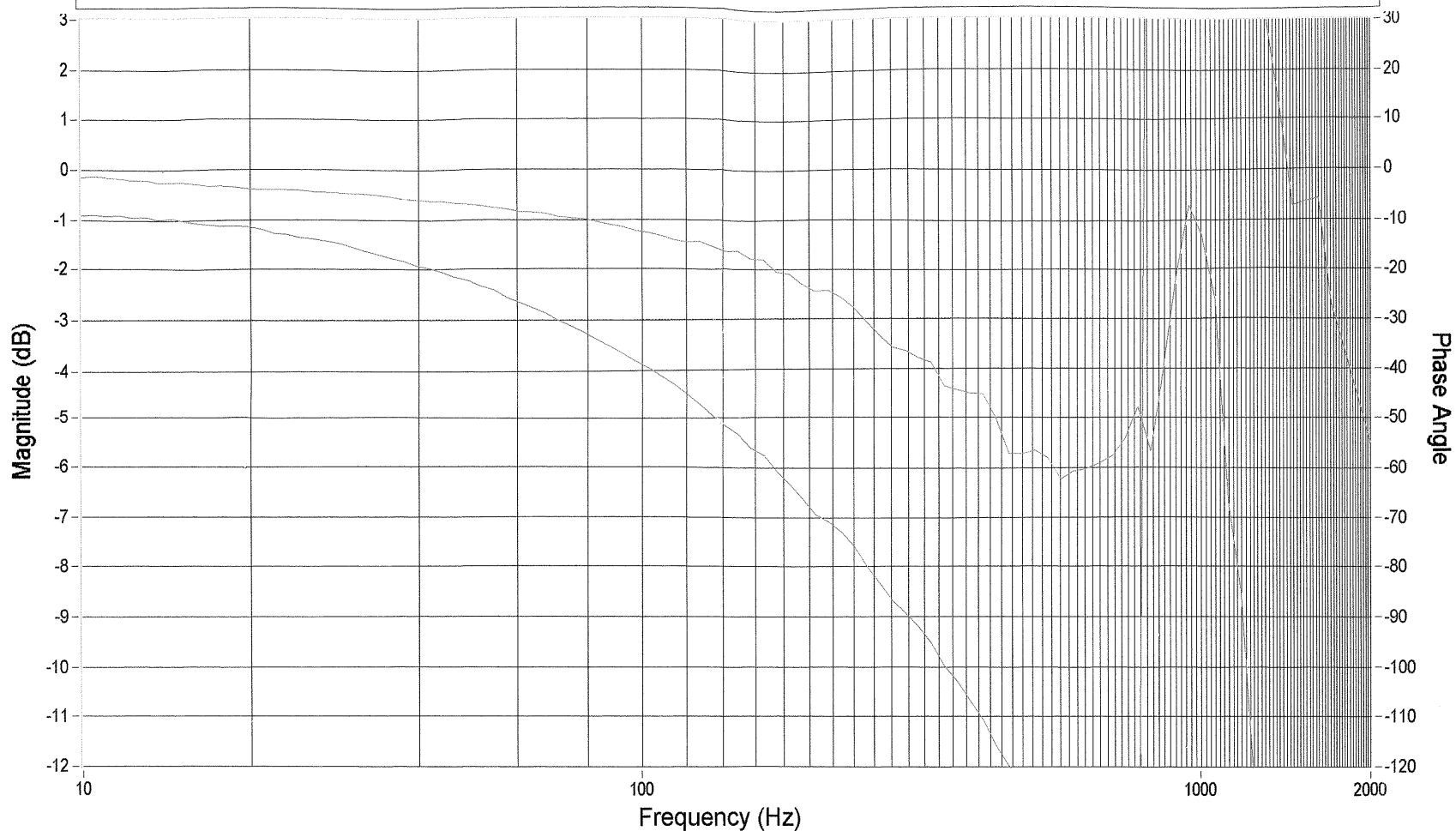
System Pressure: 4000 psi	Input Signal 10.00 mA pk-pk	Bias 0.00 mA
Operator - AL	Rev/Date NC/ 24 - 02- 03	Temp 32.0 Deg C	Time 09:44